Summary.

The reader is briefly introduced to the subject of surface thermodynamics, and to the relationship of interfacial free energies in poly-phase systems of particular interest in metallurgy.

The second part accurately defines an average surface free energy of crystalline materials, from the surface free energies of individual crystal faces, and a ratio is described which is applicable to any member of a given crystal system. This ratio is calculated for the Simple Cubic, F.C.C. and B.C.C. systems, for ideal crystals, and figures are constructed for these systems showing the variation of specific surface free energy with orientation. From consideration of the Tamman temperature, of sintering and of diffusion, temperature is shown to have little or no irreversible effect on the average ratio for refractory oxides, with some possible exceptions such as MgO. The mechanism of recrystallisation is briefly considered in terms of surface energy. Such crystal defects as growth faces, grain boundaries, dislocations and mosaic crystals are shown to have negligible effect on total surface free energy. Calculations are made of the average ratio for some polycrystalline materials with varying degrees of preferred orientation, such as compacts and wires.

The third part is involved with the calculation of the surface free energy of refractory substances. Graphite is dealt with at length, and found to have a surface free energy at absolute zero of about 3,100 erg/cm to over 5,000 erg/cm depending on the orientation of the surface: its surface entropy is also considered. The crystal structure,

the sublimation energy and the critical temperature form the basis of these calculations; and they are extended to fourteen oxides and β SiO. The solid/liquid transformation is also considered, and the surface free energy of some of these substances is calculated from absolute zero to their critical temperatures. The method used is simple and it seems to be at least as reliable as any other yet developed.

Finally, some experimental work is described, which was designed to measure contact angles continuously over long periods at high temperatures in order to estimate various interfacial parameters. The solids employed were graphite, pure and composite oxides, silicon carbide and pure iron, and the liquids were oxide slags, pure iron and iron/carbon alloys; various atmospheres were also used. Three distinct types of graphite surfaces were examined, the preparation of these and other specimens is described.

Slags made from CaO, MgO, Al_2O_3 and SiO_2 showed contact angles on graphite of 125° to 150° below 1490°C: above this temperature reaction was sometimes observed and lower contact angles resulted. Increase in SiO_2 lowered the contact angle but the effects of varying CaO, MgO or Al_2O_3 were not significant. The angles were higher for graphite of high surface free energy, and conversely. A, CO and N_2 atmospheres resulted in lower contact angles than those found in vacuo.

Liquid iron, in equilibrium with graphite at 1160°- 1247°, wet it with contact angles in vacuo of 55° and 59° depending on the orientation of the graphite. A modified surface structure is postulated to form, from a reproducible change in contact angle with time. An atmosphere of H_2 enhanced the wetting, leading to a contact angle of 37°,

but in any atmosphere wetting was hindered by impurity in the graphite or in the iron.

Oxides were not wet by liquid iron when no significant reaction occurred, and the contact angles were very similar for oxides of widely differing surface free energies. Plaques containing SiO_2 and Cr_2O_3 were found to react with the iron giving contact angles in the region of 50° for the pure oxides, and in the region 110°- 120° for composite oxides. A significant amount of FeO in any of the plaques was found to produce lower contact angles.

Some oxide slags were briefly investigated on solid iron, and contact angles of about 50° were found.

Comparisons with published work are made throughout the thesis, and practical applications of the subject are exemplified in the appropriate places.

--------- oo ---------

INTERFACIAL RELATIONS

IN

SLAG/METAL SYSTEMS.

BY

R.H.BRUCE, B.Sc., A.R.C.ST.

Thesis submitted to the University of Glasgow for the degree
of Doctor of Philosophy.

September, 1958.

Summary.

The reader is briefly introduced to the subject of surface thermodynamics, and to the relationship of interfacial free energies in poly-phase systems of particular interest in metallurgy.

The second part accurately defines an average surface free energy of crystalline materials, from the surface free energies of individual crystal faces, and a ratio is described which is applicable to any member of a given crystal system. This ratio is calculated for the Simple Cubic, F.C.C. and B.C.C. systems, for ideal crystals, and figures are constructed for these systems showing the variation of specific surface free energy with orientation. From consideration of the Tamman temperature, of sintering and of diffusion, temperature is shown to have little or no irreversible effect on the average ratio for refractory oxides, with some possible exceptions such as MgO. The mechanism of recrystallisation is briefly considered in terms of surface energy. Such crystal defects as growth faces, grain boundaries, dislocations and mosaic crystals are shown to have negligible effect on total surface free energy. Calculations are made of the average ratio for some polycrystalline materials with varying degrees of preferred orientation, such as compacts and wires.

The third part is involved with the calculation of the surface free energy of refractory substances. Graphite is dealt with at length, and found to have a surface free energy at absolute zero of about 3,100 erg/cm to over 5,000 erg/cm depending on the orientation of the surface: its surface entropy is also considered. The crystal structure,

the sublimation energy and the critical temperature form the basis of these calculations; and they are extended to fourteen oxides and β SiC. The solid/liquid transformation is also considered, and the surface free energy of some of these substances is calculated from absolute zero to their critical temperatures. The method used is simple and it seems to be at least as reliable as any other yet developed.

Finally, some experimental work is described, which was designed to measure contact angles continuously over long periods at high temperatures in order to estimate various interfacial parameters. The solids employed were graphite, pure and composite oxides, silicon carbide and pure iron, and the liquids were oxide slags, pure iron and iron/carbon alloys; various atmospheres were also used. Three distinct types of graphite surfaces were examined, the preparation of these and other specimens is described.

Slags made from CaO, MgO, Al_2O_3 and SiO_2 showed contact angles on graphite of 125° to 150° below 1490°C :above this temperature reaction was sometimes observed and lower contact angles resulted. Increase in SiO_2 lowered the contact angle but the effects of varying CaO, MgO or Al_2O_3 were not significant. The angles were higher for graphite of high surface free energy, and conversely. A, CO and N_2 atmospheres resulted in lower contact angles than those found in vacuo.

Liquid iron, in equilibrium with graphite at 1160°- 1247°, wet it with contact angles in vacuo of 55° and 59° depending on the orientation of the graphite. A modified surface structure is postulated to form, from a reproducible change in contact angle with time. An atmosphere of H_2 enhanced the wetting, leading to a contact angle of 37°,

but in any atmosphere wetting was hindered by impurity in the graphite or in the iron.

Oxides were not wet by liquid iron when no significant reaction occurred, and the contact angles were very similar for oxides of widely differing surface free energies. Plaques containing SiO_2 and Cr_2O_3 were found to react with the iron giving contact angles in the region of 50° for the pure oxides, and in the region 110°- 120° for composite oxides. A significant amount of FeO in any of the plaques was found to produce lower contact angles.

Some oxide slags were briefly investigated on solid iron, and contact angles of about 50° were found.

Comparisons with published work are made throughout the thesis, and practical applications of the subject are exemplified in the appropriate places.

------------ OO ------------

Contents

CHAPTER I - Introduction.

A. Definition of Terms:

The study of surface phenomena goes back to the beginning of the 19th century, and includes work by men as Poisson[1], Lord Kelvin[2], Gauss[3] and Laplace[4], though the modern conception of surface energy is largely due to Gibbs[5].

Surface energy is a property of condensed phases and is due to the imbalance of attractive forces at their surfaces. This causes a resultant inward attraction, and in liquids, which have sufficient mobility to change the shape of their free surface, this causes the surface to act like a membrane under tension - hence the origin of the term "surface tension". It is doubtful if such a term can accurately be applied to solids, a much better term for general use is surface energy : specific surface free energy in ergs/cm^2 is equivalent to surface tension in dynes/cm. Surface energy can be manipulated by the traditional methods of bulk thermodynamics; thus it consists of a specific surface free energy γ, which can be defined as the excess potential energy of a surface due to the imbalance of attractive forces, referred to an area of 1 cm^2, and a similar surface enthalpy ϵ related as below:-

$$\epsilon = \gamma - T\frac{d\gamma}{dT} \qquad \text{...........1.}$$

where T is the absolute temperature. The term "total surface energy" is usually applied to ϵ, but the author prefers to use the adjective "total" as below. Specific surface energy refers to one type of surface, and in a crystal with many types of surfaces, each specific surface energy may be averaged to give a total surface energy referred to weight or area (Chapter II). It is sometimes convenient to use a molar surface energy, which is referred to a surface containing one mole of the species, when the corresponding surface energy in ergs/cm^2 is multiplied by a factor $= fV^{2/3}N^{1/3}$, where f is the packing fraction (= 1.09 for close packed surfaces), V is the atomic or molecular volume and N is Avogadro's number.

The term "interfacial" is synonomous with "surface", and any interfacial energy should be stated in terms of the phases on either side of the interface; thus the subscripts $_{S,L,G}$ and $_V$ are added to denote solid, liquid, gas or vacuum respectively. Since refractory solids have negligible vapour pressures at normal temperatures, the term γ_S, for example, is often used instead of γ_{SV}, and even more loosely, the term γ_L is frequently used instead of γ_{LG} where G represents a gas (air) or the vapour of the liquid. Also the surface or interfacial energy must be defined at constant temperature, concentration and pressure

e.g. $$\gamma \equiv \left(\frac{\partial F}{\partial \sigma}\right)_{T,N,p}$$

(where F is the free energy of the substance, and σ its area), though pressure is not known to have much effect on surface energy and is ignored.

B. Effect of Temperature on Surface Energy:

The surface enthalpy is practically independent of the temperature (Frenkel[6]) though for some liquids such as silicates with abnormal surface entropies $\left(\frac{d\gamma}{dT}\right)$ (e.g. King[7]), it must vary with temperature quite markedly. There is, however, no reason to believe there is much, if any, variation with temperature in the surface enthalpy of solids which do not undergo allotropic changes. By a modification of the Nernst Heat Theorem:-

$$\lim_{T \to 0} \frac{d\gamma}{dT} \rightarrow 0$$

thus at absolute zero $\gamma^{\circ}_{sv} = \epsilon^{\circ}_{sv}$ (from equation 1). In the region of the critical temperature (see Chap. III B) γ becomes zero. So that from about 5°K to near the critical point, if a solid could be maintained at such a temperature, $\frac{d\gamma}{dT}$ may be taken as linear and approximately equal to the surface enthalpy at 0°K divided by the critical temperature (T_c °K):-

$$\frac{d\gamma_{sv}}{dT} \doteqdot -\frac{\epsilon^{\circ}_{sv}}{T_c} \qquad \text{------------} \quad 2.$$

The variation of surface free energy with temperature for liquids has been widely investigated, and many empirical equations (e.g. Partington[8], Adam[9]) have been suggested. The simplest linear form was developed by Eötvös[10] and Ramsay and Shields[11], as applied to the molar surface free energy, viz.:-

$$\gamma_L V^{2/3} = k(T_c - T - 6)$$

where k is the Eötvös constant which is approximately equal to 2.12 for "normal" liquids, and lower values are found for some associated liquids. An equation of the Van der Waals type has been found most generally applicable:-

$$\gamma_L = K\left(1 - T/T_c\right)^n \qquad \text{- - - - -} \quad 3.$$

where K and n are constants, and Lövgren[12] found n to have a value in the region of 1.2 for many unassociated liquids. An attempt to calculate the temperature coefficient for graphite from thermodynamic considerations is made in Chap.III.A, and the change in surface free energy on melting is considered in Chap.III.B.

The above changes in surface energy with temperature are, of course, reversible. An irreversible effect due to recrystallisation is considered in Chap.II, in connection with solids.

C. Effect of Concentration and Adsorption on Surface Energy:

C. Effect of Concentration and Adsorption on Surface Energy:

[illegible] d phase generally lowers the surface free energy, though a few cases of maxima in the surface energy/composition curves have been reported. A pure liquid can only alter its free energy per unit area by orientation and polarisation of its surface molecules. When another species is present with a different field of attractive forces round its molecule, that molecule with the largest attractive field will tend to pass into the body of the liquid more strongly than the molecule with the weaker field, which latter species will then occur in the surface in a higher concentration than in the bulk. This surface concentration is called adsorption. Adsorption may cause very considerable decreases in surface free energy, but large increases cannot be obtained - a solute with a large field of force exists chiefly in the bulk and the surface is little changed from that of the pure liquid. A surface excess concentration (Γ) is frequently

calculated for ideal (dilute solution) conditions from the Gibbs' adsorption equation:-

$$\Gamma = - \frac{c}{RT} \cdot \frac{\partial \gamma}{\partial c} \quad \text{------ "4".}$$

where c is the concentration, which is equal to the more correct activity, for dilute solutions.

A gas or liquid may also be adsorped on the surface of a condensed phase in which is not soluble. The driving force for this adsorption is the decrease in surface enthalpy associated with the heat of adsorption (Q), as in equation "5", modified from Rideal[13]:-

$$-(Q - \lambda) = \left(\gamma - T\frac{d\gamma}{dT}\right) - \left(\gamma' - T\frac{d\gamma'}{dT}\right) \quad \text{------"5".}$$

where γ is the surface free energy of the pure phase and γ' that of the phase after adsorption; λ is a latent heat due to the fact that some adsorped gases behave as liquids, and some adsorped liquids behave like solids (Adam[9] p.39). The sorbtion of gases by solids has been extensively studied (e.g. McBain[14], Beebe[15] and many others). Van der Waals adsorption exists at low temperatures chiefly, and with inert gases, and has a heat of adsorption in the region of 4 Kcals per gm.mole gas adsorped. Chemisorption becomes important in the region of room temperatures, and has a heat of adsorption of about 20 Kcals/mole or much higher (Garner and McKie[16] found a heat of adsorption of oxygen on charcoal above 220 Kcals/mole). These adsorped gases are extremely difficult to remove even partially : to halve any value of sorption, pressure would need to be diminished thirty-two fold; and to reduce it to 0.1%, the pressure reduction factor would be an unattainable 10^{15}

(after McBain[14] p.34)! The difficulty of measuring true surface area of adsorbents has limited the application of equation "5": the only figure known to the author is due to Parkes[17], who gives a value of 0.00105 cal/cm^2 for adsorption of water on silica, which is a reduction in surface enthalpy of nearly 4.4×10^7 ergs/cm^2, this is too high a figure by about 10^5. (Note: in this calculation $\lambda = (590) \div (V^{2/3} N^{1/3}) \doteqdot 10^{-6}$ cals/cm^2, so it is ignored). The reason for this enormous figure is probably an erroneous estimate of the surface area of the specimen used. Taking average figures, the average number of molecules on a (100) face of a simple cubic crystal $\sim 10^{15}$, giving an area per mole of $\frac{N}{10^{15}} \doteqdot 6 \times 10^8$ cm^2. With a heat of adsorption ~ 20 Kcal/mole (= 8.37×10^{11}e and assuming only one molecule of adsorbate per 100 molecules of adsorbent, the reduction in surface enthalpy = $\frac{8.37 \times 10^{11}}{6 \times 10^8 \times 10^2} \doteqdot 14$ ergs/cm^2. With better coverage this lowering may amount to 1000 ergs/cm^2 for a chemisorped fluid.

Udin et al[18] measured the surface free energy of silver wires in He and in air, finding values of 1140 and 350 ergs/cm^2 respectively. Orowan[19], from cleaving mica by a ballistic pendulum in vacuum and in air, found respective values of 4500 and 375 ergs/cm^2; the value in vacuum is about four times too high, but the ratio of these figures show a possible very large lowering of the free surface energy of a solid oxide by adsorption of air (O_2, N_2 and H_2O).

Adsorption on the surface of liquids may cause considerable lowering of the surface free energy especially of polar molecules such

as CO_2 and SO_2 as is seen from the investigations on their effect on glass by Sawai and Kubo[20]. Water has considerable effect on silicates even at very high temperatures, and raising the temperature causes some of the water to be driven off with a consequent raising of the surface free energy; thus Tamman and Rabe[21] consider water may be the cause of some abnormal positive temperature coefficients.

In a two-phase system increasing mutual solubility decreases the interfacial free energy till it becomes zero at the critical solution temperature - there is a close analogy to the critical temperature of a liquid/vapour system. If a component is added to a two-phase system, which is soluble in both phases, the mutual solubility may be raised, thus diminishing the interfacial free energy till sufficient is added to make the two phases completely miscible, when the interfacial free energy will again become zero. This latter point, which was raised by Rideal[13], is of great importance in wetting phenomena, as will be discussed below.

D. Other Factors affecting Surface Energy:

The imbalance of forces at the surface causes the atoms/molecules in the surface layer to become polarised and to change their lattice positions as discussed by Weyl[22], to decrease their surface energy. This polarisation and distortion continues into a crystal for perhaps a hundred or so layers. Very small crystals have not sufficient volume to accommodate this deformation of the lattice, so they may have higher surface energies than massive crystals of otherwise identical material.

Polarisation may be greatly affected by environment so that the surface free energies of a solution and of an interface are largely dependent on the polarisabilities of the components. Polarisation and screening offer a ready atomistic explanation of adsorption.

Edges and corners have atoms/molecules with lower co-ordination than in a surface. We may thus speak of edge energy, some calculations for which were given by Lennard-Jones[23], though it is debateable whether such edge energy contributes to the total surface energy or if it is already included in the surface energy of the component faces. If specific edge and corner energies exist they offer an explanation of active sites in some catalytic phenomena, and their contribution to the total free energy will become significant with very small particles, as the ratio of edges plus corners to surface area increases with decreasing size for geometric particles.

Strain energy in non-equilibrium structures may contribute significantly to surface energy. An apparent surface free energy for quartz was obtained by Schellinger[24] by ball-mill calorimetry, of 107,000 ergs/cm^2. This is in the region of 300 times higher than other values for equilibrium surface free energy (see Chap.III.B). Tamman and Arntz[25] report that mercury spreads several times faster on hardened copper and silver than when they are soft.

The effect of crystallographic defects is considered in Chap.II.

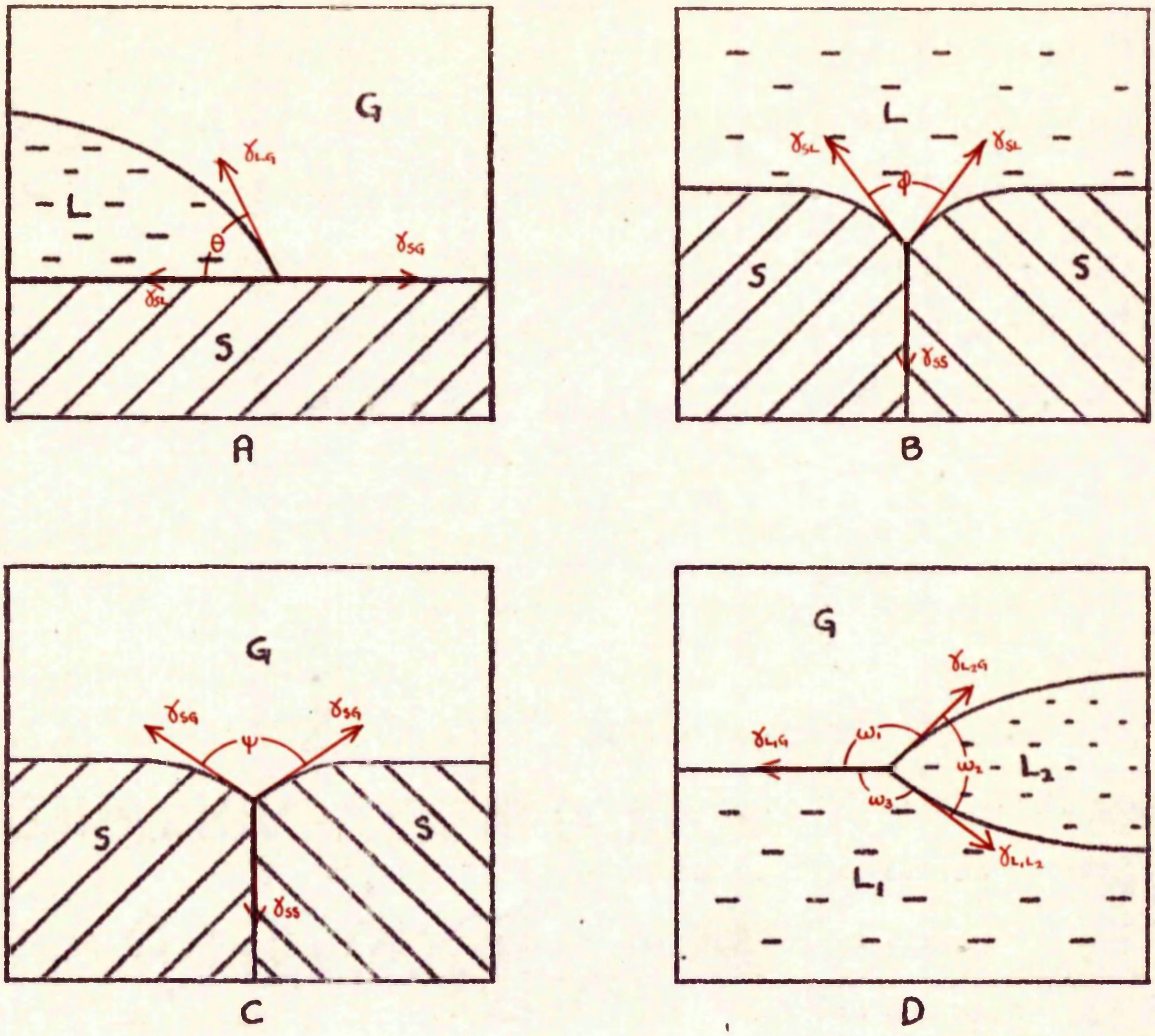

Fig. 1. Interfacial free energies at three-phase boundaries, for solid (S), liquid (L) and gas (G).

E. Spreading and Wetting:

Useful information may be derived about interfacial free energies from observations on three-phase boundaries at equilibrium. Cross sections of three-phase boundaries are shown in Fig.1. The surface tensions are regarded as forces acting tangentially at the boundary. The contact angle for a solid/liquid/gas system (θ) is the angle through the liquid between the solid surface and a tangent to the liquid surface at the three-phase boundary. Dihedral angles (φ and ψ) for a solid/fluid system are also shown. From Fig.1A the relationship is as expressed by the Dupré equation:-

$$\gamma_{SG} = \gamma_{SL} + \gamma_{LG} \cos\theta \quad \text{........ "6A".}$$

with similar equations from Figs. 1B and 1C:-

$$\gamma_{SS} = 2\,\gamma_{SL} \cos\frac{\varphi}{2} \quad \text{........ "6B".}$$

$$\gamma_{SS} = 2\,\gamma_{SG} \cos\frac{\psi}{2} \quad \text{........ "6C".}$$

γ_{SS} is the grain boundary free energy. Similar equations may be set up for the liquid/liquid/gas system as in Fig.1C. Assuming that γ_{SG} is not affected by the vapour of the liquid, observations of the three angles, together with a knowledge of one interfacial free energy (usually γ_{LG} which is readily obtained), permit calculation of all other interfacial free energies.

There is a difference of opinion over whether non-wetting should apply in cases where $\theta > 90^\circ$ or $\theta > 0^\circ$: the author prefers the former, where wetting occurs with $\theta < 90^\circ$, because a change in γ_{LG} has the opposite effect on θ when θ is initially $< 90^\circ$, to the effect of a

similar change with $\theta > 90^\circ$. The effect on θ of varying the three interfacial free energies is shown in Table I, derived from the Dupré equation (6A).

Table I. The effect on the contact angle of varying the interfacial free energies.

		$\theta < 90^\circ$	$\theta > 90^\circ$
Decrease	γ_{LG}	θ decreases	θ increases
"	γ_{SG}	θ increases	θ increases
"	γ_{SL}	θ decreases	θ decreases

A rather more detailed treatment of this variation has been given by Towers[26].

When a liquid extends its surface it is said to spread. Harkins[27] has done a great deal of work on spreading. The work of adhesion W_{AD} is the energy necessary to separate 1 cm^2 of interface, and the work of cohesion W_{CO} is the energy necessary to separate a homogeneous condensed phase over 1 cm^2 (producing in each case 2 cm^2 of surface): Harkins initial spreading coefficient is the difference in these terms, thus:-

$$\text{Initial Spreading Coefficient} = S_i = W_{AD} - W_{CO}$$
$$= (\gamma_{SG} + \gamma_{LG} - \gamma_{SL}) - 2\gamma_{LG}$$
$$= \gamma_{SG} - \gamma_{SL} - \gamma_{LG} \qquad \ldots\text{"7"}.$$

S_i is for the spreading of pure phases uncontaminated with each other: semi-final and final coefficients are obtained with partial contamination and with mutual saturation respectively. Spreading occurs to give complete coverage when $S > 0$, whereas a lens forms with $S < 0$. Mutual solution may

give quite different values of S, so that a liquid may spread completely then contract to a lens (dewetting); Bondi[28] gives several interesting examples of dewetting.

Equations such as 6A, B & C apply to systems in equilibrium. Frequently different contact angles can be observed when the liquid is advancing and receding. These angles are metastable, although they may be quite reproducible and persist for long periods, and this hysteresis, as it is termed, may be caused by a number of factors such as contamination and surface irregularities. Cleavage or condensation in a vacuum is about the only way to produce a really clean surface. All normal surfaces are more or less contaminated, though the contamination (such as adsorption of air) may be quite reproducible: the wetting liquid itself contaminates the other surface. Wetting in different atmospheres may be quite different due to adsorption of different gases at the three interfaces. The best definition of roughness is possibly the ratio of actual surface area to geometrical surface area. Wenzel[29] pointed out its effect on θ, which is such that the greater the roughness the more θ tends to 90°. Bartell & Shepard[30] showed increasing inclination of asperitis to increase the hysteresis but that their height had little effect.

Solution generally decreases the interfacial free energy between the spreading phase and the substrate, increasing the spreading tendency (from Eqn.7). In the case of metals, compounds always lead to at least initial spreading, as is seen from the many examples in Bondi[28].

F. Metallurgical Applications:

Consideration of the surface free energy of slags is very useful in assessing their structure, which is in turn useful for atomistic interpretation of slag/metal reactions. In some simple cases it is possible to predict the surface free energy of liquids (Chap.IIIC), but prediction is very difficult for complex industrial slags. Positive, and very small negative temperature coefficients are generally taken as indicative of dissociation. For example complex ring and chain networks with SiO_2 may break down to simpler molecular groups with increasing temperature, thus giving a larger number of unsatisfied valencies, increasing the surface free energy above the reduction due to thermal expansion, thus giving a positive temperature coefficient (King[7]). Even if the bonding is unchanged a reduction in size of the molecular groups will probably lead to closer packing on the surface, increasing the bond density and thus giving an increased surface free energy. In the metallic and non-metallic systems known to the author there is no abrupt change of surface energy with composition, even where solid compounds are formed. This would seem to indicate that these high temperature liquids are already largely dissociated. Also absence of a similar abrupt change with temperature shows the residual dissociation to be gradual. It would be interesting to investigate solutions of low melting liquids, which are known to form solid compounds, over a wide range of temperature.

The problem of wetting crops up very frequently. The balance of the interfacial forces is represented by a contact angle, which is of extreme importance in this connection. Where a liquid is used in heat exchanges it should wet the surface as completely as possible, for efficiency. Other examples in which wetting is desirable are in welding, brazing and soldering[28] and cladding metals by dipping.

In many cases wetting is not desirable. The penetration of liquid slag[26] or metal[31] into the pores of the wall of the furnace may amplify corrosion of the bricks: in this case, as large a contact angle as possible is desired, as hydrostatic pressure may force the liquid in against a small capilliary force in the opposite direction. With a non-wetting liquid the pores should be as small as possible, as is seen from Equation 8 where 'p' is the pressure difference across the meniscus of a liquid with contact angle θ and 'r' is the radius of the meniscus which is approximately equal to the radius of a pore.

$$p = \frac{2\,\gamma_{LG}\cos\theta}{r} \qquad \ldots\ldots\ldots\ldots 8.$$

For a wetting liquid where the capilliary forces aid penetration, the only solution is to have a completely non-porous refractory, as the smaller the pores the greater the tendency of the liquid to penetrate them (above molecular dimensions). Non-wetting is similarly desired in runners and moulds, if a metal wet the mould, extraction would be difficult and result in a dirty casting. Clean metal also requires that it should not wet the refractories with which it comes in contact to prevent exogenous inclusions, and any indigenous inclusions should

[illegible]

[illegible]

……

[illegible]

not be wet so that they will more easily separate from the metal.

In the case of slag running over coke in a blast furnace, non-wetting would lead to quicker collection of slag in the hearth, but would also mean that perhaps insufficient time of contact would lead to non-recovery of accessible metal, so that an intermediate contact angle, in the region of 90°, would be desirable to effect a balance between speed and efficiency.

The problems of nucleation in solidification[32], and in the production of gas bubbles are very dependent on interfacial free energies. From Equation 8, an infinitesimal bubble of gas (r 0) would have an infinitely high pressure in it in the centre of a liquid, or at a liquid/liquid interface (such as slag/metal), as has often been pointed out, if it were spherical, but it does not seem to have been realised that an infinitely small bubble could be lenticular and the measurable radius would cause a finite pressure difference to exist. Indeed at a liquid/solid interface (e.g. metal/refractory) where the liquid does not wet the solid, a depression, such as a crevice or pore, would result in a negative pressure difference in a bubble at that spot. In a reaction such as:-

$$MO + C \rightleftharpoons M + CO$$

the equilibrium depends on p_{co}, and hence on the rate of removal of CO. In an extreme case, the retention of a gas in a metal or slag may depend on the porosity of the vessel used to contain it, if its surface is smooth and not favourable to gas nucleation more than the equilibrium amount of gas may be retained. The study of gas nucleation

at the austenite /liquid steel interface should prove to be interesting, as in this case complete wetting would lead to a high pressure in a spherical bubble. In rimming steel gas nucleation may be brought about by favourable inclusions. Before leaving the subject of gas in liquids the problem of foaming slags must be mentioned. Kosakevitch[33] has done some work in this connection, but although it seems agreed that they are the result of surface active constituents in the slag, such agents do not seem to have been found.

Grain growth and sintering of solids are a result of them decreasing their free energy, and the processes are very largely dependent on surface forces, as will be discussed more fully in Chap.II. Also, in the important new field, cermets depend for their success on interfacial forces, in this case the work of adhesion, and on the mechanical properties of thin films, which may be quite superior to those of the bulk material, for reasons similar to the size effect already mentioned, and also due to their strained lattices. Melting point and corrosion resistance are of primary importance to cermets, but when these are suitable, consideration must be made of the interfacial relationships. This field is already too large to single out individual workers, in this necessarily brief consideration.

The kinetics of a chemical reaction may be dependent on surface phenomena such as the gas nucleation considered above. Strong adsorption of a constituent at an interface may interfere with reaction between the phases. McBain[14] quotes figures on the adsorption of charcoal showing CO_2

to be more tenaciously held than CO in the region -190°C to + 182°C, and this relationship seems to persist to higher temperatures. Now gross reaction between graphite and oxygen is known (e.g.Ohga & Ikegawa[34]) to be negligible below 500°C, increasing sharply in the region 700° - 900°C, when the reaction:-

$$CO_2 + C \rightleftharpoons 2\,CO$$

shows a strong tendency to move to the right. Thus the more strongly the adsorbate is bound, the more it tends to interfere kinetically. Another interesting example is in the reactivity of the various forms of SiO_2 towards CaO in different atmospheres, as was investigated by Hedvall & Runehagen[35]. Gwathmey et al[36] have investigated several cases where reaction (such as oxidation) and catalysis occur preferentially on some faces of single crystals, though this is possibly due as much to favourable geometrical circumstances as to surface energies.

In this vast field there is tremendous scope for basic theoretical work and for original experimentation. This work is concerned with an effort to clarify the surface energy of solids, firstly with respect to the total or average surface free energy of real aggregates, which has been almost entirely neglected or lightly dismissed; then simple attempts are made to estimate surface free energies for various refractory substances. Finally, some experimental work by the author is quoted, chiefly in the field of ferrous metallurgy, such as the wetting of graphite by slags and iron, the wetting of refractories by iron and some examples of slag on metals: in all cases only solid/liquid systems are considered. Previous work in these fields will be noted in the appropriate places.

CHAPTER II - Calculations of the Average Surface Free Energy of Allotromorphic Crystals and Aggregates of Small Crystals.

A. Introduction and Definitions:

The major difference between theoretical calculations of the surface free energy of solids and some experimental results, such as those from creep rate near the melting point and dihedral angle measurement, lies in the fact that theory in general deals with particular crystal faces, whereas the above experiments, and others, deal with an "average" surface free energy of all the faces that obtain in the particular case being considered. It is important to estimate the relationship between these values, and to establish a more exact meaning for the word "average".

Friedel et al[37] made, to the author's knowledge, the only estimate of such a relationship, in connection with the surface energy of grain boundaries in a metal; however they only dealt with a necessarily small number of planes, and their mean values are not clearly defined.

It is intended to define an average surface free energy, under what is regarded as ideal conditions, and to estimate the effect of temperature and some departures from ideality. The practical significance will also briefly be discussed.

To describe all possible planes by the customary Miller

indices (h,k,l), a three dimensional representation is necessary, with each point in this volume representing only one plane. If we now add a dimension to each point, representing surface energy, we would have a four dimensional model. Other dimensions would have to be added to account for area, temperature, pressure and departures from ideality, giving a model with a minimum of eight dimensions. A simultaneous consideration of all these factors does not seem feasible. Statistical methods are applied here to an ideal case and the effects of the other variables are considered separately.

The surface energy considered here is the specific surface free energy of a solid in contact with its own vapour only ("vacuum"), as referred to the centre of a homogeneous crystal (of the same material) with no lattice imperfections or other strain energy, and being perfectly pure and of stoichiometric composition, near absolute zero.

The examples considered are of the cubic systems (simple cubic, F.C.C. and B.C.C.) though the methods are theoretically applicable to any system, these three are sufficiently simple to allow ready analysis.

If the original crystal is assumed to exist as a perfect cube only the $\{100\}$ faces (i.e. (100), $(\bar{1}00)$, (010), etc.) are present and in equal areas. We now remove the twenty edges and corners (without causing lattice imperfections) giving 26 faces of

the three families $\{100\}$, $\{110\}$ and $\{111\}$ in such a manner that they are all equal in area. If this process of removing the edges and corners is carried out an infinite number of times a sphere results whose surface consists of all possible faces, all equal in area. This process eliminates an area factor. If we started with infinitely small crystals each of which exhibited only one face different from all the others, and then built up a sphere, each face may have a specific area. This specific area is not easily included in the calculation: it was defined as the largest plane contained in a unit cell and passing through atoms, but it was very difficult to calculate beyond the first nine families (see below) and the result was less than 1% different from such a calculation as below with faces of equal area, so this refinement was ignored.

The sphere would have to be finite (say 1 m.m. diameter) so each face would have to be very small (say 4Å^2) giving a limit to the number of different faces possible ($\pi \times 10^{14}$) ; such a limit has, as is seen below, no practical significance.

It must be assumed that edges and corners do not affect the surface energy of any face. In the limit, with a sphere, the angular difference between neighbouring faces is virtually zero so that edges and corners are more or less non-existent, and, since the neighbouring faces will be shown to have almost identical surface energies, any edge effect cannot, in an ideal spherical crystal, be appreciable.

The average surface free energy of such an allotromorphic crystal is then defined as the sum of the products of the specific surface

free energy and area for each and every face, divided by the sum of their (equal) areas.

Developments of the spherical model will be shown to be easily applied to practical cases.

D. First Calculation for the Simple Cubic System:

The simple cubic system was chosen first as it was believed to be the simplest case. In the simple cubic, and some other systems, the ratio of the surface energies of any two given planes is constant for that system, although the actual values of surface energy may vary widely from substance to substance, in that system. The surface energy is derived from a geometric factor and from an energetic factor alone, in this consideration: the energetic factor is constant for any given substance, being a fraction of the sublimation energy, called the bond energy. The lattice parameter may be included with the energetic factor, leaving a geometric factor common to all members of the system. By consideration of the spacial bond distribution about an atom, with reference to its neighbours in various planes and from the interplanar distance, this geometric factor may be expressed as a function of the Miller indices alone. Friedel et al[37] gave the corrected[38] equations below:-

Simple Cubic $$\gamma_{(hkl)} = \frac{(h+k+l)}{\sqrt{h^2+k^2+l^2}} \cdot \frac{\epsilon}{d^2} \qquad \text{..........9.}$$

F.C.C. $$\gamma_{(hkl)} = \frac{4(2h+k)}{\sqrt{h^2+k^2+l^2}} \cdot \frac{\epsilon}{d^2} \qquad \text{..........10.}$$

B.C.C. $$\left\{ \begin{array}{ll} \gamma_{(hkl)} = \dfrac{2[2h\epsilon_1 + (h+k+l)\epsilon_2]}{\sqrt{h^2+k^2+l^2} \; . \; d^2} & \text{if } h \geq (k+l) \\[2em] \gamma_{(hkl)} = \dfrac{2(h+k+l)(\epsilon_1+\epsilon_2)}{\sqrt{h^2+k^2+l^2} \; . \; d^2} & \text{if } h \leqslant (k+l) \end{array} \right\} \qquad \text{..........11.}$$

[illegible]

[illegible]

.... [illegible]

.... [illegible]

.... [illegible]

Where $\gamma_{(hkl)}$ is the specific surface free energy (near absolute zero) for the plane with Miller indices (hkl) ; ϵ is the bond strength, the subscripts 1 and 2 referring to nearest and next nearest neighbour bonds respectively in the B.C.C. system; d is the lattice parameter. These equations are to be applied when $h \neq k \neq l$, and each is positive.

In the case of the simple cubic system, $\gamma_{(100)}$ is found to be the lowest (see C, below) so all other planes may have their energy expressed as a ratio, greater than unity, with respect to $\gamma_{(100)}$. This ratio, derived from equation 9, is as below:-

$$R_{(hkl)} = \frac{\gamma_{(hkl)}}{\gamma_{(100)}} = \frac{h + k + l}{\sqrt{h^2 + k^2 + l^2}} \qquad \text{..........12.}$$

The surface energy ratio R is now seen to apply to any member of the simple cubic system irrespective of bond energy or lattice parameter, and an average ratio may be obtained which applies to all members of this system as described below.

The Miller indices are always taken as positive in this discussion, as all members of the family of planes $\{hkl\}$ have the same surface energy - indeed they are the same planes, as may be seen by rotating the axes through any whole multiples of 90°, when the signs and relative positions of the indices change as desired (e.g. $(x\,y\,z) \equiv (x\,\bar{y}\,z) \equiv (y\,x\,z)$ etc.) This is not true of more complex systems (see Chap. III).

Each family has a number (f) of members, which is obtained by simple permutation, as in Table II below, where $h \neq k \neq l \neq h$.

Table II :- Number (f) of members of a family of planes $\{hkl\}$.

Family	$\{h00\}$	$\{hh0\}$	$\{hhh\}$	$\{hhk\}$	$\{hk0\}$	$\{hkl\}$
f	6	12	8	24	24	48

We must also take $|h| \nless |k| \nless |l|$ as is required by equations 9, 10 and 11, and the families are divided into groups such that $|h| = n$ the number of the group: thus the first group where n = 1 consists of the three families $\{100\}$, $\{110\}$ and $\{111\}$ that is, of 26 planes. As $n \to \infty$ the original cube tends to a sphere.

Since the faces are made equal in area, the average ratio, R_n, for all faces up to and including those of the group n, is given by:-

$$R_n = \frac{\sum_1^n f_{(hkl)} \times R_{(hkl)}}{\sum_1^n f_{(hkl)}} \qquad \text{..........,13.}$$

Equation 13 applies to all similar systems. As $n \to \infty$ the average factor tends to the value for a sphere for which the surface energy is $R_\infty \times \gamma_{Rf}$, where γ_{Rf} is the surface energy of the reference plane; in the case of the simple cubic system, $\gamma_{(100)}$.

A further limitation is imposed, in that any plane may not be included if it is parallel to, and in the same sector, as, another plane previously considered. For example the family $\{200\}$ is not included in the calculation, although it has a real existence as it is parallel to $\{100\}$ (and has therefore the same surface energy, in this case): the spherical model does not allow more than two parallel planes on its surface (e.g. (100) and ($\bar{1}00$)). Similarly $\{300\}$ is not included, although in this case it has no real existence, that is, it does not

contain any atoms.

As an aid to extrapolation, a partial average, R'_n derived only from members in the group n, was calculated as below:-

$$R'_n = \frac{\sum_{n-1}^{n} \beta_{(hkl)} \times R_{(hkl)}}{\sum_{n-1}^{n} \beta_{(hkl)}} \qquad \ldots\ldots\ldots\ldots 13a.$$

The value R_n derived from 13 is referred to as the total average to distinguish it from R'_n.

It was hoped that R_n would tend to a limit without n being very large. However the simple cubic system required n to be about twice as high as for the other two cubic systems, before R_n tended to a definable limit. In this case the total average had to be calculated as far as n = 20, involving some 57,000 planes and a correspondingly large amount of calculation. To illustrate this calculation, Table III is given, showing the calculation up to n = 3, and Table IV shows the averages up to n = 20.

From Table IV it is seen that it is only in the region of n = 20 that the averages seem to approach reasonably close to a limit: this limit R_∞ is estimated to be 1.546 ± 0.001. The values of R'_n are seen to fluctuate irregularly, with corresponding and smaller fluctuations in R_n : the fluctuations in both values diminish as n increases, but are still present at n = 20 to give an uncertainty to R_∞ of about 0.1%. This uncertainty is, however, very much less than for any published value of the surface energy of a solid - in many cases it is better by a factor of 100 or more, so it is not profitable to take the calculation beyond n = 20 in this case.

[illegible]

[illegible]

[illegible]

[illegible] …………

[illegible]

[illegible]

[illegible]

[illegible]

[illegible]

Table III - Calculation of Partial and Total Averages for the Simple Cubic System.

n	Family	$f_{(hkl)}$	$R_{(hkl)}$	Product
	{100}	6	$1 = 1.000$	6.000
1	{110}	12	$\frac{2}{\sqrt{2}} = 1.414$	16.968
	{111}	8	$\frac{3}{\sqrt{3}} = 1.732$	13.856
	{200}	—		
	{210}	24	$\frac{3}{\sqrt{5}} = 1.340$	32.160
	{211}	24	$\frac{4}{\sqrt{6}} = 1.632$	39.168
2	{220}	—		
	{221}	24	$\frac{5}{3} = 1.667$	40.008
	{222}	—		
	{300}	—		
	{310}	24	$4(10)^{-\frac{1}{2}} = 1.264$	30.336
	{311}	24	$5(11)^{-\frac{1}{2}} = 1.507$	36.168
	{320}	24	$5(13)^{-\frac{1}{2}} = 1.386$	33.264
	{321}	48	$6(14)^{-\frac{1}{2}} = 1.604$	76.992
3	{322}	24	$7(17)^{-\frac{1}{2}} = 1.697$	40.728
	{330}	—		
	{331}	24	$7(19)^{-\frac{1}{2}} = 1.606$	38.544
	{332}	24	$8(22)^{-\frac{1}{2}} = 1.703$	40.872
	{333}	—		

$$R'_1 = R_1 = \frac{36{,}824}{26} = \underline{1.4163}$$

$$R'_2 = \frac{111.336}{72} = \underline{1.5463}$$

$$R_2 = \frac{148.160}{98} = \underline{1.5118}$$

$$R'_3 = \frac{296.904}{192} = \underline{1.5464}$$

$$R_3 = \frac{445.064}{290} = \underline{1.5347}$$

Table IV - Partial Average R'_n, and Total Average R_n, up to $n = 20$ (Simple Cubic System).

n	R'_n	R_n
1	-	1.4163
2	1.5463	1.5118
3	1.5464	1.5347
4	1.4197	1.4774
5	1.5469	1.5121
6	1.5463	1.5235
7	1.5475	1.5331
8	1.5494	1.5378
9	1.5180	1.5318
10	1.5470	1.5353
11	1.5442	1.5378
12	1.5473	1.5395
13	1.5468	1.5413
14	1.5450	1.5419
15	1.5491	1.5432
16	1.5471	1.5438
17	1.5477	1.5446
18	1.5463	1.5448
19	1.5469	1.5452
20	1.5463	1.5453

Little importance may be attached to the minima at $n = 4$ and 9, they are due to the method of grouping the planes: it is doubtful if any practical significance could be attached to these and other minima.

This average ratio was obtained from approximately 57,000 planes, so the "practical limit" ($\pi \times 10^{14}$) previously mentioned is seen to be of no consequence.

C. Second Calculation, Graphical Integration, for the Simple Cubic System:-

As the previous calculation gave only an estimate of the average factor, it was hoped that graphical integration would provide a more accurate figure: this hope was not realised, but the method adopted led to some interesting results, and to a good check on the previous figure.

Several figures were constructed showing the dependence of the surface energy ratio on the orientation of the plane, but the only representation which proved of any value was the construction of contours of this ratio on a stereographic projection. In such a projection, the orientation changes continuously with position, and the ratio was also found, as expected, to change in a continuous and regular manner, giving smooth contours of equal surface energy ratio. A stereographic projection was constructed in the usual manner, giving positions of more than 100 planes, distributed more or less evenly. This projection is shown as the transparent part of Figure 2. Only the quadrant where all the Miller indices are positive or zero is shown; the other three quadrants being identical. Figure 2 shows the contours of equal surface energy ratio as described above, and by its use an estimate (within about 5%) of the surface energy ratio may be obtained for any plane in the Simple Cubic System, and hence the surface free energy near $0^\circ K$ by multiplying this ratio by $\gamma_{(100)}$ (or by $\frac{\epsilon}{d^2}$ or by $\frac{H_s}{6d^2}$, where H_s is the heat of sublimation near $0^\circ K$).

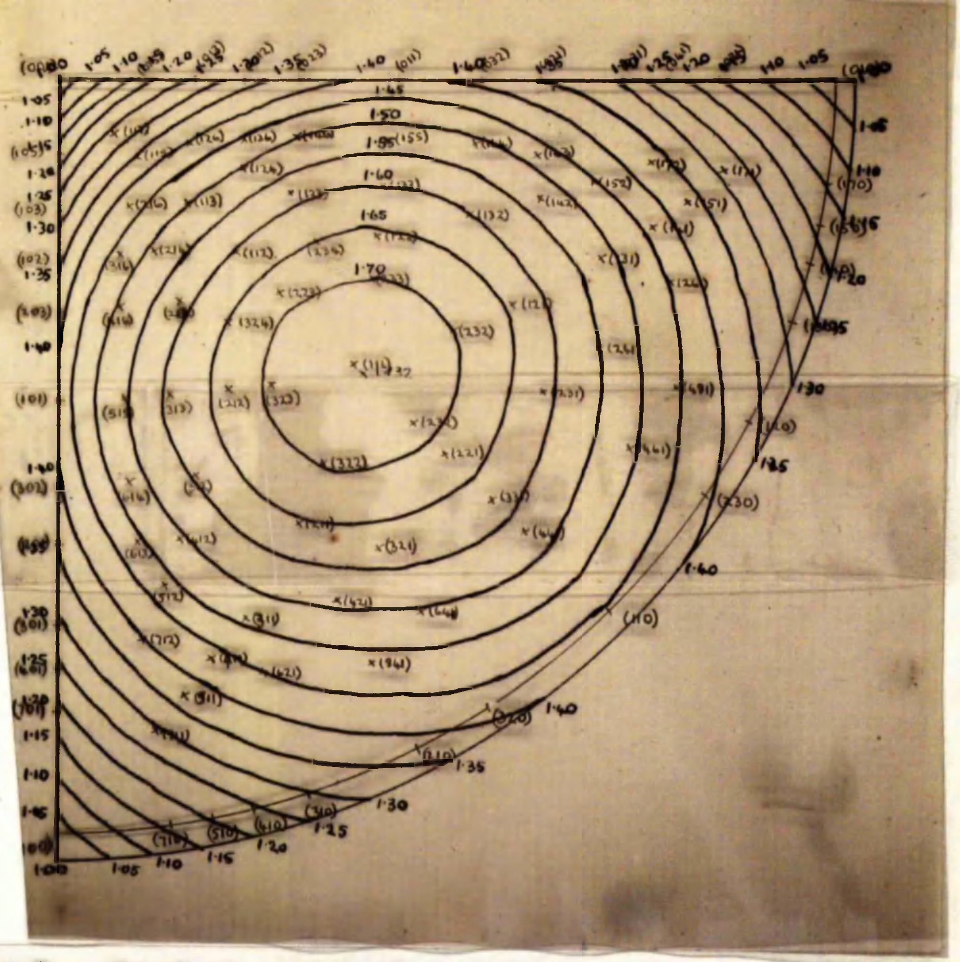

Fig.2 Surface energy ratios for the simple cubic system.

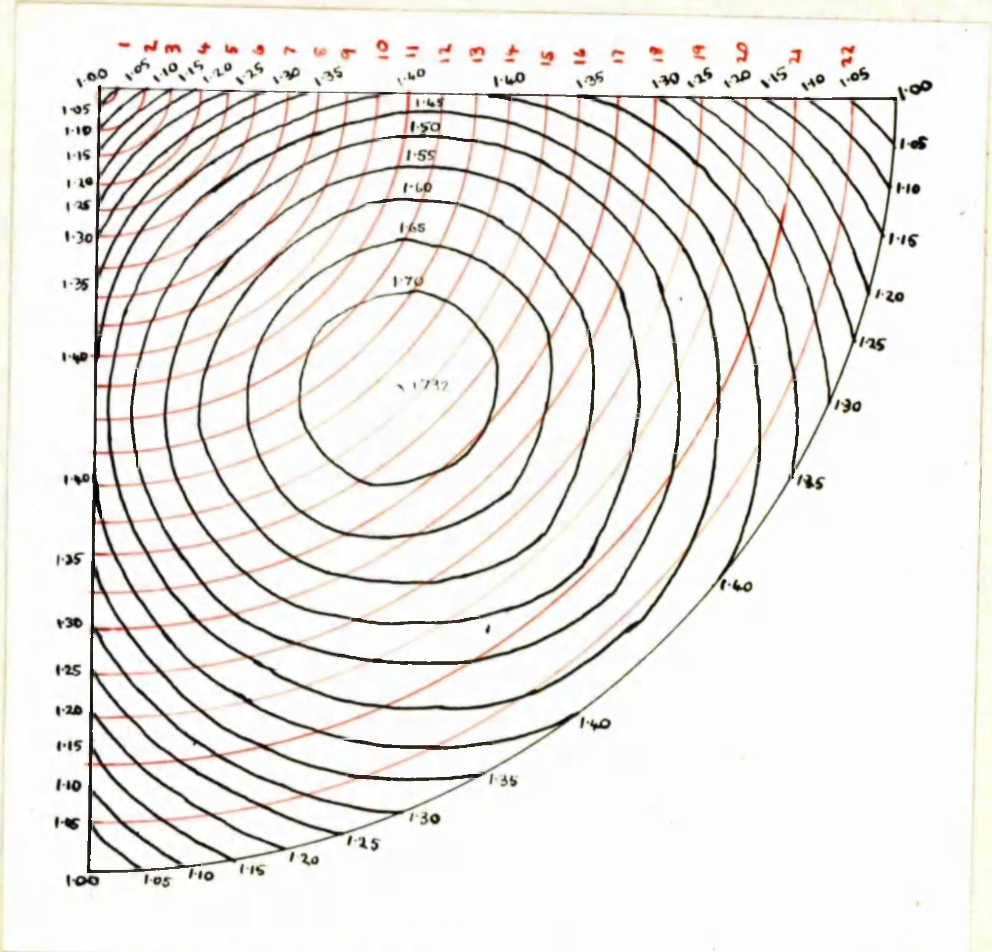

Fig.3 As in Figure 2, with medial arcs.

From Fig.2 $R_{(hkl)}$ is seen to lie between 1.000 and $\sqrt{3}$, justifying the choice of $\gamma_{(100)}$ as the reference. It is regretted that the films have shrunk unevenly and the correspondence between the two parts of Fig.2 is not very good.

The projecting sphere was divided into 22 areas by planes parallel to the plane of projection such that the edges of these areas were at 0°, 4°, 8°,------ 84° and 90° to the [001] pole. Arcs medial to these areas were projected on the stereographic contour figure, that is, at 2°, 6°, ------82° and 87° to [001]. The radii of these projected areas were obtained geometrically after the usual manner of stereographic projection. These projected arcs are shown in red in Fig.3, which is otherwise identical to Fig.2. Twenty-two vertical sections were plotted, taken along each of these arcs, with each base proportional to the arc length, and heights proportional to corresponding surface energy ratios along the arc. In each of these sections the area was obtained by counting, and these areas divided by the arc lengths gave the average values of the ratios for each 4° area. In order to find the total average, these individual averages have to be weighted by factors proportional to the areas on the projecting sphere represented by the 4° strips on the projection. This constructional work is clarified by Fig.4. ABC represents a section of the projecting sphere, OB the projection plane and OA the [001] pole. The areas on the spheres are represented by the numerals 1 - 22. OB_{10} gives the radius of the medial arc (at 38° to [001]) for the 10th area: this area is proportional to the projection XY on OA, as shown,

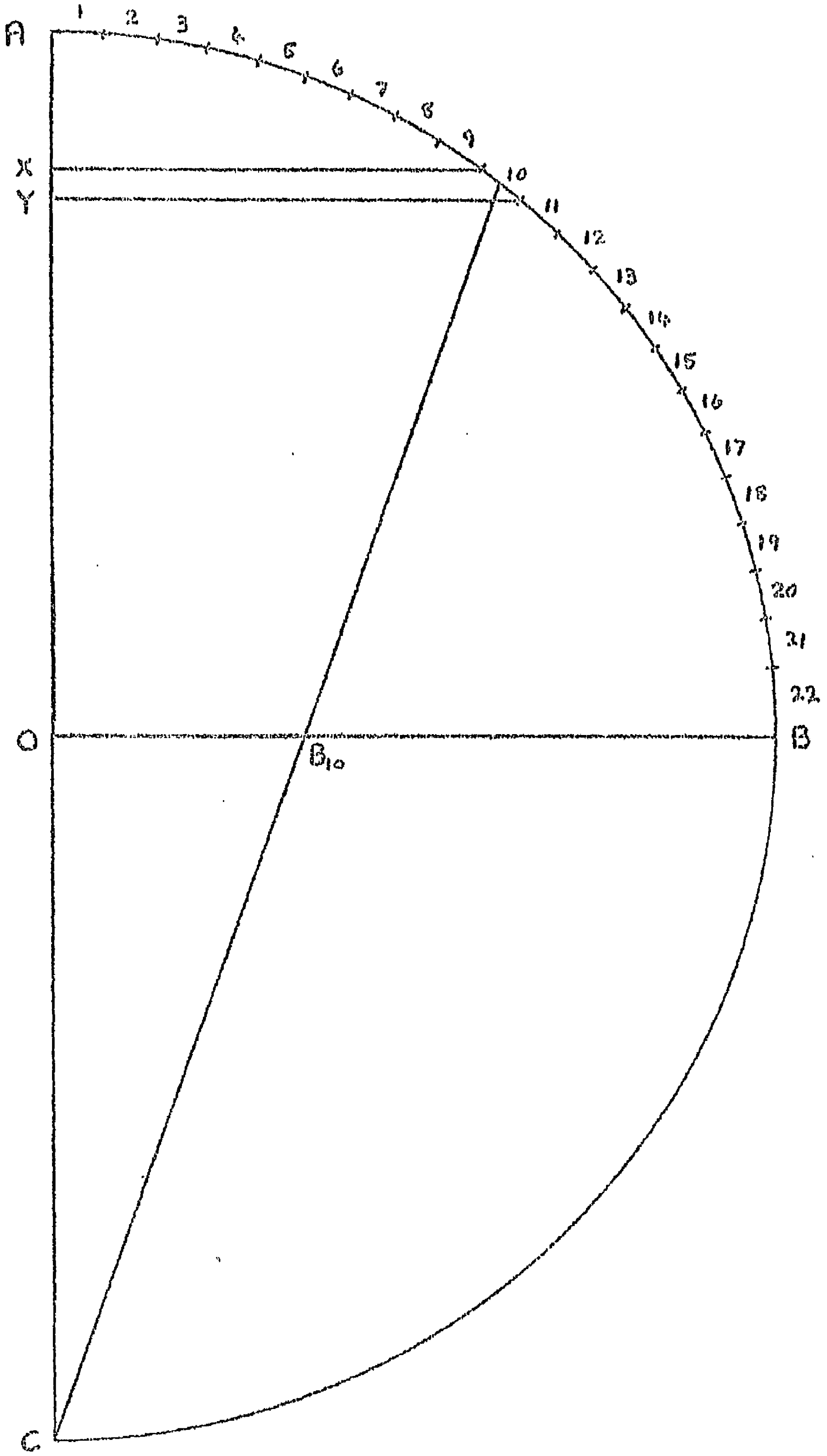

FIG. 4. GEOMETRY OF THE STEREOGRAPHIC CONSTRUCTION.

from a simple corollary to Archimedes' theorem. In turn XY is equal to OB (sin 36° - sin 40°), so the areas are respectively equal to:-

$$\frac{\pi}{2}OB^2\ (\sin 90^\circ - \sin 86^\circ),\ \frac{\pi}{2}OB^2\ (\sin 86^\circ - 82^\circ)\ ----\frac{\pi}{2}OB^2(\sin 6^\circ - \sin 0^\circ).$$

For simplicity $\frac{\pi}{2}OB^2$ is taken as 1000, to give the weights "w" in Table V below.

Table V - Graphical Integration from Fig. 3.

Area	Arc Length (ℓ)	Area (a)	Average ($A = a/\ell$)	Weight (w)
1	1.5	1.590	1.060	24
2	4.5	5.085	1.130	63
3	7.7	9.330	1.212	122
4	11.0	14.220	1.292	168
5	14.2	19.100	1.345	216
6	17.1	23.950	1.400	262
7	20.6	29.818	1.447	306
8	24.0	35.770	1.490	349
9	27.2	41.464	1.524	390
10	30.8	47.956	1.557	430
11	34.2	54.442	1.592	467
12	38.0	60.970	1.604	502
13	41.8	67.398	1.612	534
14	45.6	73.504	1.612	565
15	49.5	78.840	1.613	592
16	53.4	84.990	1.592	616
17	57.6	90.978	1.579	638
18	62.0	95.530	1.541	656
19	67.0	100.080	1.494	671
20	72.2	104.456	1.447	683
21	78.6	109.422	1.392	691
22	84.4	111.240	1.318	1045
Σ =	885.1	1316.753		9990

$$A_1 = \frac{\Sigma a}{\Sigma \ell} = \underline{1.4}$$

$$A_2 = \frac{\Sigma wa}{\Sigma w} = \underline{1.49}$$

The first average A_1, was calculated using the arc length as the weight, but the more accurate figure A_2 was obtained using the area on the projecting sphere as the weight. If the average ratio (1.546 ± 0.001) from the previous section is accepted, the errors in A_1 and A_2 here are -3.75% and -3.1% respectively. The error in drawing the contours was assumed to be ~5% due to the small number of plotted points (about 100), between which several values often had to be interpolated by visual estimation, and also to the rather inaccurate method of plotting the stereographic projection itself. A further error about 2%, in drawing the sections, must be added giving a total ~7%. It was expected that the errors in plotting would practically cancel out, due to the equal probability of positive or negative errors, but there remains an error ~3% which indicates a systematic error in plotting the contours. By using a more accurate stereographic projection, a larger number of reference planes and a larger number of sections this error could probably be reduced.

This method checked the previous figure, well within the expected accuracy. It is seen, however, that this method is no less tedious than the previous one, and the personal error is very much larger, so this method will not be used further. In the case of the F.C.C. and B.C.C. systems the first method will be shown to yield a limit for the average ratio for a much smaller number of planes, than for the simple cubic system so the second method is even less desirable in those cases.

[illegible]

[illegible]

D. The F.C.C. System:-

For this system equation 10 is used, and $\gamma_{(111)}$ was taken as the reference, giving the surface energy ratio as below:-

$$R_{(hkl)} = \frac{\gamma_{(hkl)}}{\gamma_{(111)}} = \frac{2h+k}{\sqrt{h^2+k^2+l^2}} \qquad \text{..........14.}$$

A series of values of R were calculated as in those shown in Table III, giving the partial and total averages as defined by equations 13 and 13a, in Table VI.

Table VI - Partial and Total Averages of the Surface Energy Ratio, F.C.C. System.

n	1	2	3	4	5	6	7	8	9	10
R'_n	-	1.2083	1.2083	1.2083	1.2085	1.2086	1.2085	1.2086	1.2083	1.2083
R_n	1.1397	1.1903	1.2022	1.2052	1.2069	1.2074	1.2078	1.2080	1.2081	1.2083

As is seen from Table VI a clear limit appears at n = 10 giving $R_\infty = 1.2083$ with an uncertainty possibly less than ± 0.0002. The partial averages at and above n = 2 are practically constant giving a much clearer limit than in the simple cubic system.

Figure 5 shows a stereographic contour figure for this system, constructed as before. The figure is much more complex than that for the simple cubic system, with a marked minimum at (111), surrounded by maxima of the {210} family at $R_{(210)} = 1.291$ which take the form of rather flat-topped "hills", giving each quadrant a degree of hexagonal symmetry round its respective member of the {111} family. "Saddle" inflections are seen at {100} planes with a ratio of 1.155, and at {110} planes with a ratio of 1.225.

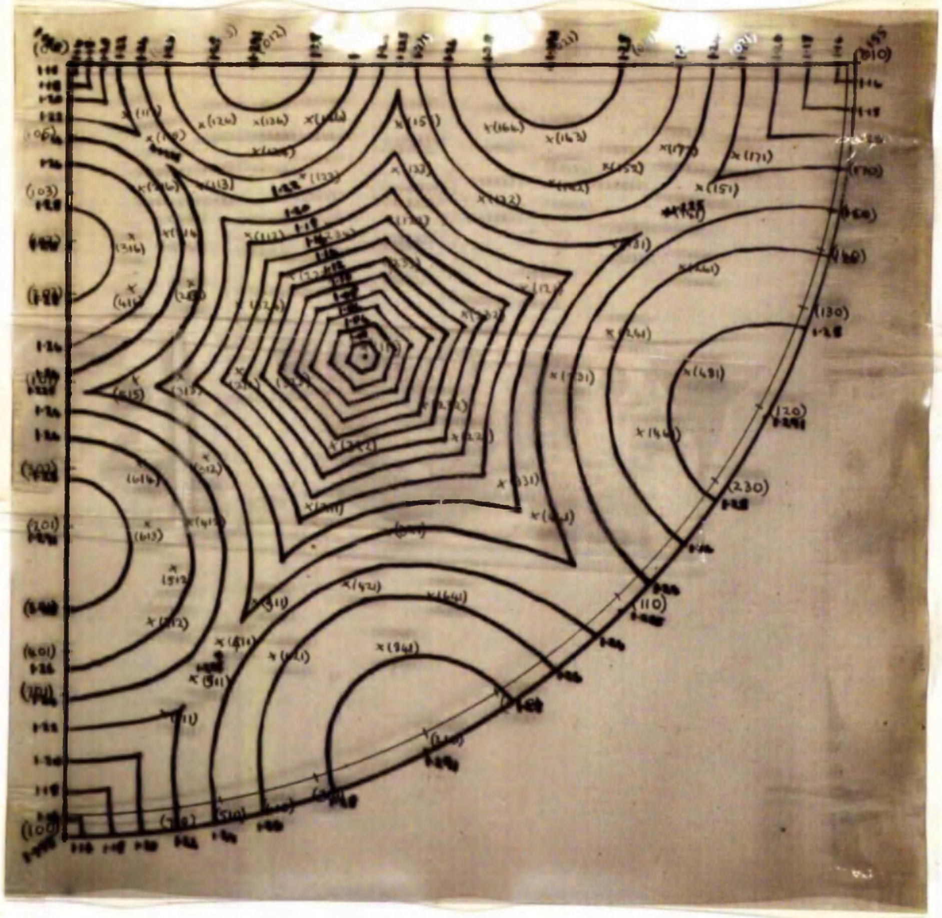

Fig.5 Surface energy contour figure, F.C.C. system.

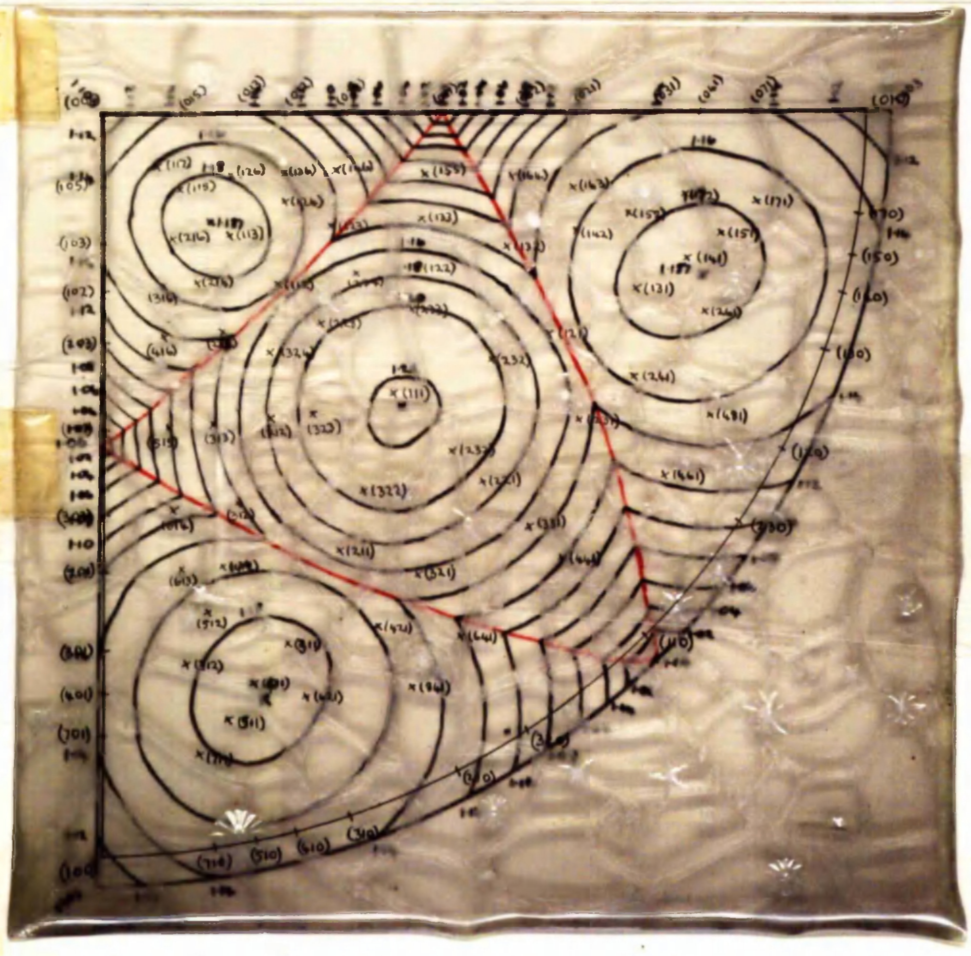

Fig.6 Surface energy contour figure, B.C.C. system (α Fe.)

E. The B.C.C. System:-

This system introduces a complication not found in the previous two systems. As is seen from equation 11, two different bond energies must be considered, derived respectively from nearest neighbour (ϵ_1) and next nearest neighbour (ϵ_2) interactions. Only in this system, of those considered, does the next nearest neighbour interaction produce a significant contribution to the surface free energy.

It is inconvenient to use ϵ_1 and ϵ_2 separately, so we may put $\frac{\epsilon_1}{\epsilon_2} = x$ and chose values for this bond strength ratio, thus eliminating either ϵ_1 or ϵ_2 for any value of x chosen.

In this case $\gamma_{(110)}$ was chosen as the reference. Putting $\epsilon_1 = x\epsilon_2$ in equation 11 where $h \geqslant (k+\ell)$;

$$\gamma_{(hk\ell)} = \frac{2[(2x+1)h + k + \ell]\epsilon_2}{\sqrt{h^2+k^2+\ell^2}\ .\ d^2}$$

$$\text{thus,} \quad \gamma_{(110)} = \frac{2\sqrt{2}\,(x+1)\,\epsilon_2}{d^2}$$

Using this value and equations 11 the following are derived:-

$$\left.\begin{aligned} R_{(hk\ell)} &= \frac{(2x+1)h + k + \ell}{\sqrt{2(h^2+k^2+\ell^2)}\ .(x+1)} & \qquad h > (k+\ell) \\ R_{(hk\ell)} &= \frac{2h}{\sqrt{2(h^2+k^2+\ell^2)}} & \qquad h = (k+\ell) \\ R_{(hk\ell)} &= \frac{h+k+\ell}{\sqrt{2(h^2+k^2+\ell^2)}} & \qquad h < (k+\ell) \end{aligned}\right\} \quad \text{..........15.}$$

From these equations it is seen that the ratio is independent of x except when $h > (k+\ell)$.

For a suitable value of x, αFe was chosen, for which Friedel et al[37] give $\frac{\epsilon_1}{\epsilon_2} = \frac{0.99}{0.78}$ i.e. $x = 1.269$; and for estimating the effect

of this bond energy ratio, x was also taken as 1.300. Two series of calculations were made with these values of x. The results are shown in Table VII. In this case the subscript n is replaced by α and β, ($x = 1.269$) and ($x = 1.300$); other notations are as before.

In the first case with $x = 1.269$ the partial average quickly approaches a value in the region of 1.1543 except for the irregular value at $n = 6$, so that the average ratio may be taken as 1.1544 ± 0.0003 for αFe.

The last line of the Table shows the ratio of the total averages for different values of x. This quickly settles down to 1.0005, so beyond $n = 6$, R_β, the total average for $x = 1.300$ were estimated from R_α using this figure; the estimated values appearing in brackets in the Table.

From these figures it is seen that the larger the value of x, the larger is the average ratio. Also the ratio of these averages for the two values of x chosen remains constant with $n > 2$. Lastly, and most important, a change in the bond energy ratio (x) of 2.44%, produces a change in the average surface energy ratio of only 0.045%, so that the value of the bond energy ratio is not very important in determining the average surface energy ratio.

The stereographic contour figure for αFe (Fig.6) shows a well defined maximum ratio of 1.225 at (111). Three secondary maxima of 1.187 at {411} also appear, together with the three minima expected at the {110} family. The planes inside the area marked by the red lines are independent of x (see equations 15) while those outside this area

Table VII - Partial and Total Averages for the B.C.C. System.

	$n =$	1	2	3	4	5	6	7	8	9	10
$x = 1.269$	R'_α	-	1.1530	1.1539	1.1543	1.1541	1.1600	1.1542	1.1541	1.1543	1.1543
	R_α	1.0930	1.1372	1.1482	1.1512	1.1527	1.1551	1.1547	1.1545	1.1544	1.1544
$x = 1.300$	R'_β	-	1.1533	1.1545	1.1548	1.1547	1.1605	-	-	-	-
	R_β	1.0939	1.1376	1.1488	1.1518	1.1518	1.1557	(1.1553)	(1.1550)	(1.1550)	(1.1549)
	$\frac{R_\beta}{R_\alpha}$	1.0009	1.00035	1.0005	1.0005	1.0005	1.0005	-	-	-	-

change with x, an increase in x producing an increase in the surface energy ratios. From inspection of the two sets of values, for a given increase in x the increase in the ratio for any plane (outside the invariant area) varies approximately with the distance of the projection of that plane from the nearest red line i.e. from the boundary of the invariant area. In other words with a change in x the stereographic contour figure (Fig.6) does not change in the area bonded in red, but the contours outside this region shift by an amount depending on their distance from the invariant region. The largest change is produced in the {100} planes which show values of 1.103 and 1.107 for x = 1.269 and 1.300 respectively.

The results for the three systems are summarised in Table VIII.

Table VIII - Total Average Surface Energy Ratios (R_∞) for the Cubic Systems.

	Simple Cubic	F.C.C.	B.C.C. (α Fe)
R_∞	1.546 ± 0.001	1.2083 ± 0.0002	1.1543 ± 0.0003
Reference plane	(100)	(111)	(110)

[illegible]

[illegible]

F. The Tamman Temperature and the Effect of Temperature on the Average Surface Energy Ratio:-

Significant changes may take place in a crystalline material well below its melting point, as is evidenced by recrystallisation and sintering, of which the latter is probably the more delicate test of these changes, and the more widely explored.

It is well known that the rate of sintering depends on the surface free energy (see Roberts[39] for a brief review), although a large amount of practical work has been concerned with the effects of deliberate impurities (such as accelerators and mineralisers) and atmosphere, both of which may be expected to lower the surface energy in many cases, and the reason for any increase in the rate of sintering may have to be ascribed to other reasons than any consequent lowering of free energy. For example the importance of small amounts of FeO in magnesite to aid dead burning is well known. FeO and MgO form a continuous series of solid solutions so the presence of liquid is not likely. The work of Taylor[40] suggests that such additions may affect the self diffusion of an oxide. The author's calculations of the surface free energies of MgO and FeO (Chap.III here) would indicate that FeO lowers the surface energy of MgO to some extent. Again the use of CaF_2 as a mineraliser for Al_2O_3 may be due to the volatility of AlF_3; and the effect of gases, particularly water vapour, on many oxides, indicates that chemical reaction, as opposed to lowering of surface energy due to adsorption, may greatly affect the ease of sinter

Results for experiments on pure oxides in inert atmospheres

are desirable but scarce. Sintering experiments lay great stress on the need for fine grinding and pressing; the former would tend to introduce or increase the proportion of high energy faces, and it is suggested that a limit to the grinding effect would be when the particles are as nearly spherical as possible. The finer the particles the larger their surface energy due to factors already considered in the introduction, but this effect is not large. Stressing pretreatment would tend to introduce or increase strain energy contributions to the surface energy, which will be considered in the following section.

Ideally then experiments should be carried out on pure, stress free material which exhibits only one type of face, or known proportions of known faces. The difficulty in obtaining material, with only one type of face present, is extreme, and the experimental determination of the types and proportions of faces present in a given material is almost insuperably difficult. The different proportions of faces present in different batches may be one reason for the lack of conformity in experimental results.

The lowest temperature, at which sintering occurs, was first investigated in detail by Tamman[41]. He stirred finely ground material, with a slow rise in temperature; the stirrer stopped, when reaction began, at a temperature which bears his name, and the ratio of this temperature to the melting temperature is described as the Tamman ratio. Volmer[42] gives rough figures for this ratio, viz. metal powders ~0.3 - 0.4, salts and oxides ~0.5, silicates ~0.8 - 0.9. Al_2O_3 was

stated to have a low ratio, about 0.26, but this is probably due to inversion of γAl_2O_3 at about 900°C and Taylor[40] stresses the effect of inversion in promoting sintering. Hutchins and Roberts[43] gave the ratio for Al_2O_3 about 0.6 and also a low value for ZnO, about 0.39. Allison et al[46] for pre-sintered, high purity MgO found a Tamman temperature about 1200°C, giving a ratio about 0.48. Clark et al[45] gave figures from which the following ratios derive:-

MgO = 0.65 CaO = 0.53 Al_2O_3= 0.55 - 0.58 Fe_2O_3= 0.70.

From these few figures, it is seen that quite different values, even for the same oxide, have been obtained by different workers (e.g. MgO = 0.48 - 0.65). It seems general, however, that the ratio is in the region of 0.5 - 0.6 for most pure oxides, with the exception of SiO_2 (see author's experiments on sintering) and silicates. This gives the temperature at which self-diffusion, be it surface or volume, begins to occur at a measurable rate. Accordingly in the region of the Tamman temperature meta-stable structures will begin to tend to pass to more stable structures: recrystallisation may then occur, and the surface energy of a solid begins to tend to a minimum.

Recrystallisation will require nucleation as well as growth. Working from the basis of kinks on a Kossel-Stranski repeatable step, Burton and Cabrera[46] worked out a critical temperature (designated T_α here), below which nucleation is required for growth and activated diffusion may be necessary. This temperature varies with the face under consideration. For example, for a typical alkali halide with

a simple cubic structure, they found T_{BC} as below:-

$$(100) = 1000^{\circ}C \qquad (110) = 400^{\circ}C \qquad (111) = -30^{\circ}C$$

These results lead to interesting deductions. If the melting point is taken in the region of 1000°C, it is seen that the ratio $\frac{T_{BC}}{T_m}$ for (110) is 0.54, that is within the range of the Tamman ratio discussed above: while for the (111) face the ratio is 0.18. Since growth on a (100) face may surely occur below the melting point, T_m is probably better taken above 1000°C, so these ratios should be lower. Although the ratio for the (111) face is lower than experimental values, it is an attractive postulate that the Tamman ratio varies from face to face in any crystal, and decreases as the surface free energy at 0°K increases. It will be remembered (section B above) that the surface free energies for this system at 0°K are in the ratio:-

$$(100) : (110) : (111) = 1 : \sqrt{2} : \sqrt{3}.$$

This idea does not seem to have been suggested previously. Similar conditions may be expected to obtain for other systems. It may well be that the Tamman ratio is a much more specific property than has been realised, requiring definition not only of the chemical composition, but the crystallographic face and perhaps even its condition with respect to adsorption and strain.

High energy faces may tend to change, with the production of lower energy faces, at comparatively low temperatures, although the rate may be slow and any face should have a temperature below which it is relatively stable. From the definition of the surface energy ratios (equations 12, 14 & 15), only the Miller indices are involved

(with the exception noted below), so that as long as a face exists its surface energy ratio is invariant: temperature only affects the factors ϵ and d. The exception is in the B.C.C. system, when $h > (k + \ell)$, and the factor x may change with temperature; but x is not likely to change much, and it has been shown that small changes in x have an almost negligible effect on the surface energy ratio. Hence below the Tamman temperature for the face with the highest surface free energy, the average surface energy ratio does not change significantly with temperature in the three systems considered. Other systems may show anisotropy of thermal expansion so that the geometrical factor, and hence the surface energy ratio will change with temperature.

Above the Tamman temperature for the face with the highest surface free energy the surface energy ratio should tend to decrease towards unity (only faces of the reference planes left). As this tendency is obviously dependent on the difference between the actual ratio and unity, the rate of decrease of the ratio will fall off with increasing time, and hence the ratio will change exponentially with time, being assymptotic to unity. We may express this as below:-

$$R_T = 1 + b\,e^{-ct} \quad \ldots\ldots\ldots\ldots 16.$$

Where R_T is the average surface energy ratio at $T^{\circ}K$ ($T_m > T > T_T$), e is the base of the natural logarithms, t is the time, b and c are constant for a given material and temperature. Just below the Tamman temperature (T_T) the rate of change of R is infinitely slow,

and at the melting point (T_m) the rate of change of R may be assumed to be infinitely fast. At any intermediate temperature the initial rate of change of R will then have an intermediate value, depending on the temperature. As a first approximation it may be assumed that the initial rate of change of R varies uniformly with the temperature as below:-

$$\left(\frac{dR}{dt}\right)_{t=o} = - k \left(\frac{T - T}{T_m - T}\right) \quad \ldots\ldots\ldots\ldots.17.$$

Where k is a constant in $(\text{time})^{-1}$. At $t = 0$, $R_o = (1 + b) \therefore b = (R - 1)$ (from 16) and on differentiating 16:-

$$\frac{dR}{dt} = -bc \quad \therefore c = - \left(\frac{dR}{dt}\right) \div b = - \frac{k\,(T - T_T)}{(R_o - 1)(T_m - T)} \quad \text{(from 17)}$$

Substituting:-

$$R_T = 1 + (R_o - 1)\ \exp\left[- \frac{k(T - T_T)\ t}{(R_o - 1)(T_m - T)}\right] \ldots\ldots18.$$

R_o is of course the initial value of R at $t = o$, and the constant value below T_T.

In equation 18 both T and t are variable so it would be useful to consider the effect with a constant heating rate from T_T to T_m. Such an integration was attempted several different ways, but additional assumptions were found to be necessary, and led to results of doubtful validity. As the temperature increases the rate of change of R at first increases; then at higher temperatures it falls off as R becomes nearer to unity. Due to the slow rate of change of R just above T_T, the actual value of T_T does not have to be very accurately known: change in T_T of the order of say 1-2% would be negligible in the R/T curve.

The constant k only applies to one allotromorphic particle as it changes isothermally towards an idoomorphic form. For more general application a diffusion constant (D - $cm^2 sec^{-1}$), and the size of the particle (r - cm), may be included such that:-

$$k = \frac{D}{r^2} k' \text{ ....19.}$$

where k' is a dimensionless number in the nature of a geometrical probability term, perhaps applicable to only one crystal system. Equation 19 is in conformity with a general description of rate processes given by Jonder[47] for solid state reactions. Unfortunately D itself is a function of temperature (Barrer[48] pp. 273 & 367) which is usually written:-

$$D = D_o e^{-\frac{E}{RT}} \text{ ....20.}$$

Where E is the activation energy. Combining equations 18, 19 & 20:-

$$R_T = 1 + (R_o - 1) \exp \left[- \frac{D_o e^{-\frac{E}{RT}} k' (T - T_T)\ t}{r^2 (R_o - 1)(T_m - T)} \right] \text{.....21.}$$

In this equation the value of k' is not very important: it will be in the region $1\text{-}5 \times 10^{-1}$, say 0.25 (see Cottrell[49]), and it does not vary much from substance to substance.

A search of literature failed to yield any values for the self diffusion of solid oxides. The diffusion of CaO in liquid slag has been measured by Towers, Paris and Chipman[50], giving $D \sim 10^{-7}$ at about 1400°C, but this value can hardly apply to pure solid CaO. However the activation energy was very large (70 ± 20 Kcal/mole) suggesting that E in the solid will also be high. The diffusion of ionic substances is a compound of the diffusion of at least two ions, which may

[illegible]

……

[illegible]

……

[illegible]

[illegible]

[illegible]

have widely differing mobilities: the rate of diffusion will then be governed chiefly by the rate of diffusion of the least mobile ion. Barrer[48] quotes several examples of large differences between the ions of a compound; the only divalent anion quoted, Se'', has an activation energy in the region of twice that for the halogen ions, for which latter D is in the region of 10^{-9} $cm^2 sec^{-1}$ a few degrees below the respective melting point, as shown by the work of Laurent and Bernard[51]. The diffusion of O'' seems to be favoured (e.g. Bengtson and Jagitsch[52]) as the governing factor in the diffusion of oxides, so that their diffusion coefficients are likely to be less than 10^{-10} $cm^2 sec^{-1}$ even in the region of their melting points. A value of D in keeping with the above considerations, was chosen as 10^{-7} $cm^2 sec^{-1}$, with the activation energy ~ 30 Kcal/mole.

Although the activation energies for sintering processes are not quite the same as for diffusion, they should be similar, so the values in Table IX are shown, taken from Clark, Cannon and White[45].

Table IX - Activation Energies for Sintering Processes[45] (Kcal/mole)

Fe O	α Al_2O_3	MgO	CaO	MgO + liquid phase	Cu
65	87	43	73	42	22

It is seen that the figure for CaO is close to that quoted above for CaO in slag[50], also the two values for MgO and (MgO + liquid) are very close. The activation energy for self diffusion of Cu is given by Barrer[48] as 57.2 Kcals/mole, but this figure is for bulk diffusion which is a more energetic process than surface diffusion, which latter is probably the chief agency in the present consideration,

so the figures in Table IX are possibly of the correct order. Purposely low values of E, viz. 20, 30 and 40, Kcals/mole, were chosen.

With the above values, values for $R_o = 1.5$, $T_r = 1000^{\circ}K$ and $T_m = 2000^{\circ}K$ were chosen to illustrate equation 21.

With an activation energy of 30 Kcal/mole and a diameter of 100μ, figure 7 shows the effect of holding at various temperatures; a logarithmic time scale is used for convenience. It may be noted that heating at 1750° K for 2 hours or more is necessary to produce a significant change in R_r, whereas at 1250° C, 2 days or more are required.

With E = 30 Kcal/mole and T = 1750° K, figure 8 shows the large effect of varying the particle size between 10μ and 1000μ. The same change in the 100μ particle heated for a day, is accomplished in the 10μ particle in under an hour. The large effect is due to r appearing as a power in the exponential term. Variation in D_o has a similar effect but change by a factor of 100 is necessary to be equivalent to change in r by a factor of 10. This figure shows that it is more profitable to sinter superfine material (< 10μ) at a fairly high temperature (1750° K), than fine material (c.100μ) at a higher temperature (1900° K), as is well known in practice.

A still larger effect is produced by variation of the activation energy, as is seen in figure 9 where T = 1750° K and r = 100μ; change in E by a factor of 2 is about as effective as a change in r by a factor of 10. Thus the activation energy for self diffusion is the most important factor, due to its appearance in

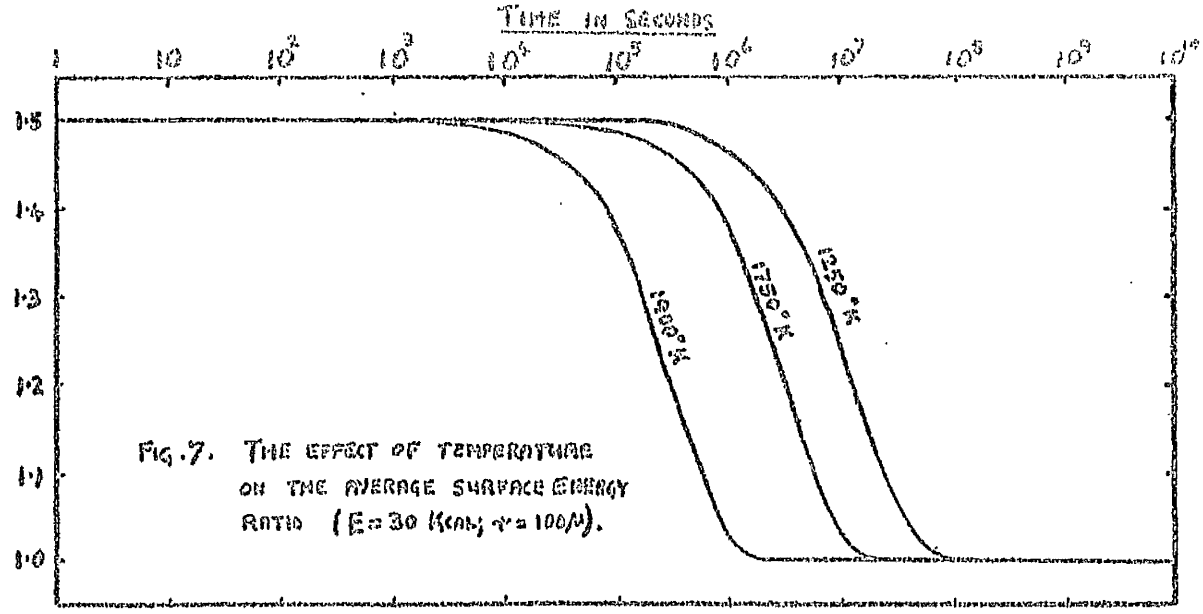

Fig. 7. The effect of temperature on the average surface energy ratio (E = 30 Kcal; r = 100μ).

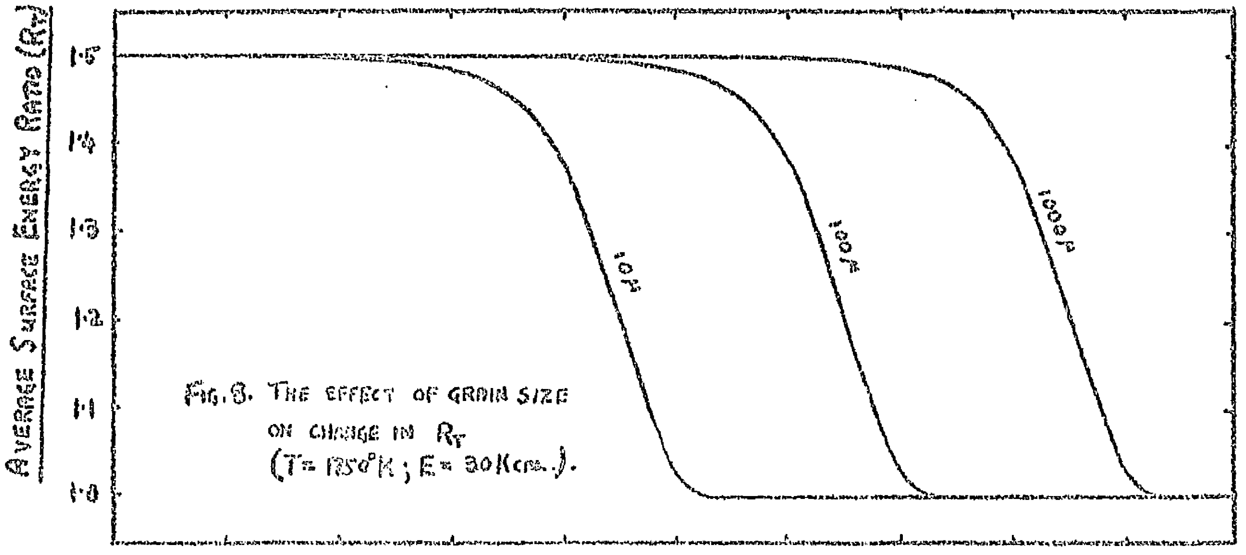

Fig. 8. The effect of grain size on change in R_T ($T = 1750°K$; $E = 30$ Kcal.).

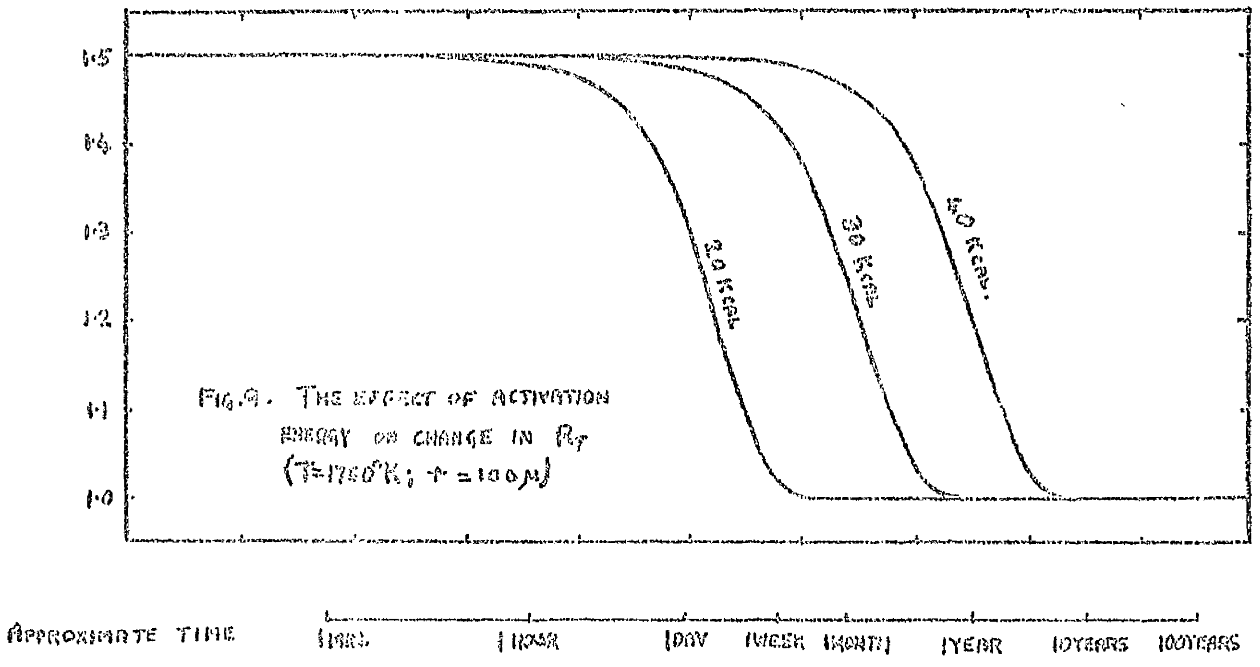

Fig. 9. The effect of activation energy on change in R_T ($T = 1750°K$; $r = 100μ$)

equation 21 in the form of a double exponential.

It may have been noticed that R_T as defined really applies to isolated planes, and cannot yet be applied to a real crystal. In this discussion recrystallisation is intended to mean change in shape towards an ideomorphic form without change in volume: this will be accompanied by a change in total surface area. R is defined specific to area, so we now have to define Γ as a surface energy ratio per unit volume (or per unit original area)($\Gamma_o \equiv R_o$). A term representing the proportional change in area with time and temperature must be applied. At equilibrium at some temperature only just below T_m, each particle will have an equilibrium shape which obtains when the total surface free energy is at a minimum (e.g. Wulff[53]) such as a cube in the simple cubic system. Let A_E be the surface area per unit volume of this equilibrium form, and A_o be the original area per unit volume then this factor is:- $\Delta A = \dfrac{A_E}{A_o}$ ....22.

As defined Γ = area ratio x surface energy ratio, this at equilibrium when $R = 1$, $\Gamma_E = \Delta A$, and this gies a different assymptotic value, viz. ΔA instead of unity. Thus the equation below was derived in an exactly analogous manner to equation 21:-

$$\Gamma_T = \Delta A + (R_o - \Delta A) \exp\left[- \frac{D_o e^{-\frac{E}{RT}} k' (T - T_T) t}{r^2 (R_o - \Delta A)(T_m - T)}\right] \text{........23.}$$

Finally the reversible temperature effect must be considered. The specific surface free energy decreases with temperature, due to the entropy term $(- \frac{d\gamma}{dT})$, which is assumed as before to be linear, for a first approximation:- $\gamma_T = \gamma_o(1 - \frac{T}{T_c})$ ....24.

From the definitions of γ, R and Γ we may combine equations 23 and 24:-

$$\gamma_T = \gamma_{Ref}\left(1 - \frac{T}{T_c}\right)\left\{\Delta A + (R_0 - \Delta A)\exp\left[-\frac{D_0 e^{-\frac{E}{RT}} k'(T - T_r)\, t}{r^2(R_0 - \Delta A)(T_m - T)}\right]\right\} \ldots 25.$$

where is the specific surface free energy (per unit area) for any crystalline material after time t at temperature T.

Equation 25 yields the specific free energy change in passing from an allotromorphic to an ideomorphic (equilibrium) form. For this to occur spontaneously γ_T must decrease, and for this condition it is easily seen that ΔA must be less than R_0. To illustrate this point let us consider the F.C.C. system. The lowest energy plane is (111), so let us see the effect of choosing an octahedron of {111} faces, with the original form being a sphere. From geometry ΔA = (area of octahedron) ÷ (area of sphere of same volume) = $\left(\frac{3\sqrt{6}}{\pi}\right)^{\frac{1}{3}} = 1.327$. R_0 for this system is 1.208 ($= R_\infty$) So a sphere will not spontaneously transform to an octahedron (as $\Delta A \nless R_0$). From basic considerations, at unit original (spherical) area the total surface free energy of the sphere $= R_\infty \times \gamma_{(111)} \times 1 = 1.208\ \gamma_{(111)}$, and for the octahedron of the same volume $= 1.327\ \gamma_{(111)}$: since the latter is higher, the previous conclusion about spontaneity will obtain.

Some simple area ratios are shown in Table X.

Table X - Area Ratios for Solids of Equal Volume.

Cube/Sphere = 1.2407
Duodecahedron/Sphere = 1.1053
Octahedron/Sphere = 1.3274

For the simple cubic system with the {100} faces of lowest energy the cube is an obvious ideomorphic form: for the B.C.C. system,

{110} planes are lowest, so a duodecahedron is possible; whilst an octahedron is possible for the F.C.C. system. From Tables VIII and X, it is seen that a sphere of simple cubic material will tend to a cube, the B.C.C. sphere will tend to a duodecahedron, but an F.C.C. sphere will not tend to change to an octahedron. This process of elimination of possible ideomorphic forms is collateral with Wulff's[53] hypothesis as expanded from Curie[54], that the equilibrium form of a crystal has faces such that their perpendicular distances from the centre of the crystal are in direct proportion to their surface energies: applied to the simple cubic system with the {100} faces at unit distance, the {110} faces will be at $\sqrt{2}$ units (i.e. cube edges) and the {111} faces will be at $\sqrt{3}$ units (i.e. the corners), the latter two families will have no effective area and the equilibrium form for this system is a perfect cube.

If the Tamman temperature varies from face to face, as was suggested above, (from Burton and Cabrera[46]), the gradual elimination of high energy faces at a particular temperature, below T_r for lower energy faces, will mean that T_r in those equations will change with time to higher values, approaching the value for the reference plane. Thus, not only recrystallisation but any sintering process will tend to a limit between the initial and reference plane Tamman temperatures, which limit varies with the temperature. Then the term $(T - T_r)$ in these equations will not be constant with time, and in an isothermal process, $(T - T_r)$ will tend to zero with increasing time, and R_r will tend to a limit between R_0 and unity, or Γ_r will tend to a limit between

Γ_o and ΔA. This will mean that the equilibrium form at $T_1 < T < T_m$ is not attained: for example in the simple cubic system, a sphere may tend to a form somewhere between a sphere and a cube, with the highest energy planes eliminated. A simple treatment of this idea, to incorporate into the above equations, does not readily suggest itself. However this process does offer a phenomenological explanation to the fact that, in isothermal sintering of a compact, a limiting porosity is often found, which limit tends to decrease to zero with increasing temperature of sintering. One such example is shown in Figure 10, for MgO, from Clark, Cannon and White[45], who also give similar figures for CaO, Fe_2O_3, Cu and Dolomite. To explain this change of limiting porosity with temperature, writers often show a variation of activation energies with temperature (e.g. Clark et al[45], Landon et al[55]), or perhaps variation of activation energy with degree of sintering (e.g. Duwez & Jordan[56]). These variations are quite probable, but possibly the above interpretation of the phenomenon is more graphic.

Figures given for the activation energies of sintering processes show considerable variation, as is exemplified (from Clark et al[45]) by calcined Dolomite, where it decreases with increasing temperature from 157 Kcal/mole to 43 Kcal/mole. In the case of oxides, with the possible exception of MgO, the activation energies for self diffusion are probably larger than 50 Kcal/mole, and possibly twice this value (see Table IX). D_o for Cu is in the region of 10 cm^2/sec (Barrer[48]) and D_o for oxides may be much larger than the figure adopted

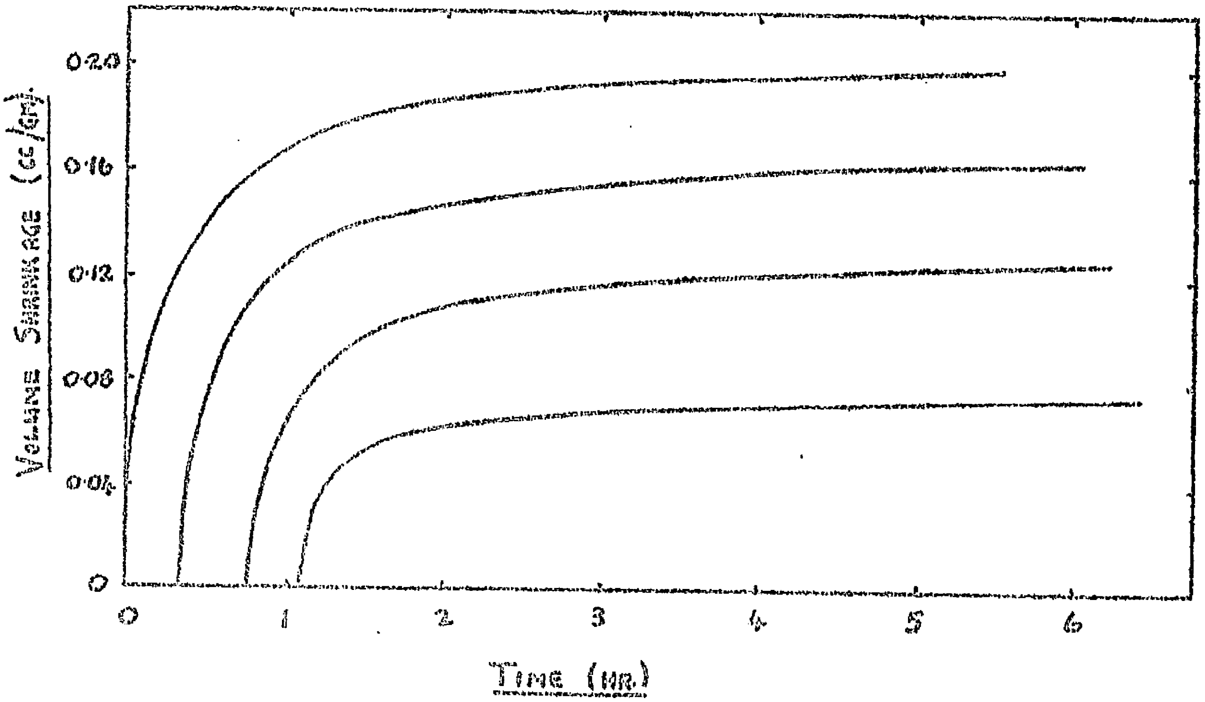

Fig. 10. Volume shrinkage against time at various temperatures for MgO compacts, initial porosity 0.26 cc/gm.; Clark, Cannon and White[65].

above for discussion of equation 21 viz. 10^{-7} cm^2/sec, but given an activation energy much higher than 40 Kcal/mole (the highest value discussed in Fig.9), the unavoidable conclusion is that very little change in R occurs except for long periods near the melting point, even for particles $<10\mu$ diameter. It would be extremely interesting to have figures for the self diffusion of MgO as a test case. In the case of metals, where the self-diffusion is apparently much greater, R may change perceptibly at lower relative temperatures (say $0.75T_m$) for very small particles ($c.10\mu$), and it may be possible to observe polygonisation in some favourable cases. Navias[57] found α Al_2O_3 spheres (m.pt. 2040°C) of about 1 mm. dia ($= 1000\mu$) developed a "loss of roundness" above 2020°C, but no effect was noticed below this temperature. It is extremely doubtful if his spheres were single crystals; probably also the method of manufacture left considerable strain energy, which would put the true temperature for beginning of observable polygonisation higher than 2020°C for stress free material. With the possible exception of MgO, it would seem that there is no significant change in R over normal periods of time (c.1 day) for isolated oxide crystals larger than 10μ, below about $0.9T_m$.

The above equations were constructed to show the interrelation amongst the various factors concerned with recrystallisation and their effect on the total surface free energy. Their form has developed partly from experimental work, chiefly in the field of sintering, whose equations it is not intended to supplant. Two factors are responsible for sintering, both derived from the lowering of the

total surface free energy, these are the lowering of the specific surface free energy by recrystallisation and the simple decrease in total surface area. Clark and White[58], Mackenzie and Shuttleworth[59], Kuczynski[60] and others (see e.g. Roberts[39], Allison and Murray[61]) have, correctly in the author's opinion, chiefly concentrated on the area change; but they take little or no account of the variation of the surface free energy with temperature and with the shape of the particles. With particles mutually in contact, as in sintering, the factor ΔA in equation 23 may become extremely small in a manner which may not yield to simple formulation, so such equations as 23 may be of little use in this field. However, it would be desirable to take account of a possible decrease in the average surface free energy in formulation of rate equations for sintering of metallic, and superfine material. Also a more precise definition of the surface energy terms in literature, along the lines suggested above, would seem desirable.

C. The Mechanism of Recrystallisation:-

The question as to whether recrystallisation is brought about by volume diffusion, surface diffusion or otherwise has been amply discussed in papers (e.g. Kuczynski[60]) on sintering, and this subject, which is still very controversial, need not be reproduced here. The chief difference between the mechanisms of diffusion, will be that surface diffusion will have a lower activation energy than volume diffusion. However, it is of interest to consider the stages in recrystallisation.

Considering the stereographic contour figures (Figs.2, 5 and 6), it is tempting to read into them a kinetic significance. If we take any given face and heat it above its Tamman temperature, it might be expected to change its orientation continuously until it reaches an energy minimum. For example in the simple cubic system (Fig.2) a (332) face might change gradually through the series — (221)--(331)--(441)----(110) and then towards either the (010) or the (100) plane through the appropriate series round the circumference of the figure. Such a view cannot be upheld atomistically, unless we could have a single isolated plane. A truer picture may be obtained from a consideration of Kossel-Stranski crystal units. In the simple cubic system, these units are small cubes of indeterminate size but having a real existence at any face other than a perfect one of the {100} family, which, of course, constitute the six faces of each minute cube. Any face may be built up of these units, as in Figure 11A, from Stranski[62]. Depending on the mode of formation of the crystal (from

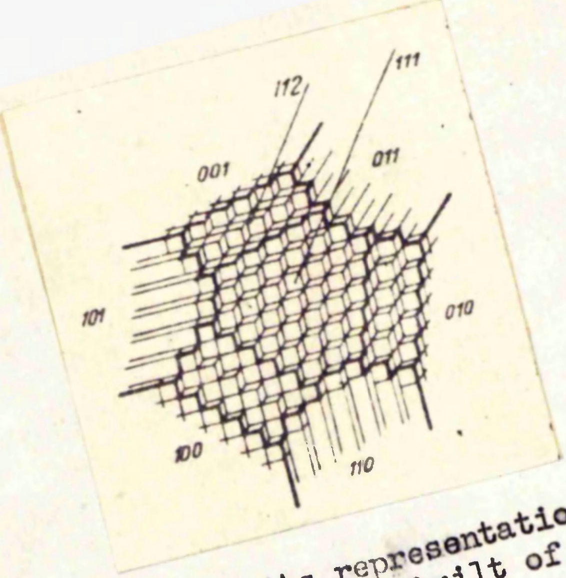

Fig. 11A. Stranski's representation[62] of faces of a simple cubic crystal built of crystal units with $\{1,0,0\}$ faces.

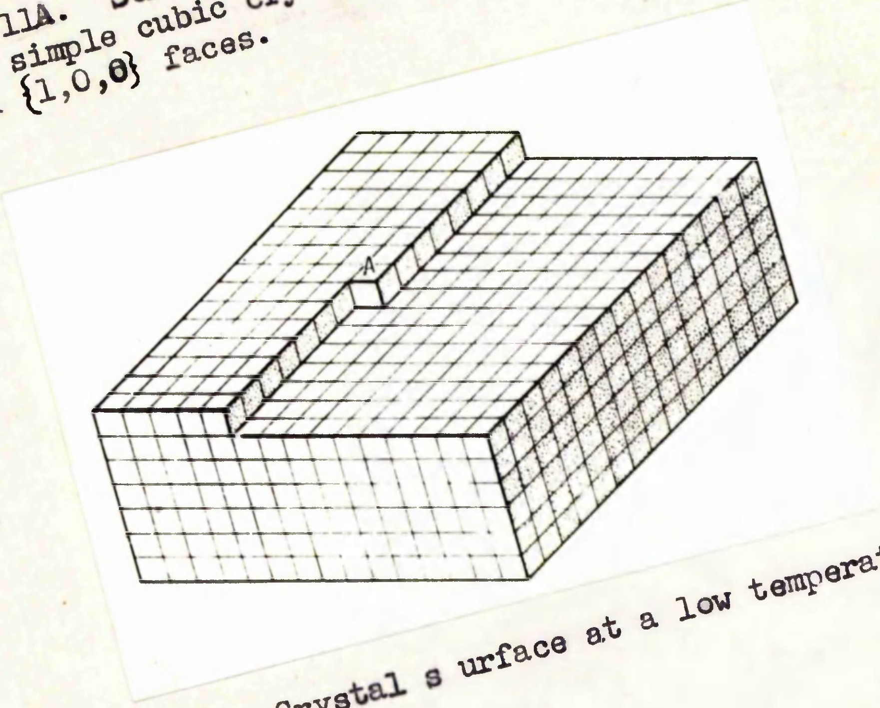

Fig. 11B. Crystal surface at a low temperature, after Verma[64].

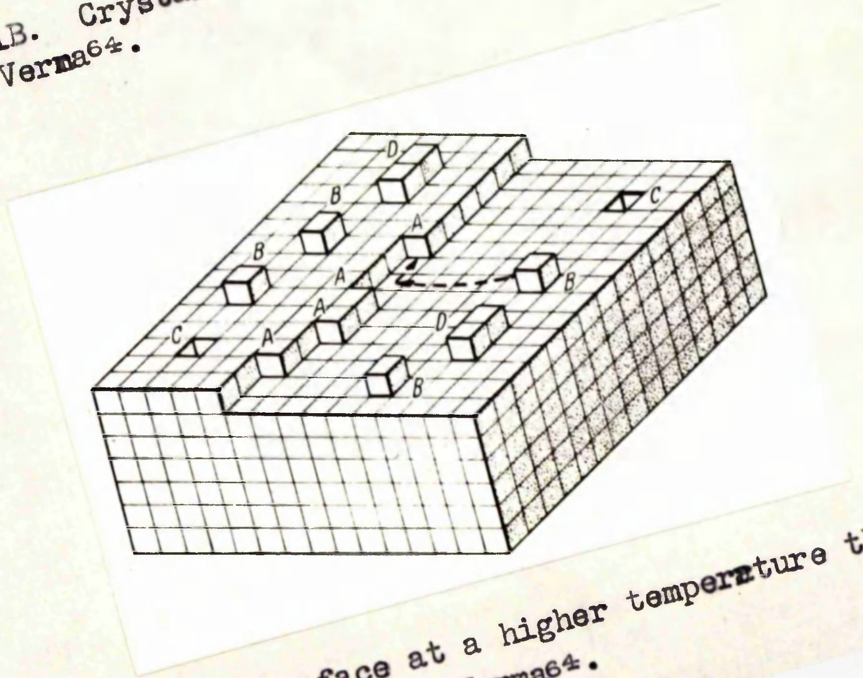

Fig. 11C. Surface at a higher temperature than in Figure 11B, after Verma[64].

solution or melt, by cleavage etc.) it may or may not show such a structure, but a high index face (any other than $\{100\}$) even if it were perfect, might tend to develop such a structure given the opportunity, that is, if there is sufficient diffusion. For lack of a better term we may call these faces "kinked", in preference to the term "stepped", which latter term may be applied to a kinked $\{h k 0\}$ face (e.g. (101) in Fig.11A). If we consider an octahedron of a simple cubic crystal composed of $\{111\}$ faces, a simple calculation shows that if it were composed of minutely kinked faces of the $\{100\}$ variety, or of perfect,planar $\{111\}$ faces, there would be no difference in the total surface free energy, provided that the kinks were extremely small compared to the crystal. Similarly a duodecahedron of $\{110\}$ faces, has no difference in total surface free energy with kinked or planar faces. These are the closest packed faces in the simple cubic system, so it may be expected that any other face would show no such difference whether it were kinked or perfect, as the density of kinks would be lower. If each kink were composed of minute $\{100\}$ faces, which were assumed to be similar in all respects, other than size, to the gross $\{100\}$ faces, there would be no change in heating them, until T_T for the $\{100\}$ faces was attained, that is, fairly near T_m. This is contrary to experiment, so the kinks must be affected by their very small size (of the order of a few unit cells), interaction between neighbouring kink faces perhaps producing a lower surface free energy and allowing diffusion to occur at about $0.5\ T_m$, if the kinks are to have a real existence. Recrystallisation might

be considered in terms of diffusion of these crystals units, but such large particles (composed of tens of atoms) would have a very high activation energy compared with individual atoms or molecules. A truer picture would be obtained by considering atoms or molecules diffusing to form more or less transitory kinks or crystal units; the function of the kink then being to act as a nucleus for, or a source of, diffusing particles, which was indeed their original purpose.

If a surface diffusion mechanism is accepted, we may consider the allotromorphic crystal changing shape on heating, by atoms/molecules diffusing about, being at a higher concentration on a low energy face than on a high energy face, due to the greater facility with which they become attached to kinks on the high energy face. As the mobile particles are removed by attachment, they will be replaced, in an attempt to preserve an equilibrium concentration, by material from kinks on the low energy face. Particles are most easily rendered mobile by thermal excitation where they are least strongly attached to the lattice, that is at the corners of kinks and at the corners between gross faces. The next most favourable position for mobilisation will be at edges. Consequently there will be a high concentration of mobile particles in these regions (corners and edges), resulting in a flow of material from them to high energy faces, as the concentration gradient of mobile particles is greatest in this direction. Corners and edges of low energy planes will then tend to degenerate with the production of vicinal faces, during growth of high energy faces. The high energy faces can only grow perpendicularly

away from the centre of the crystal, with their area decreasing towards zero. Then the next highest energy faces grow likewise, with eventual reduction in area of the vicinal faces, until more or less perfect faces of the lowest surface free energy are the only ones left.

II. The Effects of Some Departures from Perfection:

1. The effects of adsorption on the surface free energy have been briefly discussed in Chap. I. Surface non-stoichiometry may also be included in this class. A compound may adsorp atoms of an element which is already an integral part of the compound: this tendency will be governed by the change in surface free energy in an exactly analogous manner to chemisorption. Bulk non-stoichiometry and impurity, on the other hand, will possibly raise the surface free energy due to the induced strain in the lattice.

These chemical effects will also change the recrystallisation characteristics, by an amount which is also governed by their ease of removal at any temperature. Thus van der Waal's adsorption would be expected to have little effect at high temperatures (above say 400°K or less) whereas bulk impurity would probably be difficult to remove by heat alone. Chemical change on the surface and in the bulk will affect the diffusion characteristics, possibly lowering the activation energy to a value which makes a process such as sintering commercially feasible.

The effects of non-stoichiometry are sometimes difficult to evaluate experimentally. Hutchins and Roberts[43], worked with ZnO and showed that p_{O_2} could have opposite effects on sintering, depending on the source and pre-treatment of the sample. Murray, Rodgers and Williams[63] found better sintering with $UO_{2.13}$ than with UO_2. The strain in the lattice associated with non-stoichiometry might be expected to facilitate diffusion, especially when the slowest ion (O'') is chiefly affected. Thus excess oxygen (or Schottky disorders)

may be expected to speed diffusion, by providing a higher concentration of mobile O'' : but if oxygen were deficient there might not be a larger number of vacant anion sites, due to a greater possibility that the cation will occupy an interstitial position (Frenkel disorder) than will the large O''. These considerations favour a greater ease of sintering with excess/oxygen oxides (e.g. $UO_{2.13}$) than with stoichiometric oxides, but the behaviour of oxygen deficient oxides is not so easily forecast. It seems that an increasing number of non-stoichiometric oxides are being found (e.g. $UO_{1.75}$ – $UO_{2.33}$, $MoO_{1.97}$ – $MoO_{2.08}$, oxides of Ti, V and W etc.) which may exhibit excess or deficiency of oxygen: further study of these oxides in sintering would be very interesting. The oxides quoted above are probably meta-stable forms, but some (e.g. $Fe_{0.95}O$) seem quite stable and reproducibly non-stoichiometric; in such a case the surface free energy will probably be lower than for a similar stoichiometric oxide (see Chap. III for a discussion on Wüstite). The departures from stoichiometry are generally only a few percent; if such departures caused an increase in surface free energy, their concentration (of Schottky or Frenkel disorders) at the surface would be lower than in the bulk (Gibbs' adsorption equation 4) so that the increase in surface free energy would be small. On the contrary, if non-stoichiometry lowered γ similar reasoning shows that the lowering could be considerable. The sign of the change in the surface energy will depend on the relative magnitudes of the strain effect and of the adsorption effect.

2. In addition to the above chemical departures from perfection,

we must consider the effects of some physical departures from perfection. Real crystals depend for their growth, to a very large extent, on imperfections such as steps and dislocations (e.g. Verma[64]), and when growth is halted these growth features may be observed "frozen in". Thus real crystals have close packed faces containing steps and terraces, which may be considered as vicinal faces of small angular departure from the low index faces. In the simple cubic system, these vicinal faces on a {100} face will have a slightly higher surface free energy than $\gamma_{(100)}$ (see Fig.2); on a {111} face, slightly lower surface free energy than $\gamma_{(111)}$ will result; the {110} faces may be considered unchanged due to equal probability of the occurrence of vicinal faces of higher or lower energy. Thus the total or average surface free energies do not seem to be significantly changed at low temperatures, whether or not these stepped vicinal faces exist. The largest effect would obtain with only the lowest or with only the highest energy faces present in a crystal.

From photographs (e.g. Verma[64], p.97) steps may be seen to be in the region of 1,000 per cm (700 - 1500 cm^{-1}). If we consider their height to be in the region of 10 Å (viz. about 2 unit cells) the increase in area over a plane face of 1 cm^2 is seen to be 10^{-4} cm^2 and this amount is quite inconsiderable in its effect on the total surface free energy.

These steps tend to conform to one of the principal directions (e.g. [01]), and at low temperatures they tend to be straight with a few kinks (as at A, in Fig.11B). At higher temperatures, due to thermal

excitation, molecules (or crystal units) tend to break away from their original positions, as in Fig.12D, especially from kinks in the steps, which tend to increase in number (A in Fig.11C): some molecules remain adsorped as single (B) or compound (D) islands. Some holes (C) also result from molecules jumping out. At sintering temperatures (0.5 to 0.8 T) it may be shown (Verma[64] p.13) that there is, on the average, one kink for every four molecules on the step; thus the total surface energy will be increased by about 1/4 of the above figure, which may also be ignored. The adsorped molecules and holes probably give a contribution of the same order as do the kinks, so that the total contribution by steps, kinks, adsorped (indigenous) molecules and holes is in the region of 0.02% increase in $\gamma_{(100)}$.

Dislocations may give rise to terraces, such as those considered above, also with negligible effect on the free surface energy, but the centres of dislocations may have an effect in themselves. This is illustrated by the fact that screw dislocations may quite easily be etched preferentially to the rest of the surface (Horn[65]) showing them to have a higher energy. The free energy associated with a screw dislocation may be calculated as below from Cotrell[66] (p.38):-

$$\text{Energy/cm} = \frac{\mu b^2}{4\pi}\left[\ln\left(\frac{r_1}{r_0}\right) - 1\right] \quad \ldots\ldots\ldots.26.$$

where μ is the theoretical shear strength, b is the displacement of one face relative to the other, r_1 is the radius of the outside of the dislocation, r_0 the radius of a "hole" in the centre (as the stresses there are infinitely large). The energy associated with an edge

dislocation being about 50% larger. For a metal such as Cu, Cottrell[66] calculates a figure for a screw dislocation about 5×10^{-4} erg/cm. For ionic materials, μ will probably be lower than for Cu, say $\sim 10^{10}$ dyne/cm^2 (this is a rather large figure, as μ for Cu is only 4×10^{11} dynes/cm^2, and experimental shear strengths for materials like marble[67] is only in the region $(1 \text{ to } 3) \times 10^7$ dynes/cm^2. Taking $r_1 = 1000$Å, $r_0 = b = 2.5$Å, the energy associated with a screw dislocation is 2.4×10^{-6} erg/cm, and with an edge dislocation $\sim 3.6 \times 10^{-6}$ erg/cm, giving an average for either $\sim 3 \times 10^{-6}$ erg/cm. The distance between atomic layers is 1.5Å, so that the fraction of this energy which contributes to surface free energy is about 4.5×10^{-14} ergs. Cottrell[66] (p.102) also states that the maximum density of dislocations in a soft crystal is $\sim 10^8$ cm^{-2} so that the contribution of dislocations to the surface free energy is about 4.5×10^{-6} erg/cm^2 for ionic crystals; for Cu it is $\sim 7.5 \times 10^{-4}$ erg/cm^2. The magnitude of these figures needs no further comment.

Mosaic crystals may adequately be represented by arrays of dislocations such as above. If they are considered to give an equal contribution (viz. $\sim 5 \times 10^{-6}$ ergs (cm^2) in a material with $\gamma \approx 1000$ ergs/cm^2, the effect of dislocations and mosaic crystals together amount to less than 0.0001% increase in surface free energy. Any further increase in this small figure, due to interaction between dislocations, will possibly be quite negligible, though no method seems to have been suggested for calculating the magnitude of this interaction.

The contribution due to kinks, steps and adsorped molecules will increase, as their number increases, with temperature, and at

temperatures near T_m this may amount to a few ergs/cm^2 (i.e. of the order of 0.1% γ). However the energy required to form dislocations is too large for their number to be materially increased by ambient temperature fluctuations.

Grain boundaries are another departure from perfection which invites consideration. When a grain boundary intercepts the surface its effect lies in the strained areas on either side of it, and this strain will increase the surface free energy. The strain will depend on the relative orientation of the grains, and the orientation of the boundary to the surface. When the angular distortion between the grains is small ($\sim 5^\circ$) the boundary can adequately be described as an array of dislocations (Cotrell[66]). The strain energy will depend on the number of dislocations per unit area of the boundary which will, in turn depend on the difference in orientation between the grains. For angles in the region of 45°, a description in terms of dislocations is not quite accurate, as there is some boundary material which cannot be ascribed to a dislocation. When the angle is in the region of 90°, for cubic systems, the distortion is again small. Suppose every molecule in a boundary were part of a dislocation; this would give about 3×10^{-6} erg/cm (see above) for a boundary 1 molecule wide, or 1.5×10^{-5} erg/cm for an extreme case with the boundary five molecules wide, to take account of the orientation of the boundary to the surface. A very fine grained metal may show 120 grains per linear inch at x100, so that each grain is 2.15×10^{-4} cm side: if the grains are considered to be square, the boundary per grain is 3×10^{-4} cm. In such a case the

contribution to the surface free energy by the boundaries is:-

$$\frac{1.5 \times 10^{-5} \times 4.3 \times 10^{-4}}{(2.15)^2 \times 10^{-8}} = 0.14 \text{ erg/cm}^2$$

This is the largest effect so far considered in this section. The figure is for an extreme case and is less than $0.01\%\gamma$ with $\gamma = 1000$ erg/cm^2. From similar considerations, a three grain boundary, involving 75 ($\doteqdot \pi \times 5^2$) molecules in the surface; with $\frac{4}{3}$ triple points per grain, the contribution would be $\sim 9.7 \times 10^{-5}$ erg/cm^2. Quadruple points, with one per grain would give a figure of 6.5×10^{-5} erg/cm^2. So it seems that junctions of more than two grains do not contribute significantly to the total surface free energy.

The above physical effects are rather crudely calculated, but any refinements made will very probably lower their magnitude. The contribution by dislocations has been calculated as if all the excess energy in the surface molecules affected the surface free energy, whereas only a fraction ($\ngtr \frac{1}{2}$) will be effective in this manner, depending on the surface and interior coordinations. Also little attempt has been made to consider entropy, most of the figures apply to the region of absolute zero. For example the grain boundary interfacial face energy tends to zero at (or slightly above) the melting point (Mott[68]), so that any effects due to grain boundaries will quickly decrease with rise in temperature.

It is well known that a surface containing a grain boundary will change shape on heating to a high temperature, eventually to give an equilibrium dihedral angle (such as ψ in Fig.1c). The total free

energy decrease, brought about by this change, is compounded from a decrease in area of the grain boundary multiplied by γ_{ss} minus an increase in area of the solid/fluid interface multiplied by γ_{SF}, assuming γ_{SF} does not change significantly: for large dihedral angles the new curved faces will not differ much in orientation from the original plane surface so γ_{SF} will not change markedly. For oxides ψ has been found (Kingery[69]) to be in the region of 160° - 150° in air. The largest area increase will occur when the whole grain is curved, not just the edges at the boundary. It is easily shown geometrically that the ratio of areas is then approximately equal to

$$\frac{(180 - \psi)}{360} \cdot \frac{\pi}{\sin \psi/2}$$

and this gives the increase in area ($\psi = 160° - 150°$) as 0.5 to 1.2%, say 1.0%. This is a maximum effect, when the grains are small enough to be completely curved, which will only happen after a long period at a very high temperature, unless aided by solution or chemical attack. For metals, where the ratio of γ_{ss} to γ_{SF} is in the region of $\frac{1}{2}$ (Bondi[28] p.438), and ψ will be in the region of 120°, this area change will be in the region of 4.7%.

However little these above imperfections may influence the total surface free energy, they may be of the greatest importance in recrystallisation and sintering, by acting as sources and "sinks" for diffusing entities (atoms, molecules or holes) and thus greatly facilitate diffusion processes.

I. Applications to Polycrystalline Materials:

It must be stressed that all the calculations made above apply only to crystalline solids, and not directly to highly disordered solids such as glasses. Also the average factors strictly apply only to single crystals. Let us consider lead shot (Pb - F.C.C. system) for a first example in this section. In falling down the shot tower a liquid drop tends to sphere due to its surface tension. At the surface the structure of the liquid will be closely related to a solid {111} plane, as the atoms have ample freedom to move to such positions that the surface energy is minimal. Due to the fast cooling ample nucleation on the surface will occur, and it will very probably solidify such that a substantial part of the surface will consist of {111} planes of a large number of minute crystals. Then the solid shot will have a surface free energy only slightly greater than $\gamma_{(111)}$, and the surface energy ratio will be only very slightly greater than unity (c.f. $R_o = 1.208$ for a single crystal sphere). Any process which leads to preferred orientation will probably affect the average surface energy. Another such process is cold work, as is shown by the many examples in Barrett[70] (p.442 et seq.). F.C.C. metals when drawn into wires have either or both [111] and [100] poles parallel to the axis of the wire. Let us consider an aluminium wire with only [111] parallel to the axis. If a single crystal is considered with its axis along [111], its curved surface will exhibit only those planes in the zone with a [111] pole: this eliminates many other planes. By inspection, six of the {110} and six of the {211} families satisfy this condition.

Applying the Weiss zone law to the general plane $(hk\ell)$ we obtain for planes in the [111] zone:- $(h-k)=|\ell|$. With this limitation, we may apply the method as in part D of this chapter to calculate average factors as below:-

n	1	2	3	4	5	6	7	8	9	10
R_n	1.225	1.202	1.218	1.227	1.229	1.232	1.231	1.232	1.231	1.232

which show R_∞ about 1.232 ± 0.002. For a spherical F.C.C. crystal $R_\infty = 1.208$, so that such a wire, with complete orientation as above, is seen to have a higher specific surface energy for its curved surface than has a sphere. With less complete orientation, there will be a greater probability of the occurrence of lower energy planes in the surface, so that with decreasing orientation the average factor will decrease towards 1.208. Gold wires may exhibit equal proportions of crystals with [100] and [111] in the axis (Barrett[70] p.443). A similar average may be worked out as above for an F.C.C. crystal with [100] parallel to the axis: in this case the general plane is $(hk0)$, and the average factor works out to be 1.262 ± 0.002. Then for such a gold wire as above the average will be the mean viz. 1.247 ± 0.004.

B.C.C. metals have a simple [110] wire texture (Barrett[70] p.444). Two {110} planes are in this group, giving the general planes $(h\bar{h}\ell)$ and $(hk\bar{k})$ where h, k and ℓ are positive or negative but self consistent within the brackets. This analysis yields an average of 1.175 ± 0.002 which is again larger than for a sphere (viz. 1.154), using the figures for α Fe, as in part E of this chapter. These values are reproduced in Table XI.

Table XI - Average Surface Energy Ratios for Wires with Complete Orientation.

System	F.C.C.			B.C.C.(αFe)
Sphere Ratio	1.208			1.154
Example	Al	-	Au	αFe
Wire Axis	[111]	[100]	50% each	[110]
Wire Ratio	1.232	1.262	1.247	1.175

Quite a number of experimental figures for the surface energy of metals have been obtained, chiefly by Udin and coworkers[71], from the high temperature creep of thin wires. Their figures, together with an appropriate average from Table XI, and an appropriate equation (14 or 15), can yield values for any plane of the specific surface free energy.

The texture of a rolled plate also has preferred orientation (Barrett[70], p.457), but it is much more difficult to generalise such structures and apply analyses. Cold rolled αFe (Barrett et al[72]) generally has a [110] pole parallel to the rolling direction, and the (001) plane at any angle up to 45° or 55° from the rolling plane; it may also have {111} planes in the plane of the sheet. If a sheet only consisted of planes with [110] in the rolling direction, with equal probability of any planes 45° to the (001), the average factor would be the same as for the wire considered above (viz.1.175), but a preponderance of planes may exist nearer the (001) (for which $R_{(001)} = 1.103$), so that the factor would be rather less than 1.175, possibly ~1.14. Again a proportion of {111} planes exist on the surface ($R_{(111)} = 1.225$); if this proportion were 50% the ratio would be ~1.18: so it may be valid to estimate the surface energy factor on the rolled surface of cold rolled

[illegible]

[illegible]	[illegible]	[illegible]	[illegible]

[illegible]

[illegible]

αFe as 1.16 ± 0.025. For a surface perpendicular to the rolling direction, for αFe, {110} planes will preponderate (R = 1.000), with some planes in the zone with [111]; so that the average factor will be smaller in this case, possibly in the region 1.05 ± 0.05.

In general, polycrystalline materials will be largely randomly orientated, unless special methods (e.g. drawing or rolling) are used in their fabrication. We may consider a compact of randomly orientated grains, such as those common with ceramics. In cutting this compact to produce a flat surface there are equal probabilities for the production of any planes; so that here also we may use the factors developed from the spherical model, where there was a similar probability. However if the material, of which the compact was made, were flaky (e.g. graphite, mica, etc.) compacting may tend to orientate the flakes perpendicular to the direction of the applied pressure: such a case will be considered in Chap. IIIA, namely graphite. Some degree of orientation may also occur with acicular or fibrous material, such as asbestos, but no other material of interest to metallurgists suggests itself, so this class will not further be considered.

Allotriomorphic loose material, such as metal or ceramic powders, will not, in general consist of perfectly spherical particles. Cleavage is always easiest in certain directions and a material, which has been reduced in size, may tend to exhibit a preponderance of those faces which obtain from easiest cleavage: from a consideration of cohesion, these faces will be those of low surface free energy. Consequently crushed material, will have a surface energy ratio somewhere

between unity and the value for a perfect sphere, depending on the frequency of occurrence of various faces, and hence on the shape of the particles. Perhaps the best way of representing this variation is by consideration of shape factors, which are themselves averages for a large number of particles. Any shape factor $\left(\frac{d_1}{d_2}\right)$ involving the surface area of the material (e.g. d_1 the mean diameter obtained from specific surface measurement) and the average mass of each particle (e.g. d_2 obtained from numeration and weighing), will provide a useful guide to a value for the average surface energy ratio. With perfect spheres, the size factor will be unity, and the average surface energy ratio will be that for a sphere; smaller values of the ratio will result from larger values of the size factor, until the ratio is unity at a size factor obtained by simple geometry, when the particles consist only of the reference faces. The history of the material and its ability to be cleaved are the chief factors governing the size factor: material produced by crystallisation will have grains approximating to their ideomorphic forms (e.g. common salt), abraded material will tend to have particles of a spherical character (e.g. desert sand), and crushed material tends to be angular (e.g. crushed quartz) with a character intermediate to the ideomorphic and spherical forms. In abrasion the actual size of the particles may also affect their shape, large particles possibly having a greater tendency to a spherical form than smaller particles.

It is unfortunate that the great difficulty in constructing, for other systems, equations similar to 9, 10 and 11, precludes accurate

estimates for average surface energy of materials in systems more complex than the three cubic systems discussed. Rough estimates may be made (as in Chap.III) for some other systems. Due to the similarity between the F.C.C. and C.P. Hex systems, one might expect similar surface energy ratios, but the introduction of second nearest neighbour bonds will complicate the analogy.

J. Conclusions:

1. An average surface free energy ratio has been defined.
2. The average ratios for spherical, perfect crystals, near absolute zero, have been clcculated for the simple cubic, face-centred cubic and body-centred cubic systems, by two methods (Table VIII). Differences in relative bond strengths in the B.C.C. system have been shown to have little effect on the average ratio.
3. Figures showing the variation of specific surface free energy with orientation of a face, have been constructed (Figs.2,5 and 6).
4. From consideration of the Tamman temperature, sintering and diffusion, temperature has been shown to have little or no irreversible effect on the average ratio for refractory oxides (with the possible exception of MgO), except for very long times near the respective melting point. In addition to the reversible entropy $(\frac{d\gamma}{dT})$ effect, anisotropic materials may show a reversible change, due to anisotropy of thermal expansion, in the surface energy ratio.
5. The mechanism of recrystallisation has been considered for an isolated, allotromorphic crystal, and, briefly, for an aggregate of crystals with reference to sintering phenomena.
6. The following physical defects in crystals have been shown to have negligible effects on total surface free energy:-
    a. Vicinal growth faces, steps/with or without kinks on them (near T_m, <0.1%).
    b. Grain boundaries (c.0.01%).
    c. Dislocations and Mosaic crystals (c.0.001%).
7. Calculations have been made of the average ratio for some poly-crystalline materials with varying degrees of preferred orientation, and random orientation.

Chapter III - Calculations of Some Surface Free Energies.

A. Graphite.

The calculations below for graphite were the first ones attempted by the author in the series in this chapter, so it is reproduced first, although it is by no means the simplest of those calculations. Previous work is considered more fully in part B2 of this chapter.

1.The Structure of Graphite:

Graphite is not a rare substance, but there is a surprising absence of good, large crystals, judging from the paucity of reports on such material in literature. Also, due partly to the low atomic weight of carbon, X-ray diffraction presents some difficulty, and due to variation of lattice parameter with crystal size, the X-ray reflections are broadened. The position today regarding the structure of graphite is the same as it was when Arnold[73] said, "A final solution to this problem does not yet exist." A brief review is given below.

Debye and Scherrer[74] introduced the idea of a rhombohedral structure with a unit cell of three layers of hexagonally arranged carbon atoms, but this structure was not proved to exist for another 25 years. Meanwhile Bernal[75] demonstrated graphite to consist of hexagonally arranged atoms, in layers of two per unit hexagonal cell.

Experimental evidence[76 & 77] was found to indicate that the Bernal structure was not comprehensive, but proof of the existence of the Debye-Scherrer structure was finally found by Lipson and Stokes in an artificial graphite which consisted of 80% Bernal, 14% Debye-Scherrer structures with the remainder being turbostatic graphite, which consists of particles of only a few hexagons, similar to the old "amorphous" carbon. Additional evidence was furnished by Rooksby and Steward[79], who found 25% Debye-Scherrer structure in one specimen, whose origin was not given.

For the study in hand it is advantageous to consider both these structures as belonging to the hexagonal system, three unit rhombohedrons being incorporated in one hexagonal cell. Fig.12 A. and B, shows interpretations of the Bernal and Debye-Scherrer structures respectively; from 12B it may be seen how the hexagonal network of atoms is arranged in the first layer (layer A). There are three possible orientations of this network relative to the unit cell, as in layers A, B and C; the Bernal cell being chosen as layers ACA. Different stackings for each cell are possible (e.g. ACBA and BCB respectively) giving equivalent structures, and only affecting the positions of the x,y and z axes. Different stacking may lead to different Miller indices for any plane, accordingly the structures as in Fig.12 are rigidly adhered to below.

Each carbon atom has three equivalent bonds in the layer, termed σ bonds, and one π bond extending between the layers. The π bonds are shown only in the Debye-Scherrer structure (Fig.12B), extending perpendicularly in alternate directions for neighbouring atoms in a

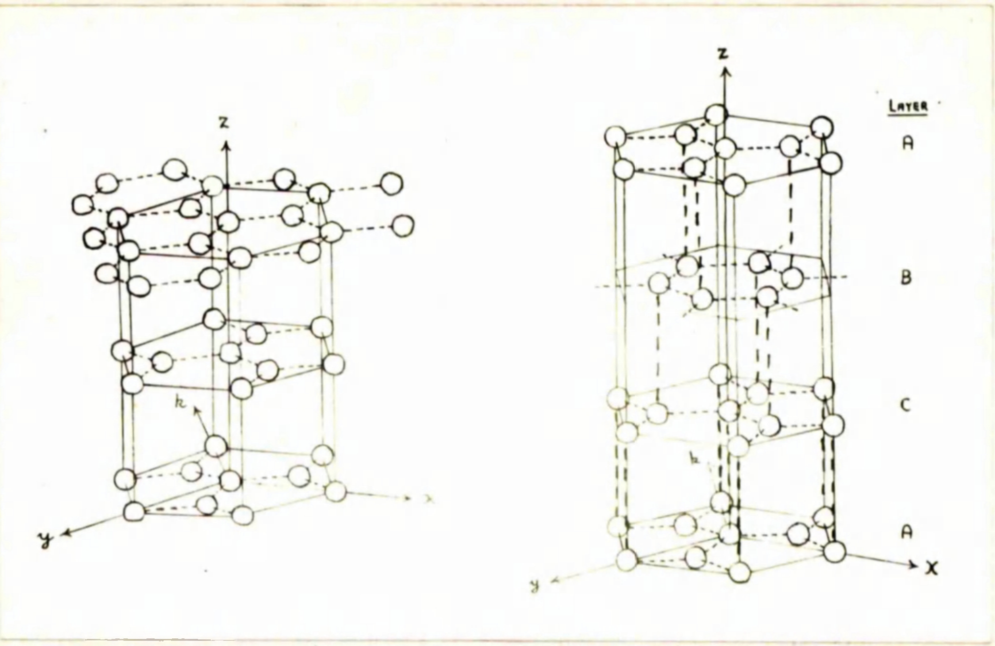

Bernal-structure Debye-Scherrer structure

Fig.12 Unit hexagonal cells of graphite.

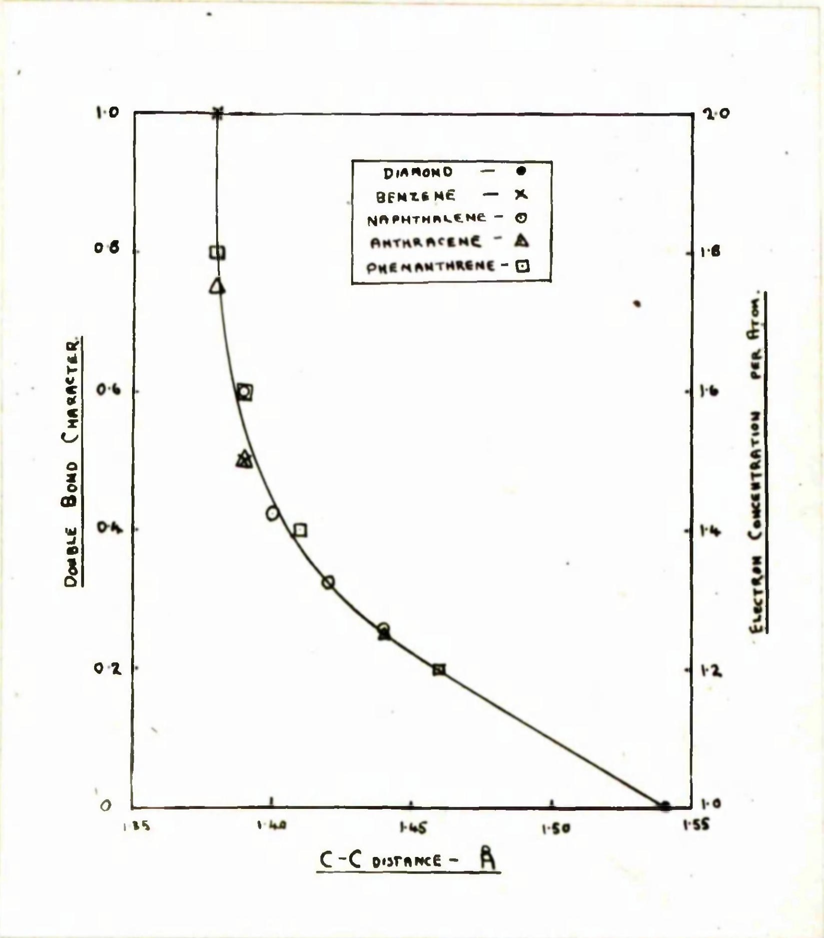

Fig.13 Double bond character and electron concentration versus the C-C interatomic distance.

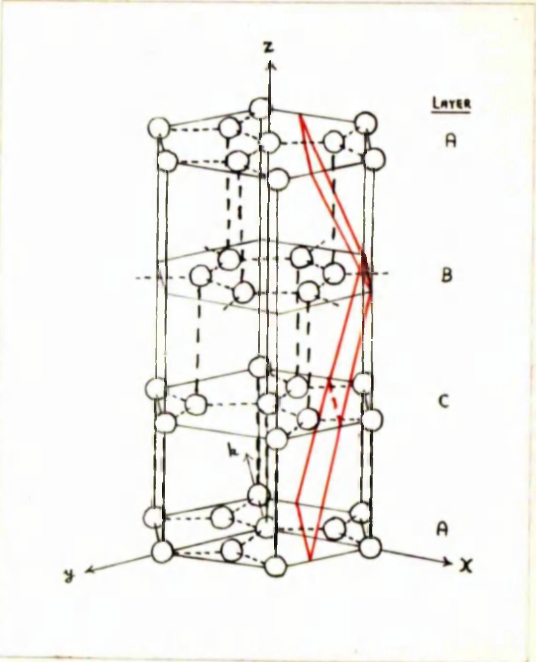

Fig.14 The character of $(3,\bar{3},0,0,)_{\text{MOD}}$.

layer. It will be seen that it is not possible to draw π bonds perpendicular to the layers in the Bernal structure, unless each alternate atom has two π bonds, one in each direction, the other atoms having none. Alternatively a Bernal crystal may be described as a huge resonating molecule, with each atom having a choice of three atoms in each neighbouring plane, with any one of which it may form a π bond. These interpretations are only pictorial, the π bonds being very diffuse: indeed a more accurate description would be obtained by considering the bonds to be in the nature of an electron cloud, as in metals; the number of free electrons per atom being in the region of 10^{-4} (Arnold[74]). However in the following calculations, π bonds are considered to exist, however non-localised they may be, and the planes chosen are such that there can be no confusion as to the number of π bonds they contain.

Before leaving this subject, it may be observed that there is a possibility that the two forms co-exist to some extent in any given "crystal". This idea was suggested by Arnfelt[80], not specifically as above, but he stressed the ease of slip parallel to the layer planes, and suggested somewhat "displaced lattices". There is an energy minimum on either side of the carbon atoms perpendicular to the layer plane, though from the ease of slip, the minimum cannot differ much energetically from any other point at a similar distance from the layer plane: these minima result in the three distinct relative orientations (layers A, B and C Fig.12). There seems to be no cogent energetic reason why the stacking should not be quite random, as long as two

similar layers are not neighbouring: the π bonds are very distended, and it seems very unlikely that a layer plane should exert any significant force on a second nearest layer plane, sufficient to cause a preferential orientation among the three possible. The two structures have the same 'c' parameter as far as can be determined, so from this there would seem to be no significant energy difference in the relative stacking of the layers. If a material consisted solely of one structure, grinding would cause slip, and it would seem inevitable that a proportion of the other structure, or a random stacked structure, would be generated, which would probably behave as a mixture of the two ideal structures. Unfortunately, by far the most of the work on graphite has been done on material which has been ground. It might be interesting to compare results with the same material re-ground and examined as before.

From the few results available (see above), the Debye-Scherrer structure is found to the extent of 10-20%; a figure of this order may be expected when it is remembered that the three Bernal forms (--ABAB---),(---ACAC---) and (--BCBC---)are quite equivalent, and therefore the Bernal form has at least three times the probability of occurrence as has the Debye-Scherrer form (giving the maximum percentage of Debye-Scherrer form as 25% - which value has been found only once, and none higher). If the probability of occurrence were also inversely proportional to the repeat number of layers, the total probability for occurrence of the Debye-Scherrer would lead to a value in the region of 17%. Some other factor may be responsible for the lower values

found in the region of 10%, if the values reported are indeed accurate; they are not easily obtained by the method of Lipson and Stokes[78], and it is the only one so far reported.

2. The Rotative Bond Strengths:

If it were assumed that all four bonds of the atom in graphite were identical, the bond strength would be half the sublimation energy. This latter quantity is even yet somewhat uncertain, different values have been given in practically every one of the many papers on the subject, ranging from $Q_s \sim 120$ to over 200 Kcal/mole (e.g. see Bichowski and Rossini[82]; though most of the values are in the region of 170 Kcal/mole (e.g. Kynch and Penney[83]), dozens of older results could be quoted over a wide range. The recent work of Glocker[84] seems to establish $Q_s = 170$ Kcal/mole. Apart from the experimental difficulties of working at such necessarily high temperatures (in the region of 4000°C) there has been trouble identifying the ground state in spectrographic work, and there is ample evidence that the vapour is a mixture of three chief forms C, C_2 and C_3: Glocker[84] found the relative quantities for these species to vary with the temperature, and gave sublimation energies for the production of each form:-

$$C,\ Q_{s1} = 170 \text{ Kcal/mole};\quad C_2,\ Q_{s2} = 210 \text{ Kcal/mole};\quad C_3, Q_{s3} = 190 \text{ Kcal/mole}$$

The polyatomic molecules are each capable of resonating among a number of different structures; each form having a resonance energy, estimation of which does not yet seem possible. If the resonance energies were known, they could be added to the respective Q_s, and the absolute bond energies for the π and σ bonds could be obtained. This resonance

energy is a possible reason for Q_{s3} being lower than Q_{s2}, as the triatomic molecule would have the greatest resonance energy. This point does not seem to have been raised previously, despite the great volume of literature on the subject.

It remains, then, to divide Q_s amongst the π and σ bonds by other methods.

Pauling[85] gave values of the "double bond character" for different carbon-carbon interatomic distances in various organic molecules and in the diamond. Fig 13 is drawn from these figures: the right-hand ordinate assumes an electron concentration of unity for a single bond and a linear increase to the double bond value of 2. The interatomic distance in the layer (1.421 A) is seen to be equivalent to 1.325 electrons per atom. Coulson[86] favours a value in the region of 1.54, though it is difficult to see the significance of a figure greater than $1\frac{1}{3}$, which assumes all the valency electrons to be in the layer (i.e. associated with the σ bonds), whereas Arnold[74] gives the electron concentration between the layers as 10. So it does not seem profitable to attempt a calculation of the relative bond strengths from electron densities.

Two other methods remain. Ruff[87] calculated the heat value for the π bonds in graphite oxide, and the heat value for all four bonds, giving a ratio of bond strengths $\left(\frac{\pi}{3\sigma+\pi}\right) = \frac{29.3}{211.3} = 0.1387$; otherwise, the σ bond is just more than twice as strong as the π bond. No account is taken of alteration of electron density and polarisation, by introducing the oxygen into the graphite lattice, nor is account

taken of probable distortion of equilibrium bond angles: both these factors would lead to a lower ratio of bond strengths so this ratio may be regarded as a maximum. Possibly a result derives from considering that only van der Waal's forces operate between the layer planes. Syrkin and Dyatkina[88] considered this force in graphite, for which a value of 2.25 ± 0.5 Kcal/mole is suggested. The energy remaining from the deduction of this figure may be divided equally amongst the three σ bonds. The results are shown below:-

Ruff's Method: Bond strength of $\pi = B_\pi = \frac{2 \times 170 \times 10^3 \times J}{N} (0.1387)$

$$= \underline{3.287 \times 10^{-12} \text{ erg/bond.}}$$

$$B_\sigma = \frac{2 \times 170 \times 10 \times J}{N} \left(\frac{1 - 0.1387}{3} \right)$$

$$= \underline{6.782 \times 10^{-12} \text{ erg/bond.}}$$

van der Waal's force: $B'_\pi = \frac{2.25 \times 10^3 \times J}{N}$ $\quad B'_\sigma = \frac{(2 \times 170 - 2.25) \times 10^3 \times}{3N}$

$$= \underline{1.564 \times 10^{-13} \text{ erg/bond.}} \qquad = \underline{7.822 \times 10^{-12} \text{ erg/bond.}}$$

3. The Surface Free Energy.

Lattice summations of the potential energy have been made by Girifalco and Lad[89], who also quote wave mechanical calculations of the surface free energy of graphite, but the Lennard-Jones potential does not seem to be strictly accurate, and choice of different wave functions leads to values of the free surface energy of the basal plane (0001) from 35 to 513.5 erg/cm^2; also, only values for the basal plane were obtained.

Ideally, a bond direction should only be associated with

ionic models; homopolar materials, like graphite, cannot have their bonds clearly defined in space, but only in terms of maximum overlapping of orbitals. However similar calculations to the one below have been carried out for metals (e.g. Friedel et al[37]) and the diamond (Harkins[90]), so this estimation would seem permissible, even although the π bond is very diffuse.

Since 2 cm^2 of surface are formed by rupture over 1 cm^2 cross-section, the surface free energy per bond is half the cohesive bond strength , denoted B above. The surface free energy per bond ($\Sigma = \frac{1}{2}B$) now needs to be multiplied by an appropriate bond density (ρ bonds/cm^2) for any given plane, to give the specific surface free energy. In general the plane with the lowest bond density has the lowest surface free energy, and it can quite readily be recognised by visual examination of a model or sketch of the unit cell, as can close packed planes, though they are not necessarily the same planes. If a crystal is broken up preferential cleavage will tend to occur along these planes with lowest surface free energy and with densest packing, and as all these planes may be listed from visual examination, any plane not listed has little chance of existence unless special methods (sawing etc) are used to obtain it. These other planes may be considered as vicinal planes composed of the listed planes and accordingly of intermediate surface free energies (see Chap.II). The bond densities were obtained by counting the bonds cut to give a certain plane through one unit cell, or in rare cases two neighbouring cells, giving a small integral which was divided by

the corresponding area of the plane, calculated geometrically from the lattice parameters. The lattice parameters were obtained from "Structure Reports"[91]. The distance between the atoms in a layer in large crystals is 1.4210Å, and the distance between the layers is given for the Bernal cell as 3.3540Å, and for the Debye-Scherrer cell as 3.3546Å; the difference is not significant, so the mean value 3.3543Å was used.

Each plane designated below may stand for a class of planes with the same surface free energy, as discussed in the previous chapter. Some planes (e.g.(0001))are identical in both Bernal and Debye-Scherrer forms, but the same indices may apply to different planes and the same plane may have different indices, in these forms; so the plane and the form both need to be specified. As a specimen calculation, the plane $(10\bar{1}2)$ in the Debye-Scherrer form, is considered below:-

$$\rho = (1.115 \times 10^{15}\,\sigma\,\text{bonds} + 1.115 \times 10^{15}\,\pi\,\text{bonds})\ \text{per cm}^2$$

Using van der Waal's force method:-

$$\Sigma_\sigma = 3.911 \times 10^{-12}\ \text{ergs/bond} \qquad \Sigma_\pi = 7.818 \times 10^{-14}\ \text{erg/bond}$$

$$\therefore \gamma^\circ_{(10\bar{1}2)} = (1.115 \times 3.911 \times 10^{3} + 1.115 \times 7.818 \times 10)\ \text{erg/cm}^2$$

$$= \underline{4438\ \text{erg/cm}^2}.$$

$\gamma^\circ_{(10\bar{1}2)}$ being the surface free energy of $(10\bar{1}2)$ near absolute zero, as before. Similar calculations were made for six other principal planes as listed in Table XII, to the nearest 5 erg/cm^2.

Table XII -
Surface Free Energy of Various Planes in Graphite, near 0°K. (erg/cm^2).

Form	Both			D-S$^+$ only			B$^+$ only
Plane	(0001)	$(2\bar{1}\bar{1}0)$	$(3\bar{3}00)$	$(3\bar{3}00)_M$	$(30\bar{3}3)$	$(10\bar{1}2)$	$(30\bar{3}2)$
Van der Waal's Method	149	5475	6320	4765	4635	4440	4555
Ruff's Method	3125	4735	5475	4770	4020	5610	4860

+ D-S - Debye-Scherrer form; B - Bernal form.

Apart from the basal plane (0001), the energies are little dependent on the value of the van der Waal's force, variation in which by 25% produces less than 0.5% in the surface free energy, in the third line of the table.

The plane $(3\bar{3}00)_M$ was investigated after some experimental work, to be discussed later, had suggested a low energy plane perpendicular to the layer planes (i.e. parallel to the z axis). It is an atomically kinked plane, formed by slight rearrangement of atoms in a $(3\bar{3}00)$ plane, such as could be obtained as marked in Fig. 14.

The only previous attempts on this problem found by the author are given by Girifalco and Lad[89], on which brief comment has already been passed. The best of these results were stated to lie in the range 130-165 erg/cm^2 for the (0001) plane, the former value being derived from data on heat of wetting. Thus the method used here with the van der Waal's force is in good agreement with those figures. However

evidence will be shown (in Chap. IV, C2) that $\gamma^{\circ}_{(0001)}$ cannot be less than about 1100 erg/cm^2, and so the above lower figures cannot be substantiated experimentally. Thus the only remaining theoretical figures derive from the more empirical calculation involving Ruff's method, and only these figures will be considered in the following work.

The planes may be divided into three classes as below:-

a. the basal plane, and those parallel to it.

b. planes perpendicular to (0001)

c. planes at an angle other than 90° or 0° to (0001)

The last class is not of immediate interest, but if we assume 25% of the Debye-Scherrer and 75% of the Bernal structures we obtain the following averages for class 'b' planes:-

$$= 5100 \text{ erg/cm}^2 \text{ (excluding } (3\bar{3}00)_M \text{)}$$

$$= 5020 \text{ erg/cm}^2 \text{ (including } (3\bar{3}00)_M \text{)}$$

4. The Temperature Coefficient:

As discussed previously the simplest method of obtaining the temperature coefficient of surface free energy is by use of the critical temperature. For graphite T_c is given as 7000°K by Basset[92], and this figure is regarded as adequate. Thus the following equation may be used for any plane:-

$$\gamma^{T} = \gamma^{\circ} - \frac{\gamma^{\circ}}{7000} T$$

An alternative theoretical attempt was made, to calculate this coefficient for solids, in particular graphite.

From equation 1, by analogy to usual thermodynamics the

following was suggested:-

$$\frac{d\gamma}{dT} = -\int_0^T \frac{\Delta C_s}{T}\,dT$$

Where C_s is the specific heat in ergs/cm^2/°C, thus $C_s = C'_p \times W \times J$ where C'_p is the surface excess specific heat in cals/gm, and W is the weight of atoms per cm^2 in the plane under consideration.

Now $W = \dfrac{W_0}{1 + \kappa T}$ where κ is the coefficient of superficial thermal expansion assuming it to be linear. Writing C'_p in the form:-

$$C'_p = \alpha + \beta T + \delta T^2 + \lambda T^3 + \text{-----}$$

we have:-

$$\frac{d\gamma}{dT} = -\int_0^T \frac{W_0 J\,(\alpha + \beta T + \delta T^2 + \lambda T^3 + \text{----})}{(1 + \kappa T)T}\,dT$$

By the Nernst heat theorem, at 0°K, $\dfrac{d\gamma}{dT} = 0$ so the constant term in the integration is zero.

$$\frac{d\gamma}{dT} = -W_0 J\left[\alpha\,\ln T + (\beta - \kappa\alpha)T + \frac{(\delta - \kappa\beta + \kappa^2\alpha)}{2}T^2 + \frac{(\lambda - \kappa\delta + \kappa^2\beta - \kappa^3\alpha)}{3}T^3 \text{----}\right. \quad\text{---- } 27.$$

κ is in the region of 0.000005 (twice the coefficient of linear expansion). Assuming $C'_p = k C_p$ where C_p is the bulk specific heat and that k is a temperature invariant constant, we may as a first approximation put:-

$$C'_p = k(7.638 + 3.906 \times 10^{-4} T - 4.302 \times 10^{-7} T^2 + 2.957 \times 10^{-10} T^3 + \text{---})$$

with values for C_p from Internat. Crit. Tables (Vol.V,P.94).

W_0 is readily obtained from the geometry of (0001) and the weight of the hydrogen atom (1.67×10^{-24} gm). Taking $T = 300^{\circ}$K and calculating as far as the T^3 term $\dfrac{d\gamma}{dT} = -3.1$ erg/cm^2/°C.

A rough approximation for k can be obtained from the work of Melford and Hoar[93], who found, for Pb and Sn, the ratio $\frac{C_p'}{C_p}$ to be approximately 0.05 and 0.01 respectively. Adopting a ratio of 0.01 for graphite, the value for the coefficient becomes about -0.03 erg/cm^2/°C, which is of the correct magnitude, as by simple division, $-\frac{\gamma^\circ}{T_c} = -0.0213$ for this plane. However, uncertainty in the value of k would indicate this agreement to be fortuitous, and equation 27 cannot be used, except perhaps for Pb and Sn where k is known with some degree of accuracy. The best method of obtaining the temperature coefficient is probably by use of the critical temperature. From $T_c = 7000$°K the values in Table XIII were derived.

Table XIII.

Surface Free Energy of Graphite as a Function of Absolute Temperature (T°K).

Basal section, (0001) $= 3125 - 0.446\,T$
Section perpendicular to (0001), normal $= 5100 - 0.729\,T$
Section perpendicular to (0001), modified $= 5020 - 0.717\,T$

5. Conclusions:

As expected, the lowest energy faces, (0001), are found to preponderate in well crystallised graphite. The next lowest energy faces are oblique, such as the $(10\bar{1}2)$, so they would be expected to form the edges of a well developed crystal, at an angle of 103°45' to the basal plane in the Debye-Scherrer form. In the Bernal form, the next lowest energy face is the $(30\bar{3}2)$, at an angle of 110°9' to the basal plane. Thus if only one form of graphite were present in a well developed single crystal, simple goniometry could establish whether it was of the Bernal or of the Debye-Scherrer form. A specimen of

flake graphite was examined under a low power binocular microscope, and although the edges of the flakes were all very irregular, many grains showed tiny steps running across their faces, sometimes in two series at 60° to each other. A goniometer of sufficient sensitivity was unfortunately not available: the steps being estimated to be of the order of 10 cm or less in height.

Flake graphite has a large area of the (0001) face with edges of the order of about $\frac{1}{500}$th of this area. If the average surface free energy for the edges is taken as 5,000 erg/cm^2, the total surface free energy may be stated approximately as $\gamma^T = 3155 - 0.448T$ erg/cm^2. For turbostatic or very finely divided graphite the total surface free energy should be 5,000 erg/cm^2 or more, with a much larger proportion of the high energy faces present. Artificial graphite, such as the cross section of an extruded electrode, may also show values in the region of 5,000 erg/cm^2, as the planes cut are chiefly of class b, perpendicular to (0001) (see Bruce[94]).

The very high values of surface free energy of finely divided graphite explains the great tendency for adsorption of fluids, and the difficulty of their removal. An example of a possible effect of this adsorption on the reactivity of graphite has already been given (Ch.I,F).

This method of calculation seems to be as justifiable as any other yet put forward, and it is the only one which gives surface free energy values for faces other than the basal plane, and values which are upheld by experiment.

B. - Other Refractory Substances.

1. Introduction.

Experimental determinations of the surface energy of solids has been done by three methods:-

a) Creep of fine wires or foil near the melting point.
b) Dihedral and contact angle measurements.
c) Calorimetric determinations on particles of different sizes.

Method 'a' is obviously inapplicable to most refractories due to difficulties of fabrication; it has been applied to fused quartz by Parikh[102]. Method 'b' has been applied to Al_2O_3 and ZrO_2 by Kingery[69] at 1350°C. The third method is the only one applicable much below the melting point and has been used by a number of workers such as Fricke et al[103] on the heat of solution, and Jura et al[104] on the specific heat. The most satisfactory of these methods is probably the last, but this also has many limitations as discussed in the papers.[104]

On the theoretical side wave-mechanical calculations have been made by several different methods, from that of Lennard-Jones[105] onwards, for the alkali halides and some other simple compounds. The early calculations assumed an inverse power law of the Born type for the repulsive energy term, with powers assessed from such data as compressibility results; whereas modern work indicates an exponential form to be more accurate. Also Lennard-Jones et al did not include van der Waal's attractive energy in their calculations. Brill, Hermann and Peters[106], from electron density determinations deduce that MgO is not completely ionic in the solid, so that treatment on a purely

ionic basis will not in this case at least, be very accurate. More serious objections were raised by Benson and McIntosh[107] who show the extreme sensitivity of the results to the choice of the co-efficients used, and conclude that great caution must be exercised before accepting the surface energies arrived at by such calculations. Before leaving this part, the subject of polarisation and surface distortion should be discussed. Miss Dent[108] made more some calculations on the corrections, due to these factors, of some of Lennard-Jones' figures: these corrections, in the nature of a decrease of 10-25%, only apply to the surface free energies of the (100) planes, as shown in Fig.15 plotted against the cation/anion radius ratios obtained from Pauling.[109] These figures show a wide scatter but seem to indicate a tendency for the corrections to become smaller as the radius ratio becomes smaller, which is contrary to expectation, as small cations increase the polarisation. Shuttleworth[105] made less specific reductions. But Molière, Rathje and Stranski[110] showed that no polarisation deformation was to be expected for NaF, KF and KCl, edge deformations only for NaCl and KBr, and some surface deformation for NaBr, NaI and KI. The lack of agreement on this subject tends further to invalidate the wave mechanical calculations.

Table XIV shows some of the results obtained for the (100) face of NaCl at 0°K.

Table XIV - Surface Free Energy at 0°K for the (100) face of NaCl.[105,108]

Lennard-Jones et al	96	erg/cm^2
Biemuller	87	"
Shuttleworth	155	"
Dent	77	"

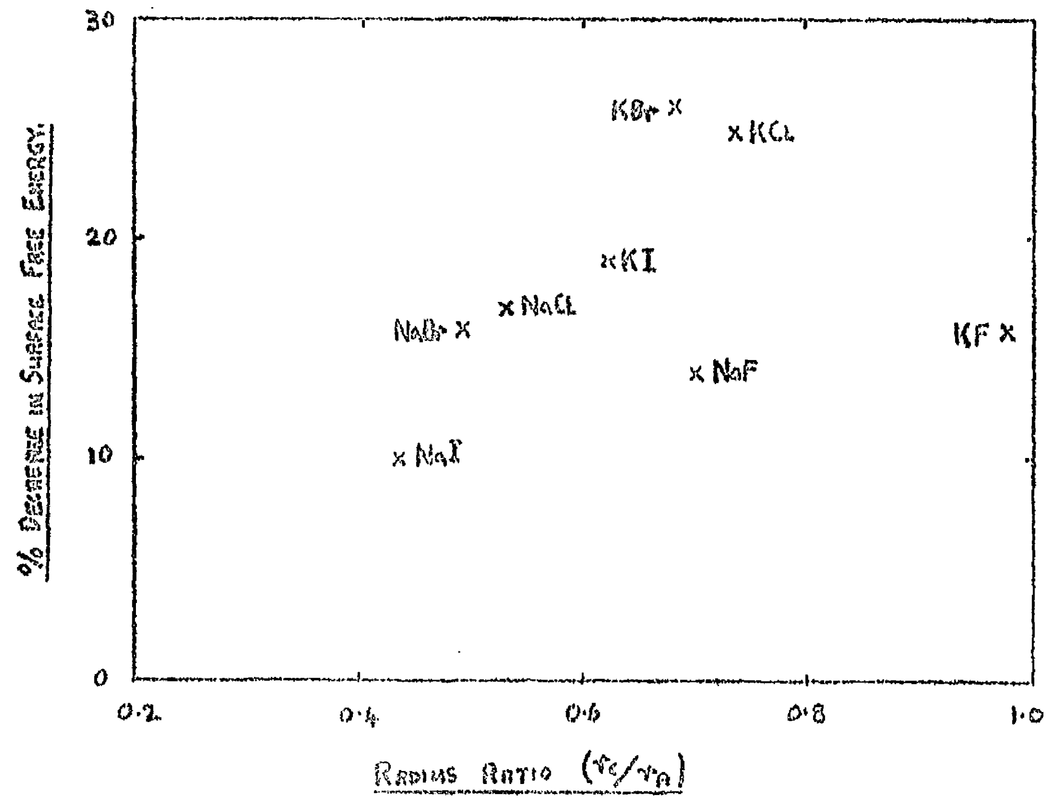

Fig. 15. Percentage decrease in calculated surface free energy (Dent[107]) versus cation/anion radius ratio.

Jaeger[111] found experimentally that the surface tension of liquid NaCl at its melting point was 114 erg/cm^2, which is equivalent to a surface free energy for solid NaCl at its melting point of about 172 erg/cm^2, as will be shown in part 4 below. Heat of solution values[112] are in the region 300-400 erg/cm^2 at 25°C. Even allowing a proportion of higher energy planes to be present in the latter work, these figures suggest that the values calculated as in Table XIV are too low.

Empirical estimations have been made by Livey and Murray[113], chiefly from a consideration of lattice energy and molar volume; but these were based on rather uncertain values of surface free energies for MgO and CaO.

Estimates have been extrapolated from values for liquids; this method will be considered in part 4 below.

A remaining method, which is the one adopted here, is based on the sublimation energy. Fricke[114] was one of the first to use such a method but his calculations were also involved with a rather complex consideration based on Volmer's[115] treatment of Stranski's half crystal position. Fricke's results for metals are very high, for salts and oxides they seem to be reasonable, if a little low (e.g.NaCl $\gamma^\circ = 152$ erg/cm^2). The method used here, as in the previous chapter, assumes interaction to occur only between nearest neighbour atoms of opposite types in a localised manner, along co-ordination bonds. Interaction between similar atoms and between second nearest neighbours are considered to be negligible; all the crystals considered

below have atoms of different types as nearest neighbours. The sublimation energy is proportioned according to the co-ordination in each crystal, giving the energy required to break each bond; all the sublimation energy is allocated to nearest neighbour bonds, this energy would be less if other bonds were considered but the end result for the surface free energy would be little different, perhaps of the order of a few percent also no satisfactory method seems to exist for calculating the energy of bonds other than nearest neighbour bonds for compounds.

When a bond is broken, half the energy supplied applies to each atom. Alternatively, when a column of condensed phase of area 1 cm^2 is cut, two areas each of 1 cm^2 are formed; thus giving the factor 1/2 in converting bond energy to surface energy per bond. The contribution to the surface free energy, σ, is then:-

$$\sigma = \frac{1}{2}\frac{H_s \times J}{C \times N}$$

where H_s is the heat of sublimation in calories/gm mole,
J is Joules' equivalent,
C is the molecular co-ordination (number of bonds per molecule),
N is Avogadro's number.

In the simple cubic system each atom is surrounded by six nearest neighbours of the opposite type and thus possesses six "half bonds", each molecule of two atoms thus possesses six complete bonds and $C = 6$.

σ is multiplied by the number of bonds per cm^2 (ρ) for the material and plane under consideration to give the specific surface free energy. ρ is easily obtained for simple planes by inspection

of a model. It is quite simple to find the plane with the lowest bond density and, in many cases, this plane has the lowest surface free energy. Unfortunately inspection is not so reliable in obtaining maximum values for ρ. Only simple, low index planes are considered in this place, as high index planes have been shown (Chap. II) to have similar values, but some suggestions are made concerning approximate average surface free energies.

This method requires rather a precise definition of a dividing plane, and objection may be raised, on the grounds of Heisenberg's uncertainty principle, that this may lead to uncertainty in the surface energy. With the usual notation:-

Variation of momentum (mv) x variation of position (Δr) $\sim$ h

Thus variation in energy $= \frac{1}{2} mv^2 \sim \dfrac{h^2}{2m(\Delta r)^2}$

Referring to a molecule, $\Delta E \sim \dfrac{h^2 N^{2/3}}{2(\Delta r)^2 V^{2/3}}$, where V is the molar volume.

Assuming $\Delta r \sim 0.1$ Å and V $\sim$ 10 cm^3 (V for MgO = 11.17 cm^3), this gives:-

$$\Delta E \sim 3.3 \times 10^{-20} \text{ erg/cm}^2.$$

Similarly a definition of the dividing surface to an accuracy of 10 Å would lead to an uncertainty in surface energy of about 3 erg/cm^2. The magnitude of these figures requires no further comment.

In this method all the members of a crystallographic system have identical surface energy ratios for the same planes; e.g. in the simple cubic system the ratios are:-

$$(110) : (110) : (111) = 1 : \sqrt{2} : \sqrt{3}$$

The other theoretical calculations may give different ratios for different members of the same system. The ratio for (100) : (110)

varies from about 2.5 to 4.7 (for NaF and CaS respectively) according to Lennard-Jones[105], or from about 2.0 to 3.06 (NaF and KI respectively) according to Shuttleworth[106], and the latter's ratios for (100) : (111) varies between 2.5 and 3.75 (KBr and NaF respectively). It will be seen that these other methods do not permit the calculation of average values for the cubic system as a whole. The method used here allows the bond densities to be used for any member of the appropriate system, with the use of the appropriate lattice parameter.

Before proceeding with the calculations critical temperatures and sublimation energies must be considered.

2. The Critical Temperatures of Refractories:

A study of literature produced no figures for the critical temperature of any refractory material other than graphite, so it was thought advisable to make some estimations in this respect.

It has long been realised that the free surface energy of a liquid vanishes at or just below its critical point. Ramsay and Shields[11] were among the first to postulate a critical region, with the surface tension vanishing about 6°C below the "true" critical temperature. This idea has been revived by Maas and Geddes[95] who introduced a concept of a temperature of meniscus disappearance, which was extended theoretically by Mayer[96]. More recently, however, the critical range is considered to be negligible: Kobe and Lynn[97] exemplify this with the case of water; its meniscus disappears at a temperature identical with the T_c determined from pressure/volume isotherms; and they point out that a highly associated liquid like

water would be expected to show large differences in these temperatures. In any case, when dealing with refractories, 6° may be entirely ignored, indeed 600° may be within the limits of error in estimating their critical temperature.

With substances, like SiO_2 and Al_2O_3, which dissociate fairly readily into lower oxides, it is difficult to attach any meaning to their critical temperature, except to define it as the temperature at which the surface free energy would be zero, if the substance were still stable as a condensed phase to just below this temperature.

Quite a number of empirical methods have been proposed for estimating T_c, but, without exception, they suffer from the necessary drawback that they have been constructed from data on substances with readily accessible critical points; water having about the highest T_c (647.4°K) investigated. Consequently the estimation of T_c for substances like MgO must be regarded as little better than guesswork.

Guldberg[98] was among the first to notice a relation between T_c and T_b (the boiling point at one atmosphere) giving a ratio $\frac{T_b}{T_c} = 0.66$. Other figures have been given for this ratio, generally tending to the region of 0.63.

The parachor, [P], has also figured in some of these estimations. Lewis[99] proposed the form:- $T_c = 2.33\,[P] + 63$ from which T_c may be readily assessed if the appropriate atomic and other parachors are known. This equation is of little use here, as when it is applied to BeO it results in a critical temperature of 207.5°K, on which figure no comment need be passed.

Meissner and Redding[100] divided compounds into four classes, with an appropriate equation for each class; the applicable one in this case, coming under "other compounds", viz:-

$$T_c = 1.027T_b + 159.$$

A more detailed treatment by Herzog[101] yields three possible equations:-

$T_c = 1.112\,T_b + 131.8$ (for compounds free from halogens & sulphur)

$\frac{T_c}{T_b} = 2.544 - 0.4429 \log [P]$ (for some inorganic oxides e.g. $SO_2, O_2 H_2O$, etc)

$\frac{T_c}{T_b} = 1.783 - 0.1479 \log [P]$ (for "anhydrides" e.g. CO_2, H_2, etc)

Since these formulae were derived from such a miscellany of substances, it was decided to investigate them with oxides only, with data chiefly from Kobe and Lynn[97], the parachors being taken from Herzog[101]. The results are shown in Table XV, in which were used some of the above relationships, denoted as below:-

$$\frac{T_c}{T_b} = 0.63 \quad \text{———— 1.}$$

$$\left.\begin{array}{ll} T_c = 1.027\,T_b + 155 & \text{———— 2.} \\ T_c = 1.112\,T_b + 131.8 & \text{———— 3.} \end{array}\right\} \text{For compounds with } T_b < 235^{\circ}K.$$

$$\frac{T_c}{T_b} = 2.544 - 0.4429 \log [P] \quad \text{———— 4.}$$

$$\frac{T_c}{T_b} = 1.783 - 0.1479 \log [P] \quad \text{———— 5.}$$

Other than relation 1, these are stated to be accurate to 5% or less, under their respective conditions.

Table XV - Estimated and Experimental Critical Temperatures.

Compound	T_b °K	T_c (Exp)	Relation				
			1	2	3	4	5
H_2O	373	647.4	593	542	546	675	576
CO	82	133	130	-	-	155	129
CO_2	194.5	304.2	309	-	-	349	298
NO	122	180	194	-	-	225	188
NO_2	294.3	431	468	479	459	519	443
SO_2	263	430.7	418	429	424	441	393
SO_3	317.6	491.4	505	485	505	521	471

The simple ratio 1 is seen to give quite good agreement in some cases, as do the other relations except 4 which gives consistently high results. In dealing with high boiling point substances a relation involving the ratio $\frac{T_c}{T_b}$ seems to be preferable. Atomic parachors are available for Al, Be, Cr and Si; although they are obtained from low boiling compounds, and their use must be regarded with suspicion in connection with refractory oxides. The values calculated from relations 4 and 5 in Table XV are respectively 12% and 3.4% high in the $\frac{T_c}{T_b}$ ratio compared with experimental values; accordingly ratios calculated from these relations were reduced by these amounts. The average $\frac{T_c}{T_b}$ ratios for the four refractory oxides are given below:-

BeO - 1.515 ; SiO_2 - 1.500 ; Al_2O_3 - 1.397 ; Cr_2O_3 - 1.391.

It would seem encouraging that the ratios for Al_2O_3 and Cr_2O_3 are so close; and that they are lower than the other two, as these

oxides have a strong tendency to dissociate at very high temperatures which would lead one to expect low ratios.

No other data are available for metals or compounds of interest, so for want of a better criterion oxides are grouped according to their valency and allotted the following ratios:-

$$MO \quad \frac{T_c}{T_b} = 1.52$$
$$MO_2 \quad \frac{T_c}{T_b} = 1.50$$
$$M_2O_3 \quad \frac{T_c}{T_b} = 1.40$$

Any estimate of error for these ratios must be purely tentative; it is possibly ~15%.

No account was taken of strain parachors, due to entire lack of data. This may affect the polyvalent oxides, decreasing their parachors and consequently increasing their $\frac{T_c}{T_b}$ ratios. If a strain parachor of -9 were adopted for SiO_2, its ratio would rise to 1.515 (c.f. BeO); a comparative value for Al_2O_3 would be -18, raising its ratio to 1.410; but these strain parachors are almost entirely guesswork, so they were ignored.

Two of the most comprehensive references on oxides, Brewer[117] and Kubaschewski and Evans[116] were consulted to obtain boiling temperatures. They differed slightly, if at all, except for MgO, for which Brewer's figure was adopted. No figure seems to have been suggested for the hypothetical normal boiling point of SiO_2 so the figure in Table XVI was estimated by analogy with similar oxides (e.g. TiO_2, VO_2, Al_2O_3 and MnO). The melting temperatures and latent heats of fusion are also noted. The prescript 'd' indicates dissociation at or below that

temperature. Possible errors in T_c in the table must be in the region of 20%, due to uncertainty in boiling points, with the exception of BeO, where it is possibly in the region of 15%.

Table XVI - Thermal Data on Some Refractory Oxides.

Oxide	$\frac{T_c}{T_b}$	T_b (^oK)	T_c (^oK)	T_m (^oK)	Lf(Kcal/mole)
MgO	1.52	3600	5470	3075	18.5
CaO		3800	5770	2860	19.0
FeO		d.3400	5170	d.1644	7.4
MnO		d.3400	5170	2058	13.0
BeO		4390	6680	2820	17.0
SiO_2	1.50	(d.3200)	4000	1986	3.6
TiO_2		d.3200	4800	2400	15.5
Al_2O_3	1.40	d.3700	5180	2300	26.0
Cr_2O_3		d.3300	4620	2710	-

3. Sublimation Energies:

Direct determination of H_s for refractory substances is extremely difficult. Apart from the experimental difficulties of working at very high temperatures, many compounds tend to dissociate at high temperatures. Consequently there is a large uncertainty in any results obtained. The Born-Haber cycle was used to calculate H_s in all cases, to give self consistent values. The calculation is exemplified below:-

$$Na_c + \tfrac{1}{2} Cl_{2_g} \rightarrow NaCl_c \qquad \Delta H_f = -98.7 \text{ Kcal/mole}$$

$$Na_c \rightarrow Na_g \qquad \Delta H_m = +26 \quad ''$$

$$\tfrac{1}{2} Cl_{2_g} \rightarrow Cl_g \qquad \Delta H_x = +28.9 \quad ''$$

$$NaCl_g \rightarrow Na_g + Cl_g \quad D = +98 \quad ''$$

$$NaCl_c \rightarrow NaCl_g \qquad H_s = \Delta H_m + \Delta H_x - \Delta H_f - D$$

$$= +55.6 \text{ Kcal/mole.}$$

The experimental value is 55.1 Kcal/mole.

Calculations were made as in Table XVII for some simple refractory substances; three published values[116] are also quoted.

ΔH_f was obtained from Kubaschewski and Evans[116]. Other sources[82 & 117] were also consulted for the other values. The figures refer to one mole at 25°C for convenience, the transformation to 0°K being small (about 1-2 Kcal/mole) and in many cases uncertain.

Table XVII - Heats of Sublimation at 25°C (Kcal/mole).

					H_s	
	$-\Delta H_f$	ΔH_m	ΔH_x	D	calc'd	rep'd
MgO	143.7	36	59.1	110	129	130
CaO	151.9	47	59.1	116	142	149.5
FeO	63.5	95.2	59.1	92	126	-
BeO	143.1	77	59.1	124	155	155
SiO	12.4	87	170	64	205	-
SiO_2^+	209.3	87	118.2	246	168	-
TiO_2	225.5	112	118.2	320	135	-
Al_2O_3	400.0	154.8	177.3	261	470	-
Cr_2O_3	270	188	177.3	236	399	-
Fe_2O_3	197	190	177.3	175	389	-

$^+$ β Cristobolite

The D values are uncertain in the last five cases, as few values are reported other than for monoxides. For SiO_2, the D value for SiO was multiplied by the ratio of D values for CO_2 and CO: for TiO_2 a similar adjustment was made from a consideration of ZO_2 and ZrO. With Al_2O_3 no simple adjustment from the value for AlO was possible, so one of the lowest values of D for AlO[118] was multiplied by three; the values for Cr_2O_3 and Fe_2O_3 were obtained analogously.

The possible error in H_s for the monoxides is 10% or less,

[illegible]

[illegible]	[illegible]	[illegible]	[illegible]	[illegible]	[illegible]	[illegible]
[illegible]	[illegible]	[illegible]	[illegible]	[illegible]	[illegible]	[illegible]
[illegible]	[illegible]	[illegible]	[illegible]	[illegible]	[illegible]	[illegible]
[illegible]	[illegible]	[illegible]	[illegible]	[illegible]	[illegible]	[illegible]
[illegible]	[illegible]	[illegible]	[illegible]	[illegible]	[illegible]	[illegible]
—	[illegible]	[illegible]	[illegible]	[illegible]	[illegible]	[illegible]
—	[illegible]	[illegible]	[illegible]	[illegible]	[illegible]	[illegible]
—	[illegible]	[illegible]	[illegible]	[illegible]	[illegible]	[illegible]
—	[illegible]	[illegible]	[illegible]	[illegible]	[illegible]	[illegible]
—	[illegible]	[illegible]	[illegible]	[illegible]	[illegible]	[illegible]
—	[illegible]	[illegible]	[illegible]	[illegible]	[illegible]	[illegible]

[illegible]

[illegible]

this figure rising to possibly more than 20% for the sesquioxides. For SiO_2 D is felt to be rather more uncertain with a possible error in H_s of perhaps 30%, 205 Kcal/mole seems rather high.

In the rupture of a bond in a NaCl crystal, the Na atom may be thought to be left deficient by $e/6$ from neutrality with a corresponding excess in charge in the Cl atom. However, every plane except those of the {111} family contain equal numbers of both types of atoms and neutrality will be preserved. In a {111} plane three bonds are ruptured per atom giving a charge of $\pm e/2$ per atom depending on whether the plane surface consisted of Na or Cl atoms: in separating the two planes, an extremely high electrostatic field would exist, and charged atoms would be exchanged practically instantaneously, the process tending towards electrical neutrality with the production of kinked faces. Even in this extreme case an atom cannot have more than half the charge it would possess if it were a true ion (viz. Na^+ and Cl^-). Accordingly, the lattice energy, involving the production of ions from a crystal, cannot be used to derive an energetic term to be employed in cohesive or surface forces; thus justifying the use of a term derived from the sublimation energy. Again, NaCl has a lattice energy of about 185 Kcal/mole, against $H_s = 56$ Kcal/mole, so that unique use of the former would lead to values more than three times those obtained from the latter: the use of $H_s = 56$ Kcal/mole leads to high values of the surface energy, so that use of the lattice energy would lead to ridiculously high values.

4. Example of Calculation - NaCl:

All the crystal parameters were taken from Donnax and Nowacki.[119]

The structure is too well known to require description, and the sublimation energy has already been discussed, giving:-

$$\sigma = \frac{1}{2}\frac{H_s \times J}{CN} = \frac{56 \times 10^{3} \times J}{2 \times 6 \times N} = 3.243 \times 10^{-13} \text{ erg/bond.}$$

The (100) plane has four bonds per unit cell of side $a = 5.639$Å, giving:-

$$\rho_{(100)} = \frac{4}{a^2} \qquad \therefore \gamma^{\circ}_{(100)} = \frac{4\sigma}{a^2} = 408 \text{ erg/cm}^2.$$

γ° is equivalent to the surface enthalpy, the entropy being obtained by consideration of T_c. $T_b = 1465^{\circ}$C and $\frac{T_c}{T_b} \doteqdot 1.52$, giving $T_c = 2620^{\circ}$K. Thus an approximation is obtained:-

$$\frac{d\gamma}{dT} = -\frac{\gamma^{\circ}}{T_c} = -0.1557 \text{ erg/cm}^2/^{\circ}\text{C.}$$

$$\therefore \gamma^{T}_{(100)} = 408 - 0.1557\,T.$$

This expression yields surface free energies of 352 and 241 erg/cm^2 at 25°C and the melting point (801°C) respectively. The former value is in good agreement with the heat of solution values (300-400 erg/cm^2).

As already discussed, immediately before melting the solid surface of a crystal of this system is composed essentially of {100} faces. Assuming that the latent heat of melting contributes to lowering the free surface energy on melting, we have an expression of the form:-

$$-\Delta\gamma \doteqdot \frac{\Delta H_f}{A.N} \qquad \text{.............28.}$$

where $-\Delta\gamma$ is the lowering of the surface free energy, ; ΔH_f is the molar heat of fusion; A is the surface area associated with one molecule ; and N is Avogadro's number. Bondi[28] favoured equation 28 for high melting metals. For refractory substances this yields too great a lowering (see below) and the author would introduce the form:-

$$-\Delta\gamma = B\frac{\Delta H_f}{A.N} \qquad \text{............29.}$$

[illegible]

[illegible]

[illegible]

……

[illegible]

……

where B is a factor obtained from a geometrical consideration of the lattice and plane in question, viz. the number of bonds cut divided by the co-ordination for one molecule. In this case with a (100) plane in NaCl, $B = \frac{1}{6}$. Rigby[120] gives the linear coefficient of expansion for NaCl = 40×10^{-6} °C, giving 'a' at 801°C = 5.657Å, thus

$$-\Delta\gamma = \frac{1}{6}\,\frac{6.9 \times 10^{3} \times J}{\frac{a^{2}}{2} \times N} = 57.8 \text{ erg/cm}^2$$

and

$$\gamma_L^{801} = 241 - 57.8 = 183 \text{ erg/cm}^2.$$

This is rather high compared with the experimental value[111] of 114 erg/cm^2 for the liquid, but the difference may be attributed to impurity and adsorption. If equation 28 were used the lowering would be 347 erg/cm^2, which is ridiculous, as it would lead to a negative surface free energy for the liquid.

Assuming equation 3, as modified by Lövgren, to hold for high melting substances, we have for liquid NaCl with $\gamma^{801} = 183$ erg/cm^2, and $T_c = 2620$°K:-

$$\gamma_L^{T} = 567\left(1 - \frac{T}{2620}\right)^{1.2}$$

where T is the temperature of the liquid in degrees Kelvin.

Again, with $T_c = 2620$°K and $-\Delta\gamma = 57.8$ erg/cm^2, Shuttleworth's value[105] would yield a liquid surface free energy of 33.7 erg/cm^2, which is too low; the result from the figure of Lennard-Jones et al[105] would be negative (-17.4 erg/cm^2). So that these other values calculated for the solid seem again to be too low.

5. Calculations for Refractory Substances:-

Eight crystal systems were examined, containing fifteen

substances of interest to ferrous metallurgy.

Crystal structures were obtained from Bragg[121] and from Wells[122], lattice parameters from Donnax and Nowacki[119], and thermochemical data from Table XVI unless otherwise noted.

5.1 Simple Cubic:-

This system has already been considered and exemplified. Results are noted below:-

MgO : $a = 4.213$ Å; $\gamma^{T}_{(100)} = 1680 - 0.308T$ (erg/cm); $\gamma^{T}_{a} = 2600 - 0.476T$ (erg/cm)

CaO : $a = 4.812$ "; " $= 1420 - 0.246T$ " ; " $= 2200 - 0.381T$ "

FeO : $a = 4.299$ "; " $= 1580 - 0.306T$ " ; " $= 2440 - 0.472T$ "

The linear coefficient of expansion for MgO was extrapolated from data by Whitmore and Ault[123]; from room temperature to melting point it is $20.5 \times 10^{-6}\ {}^{\circ}C^{-1}$, whence at 2800°C, $a = 4.455$Å, giving, with $H = 18.5$ Kcals/mole, a lowering of 215.8 erg/cm^2.

Thus for liquid MgO, $\gamma^{T}_{L} = 1387(1 - \frac{T}{5470})^{1.2}$

For FeO, the expansion coefficient was similarly extrapolated from Rigby, Lovell and Green[124], giving $\gamma^{T}_{L} = 1562(1 - \frac{T}{5170})^{1.2}$

Calculated values are compared with previously published values in part 6 below.

5.2 Wurzite Structure:-

This hexagonal structure is exemplified by BeO, which entails a considerable degree of covalency and would be difficult to treat wave-mechanically but the calculation below is at least as valid as that for graphite (Chap.IIIA).

The structure consists of interlocked hexagonal layers; each

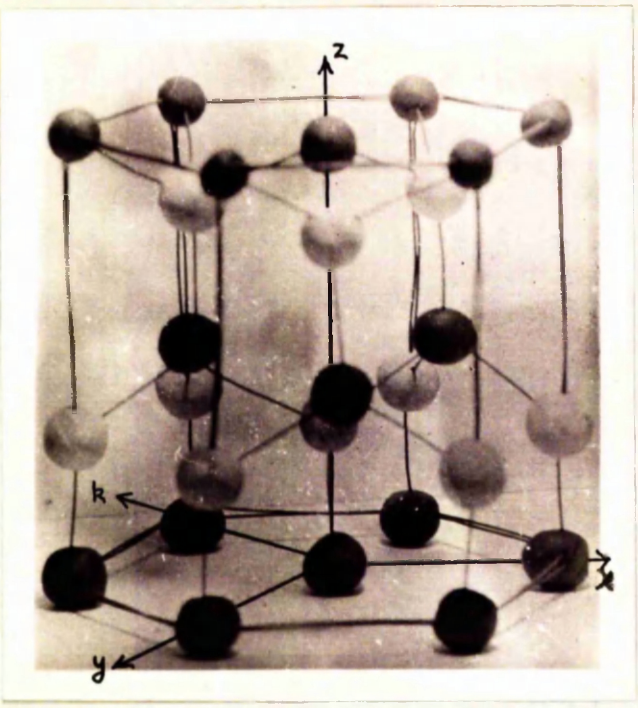

Fig.16 A unit cell of Wurzite.

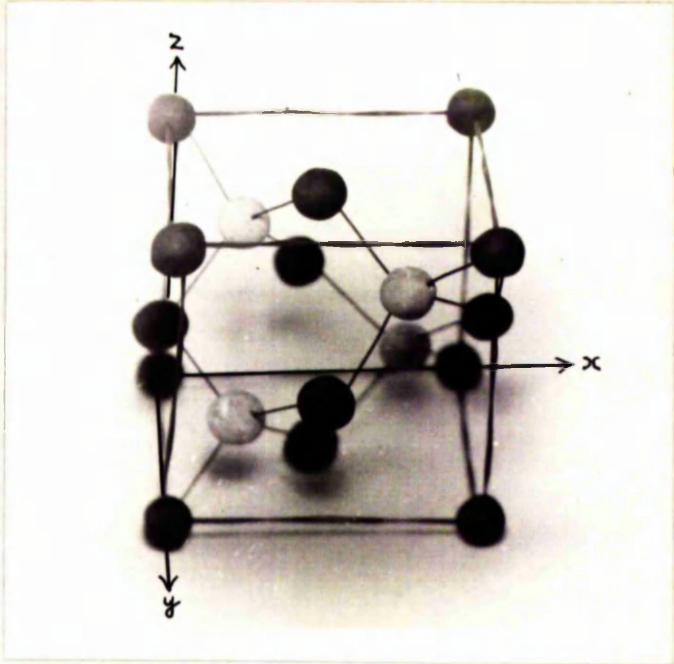

Fig.17 A unit cell of β SiC.

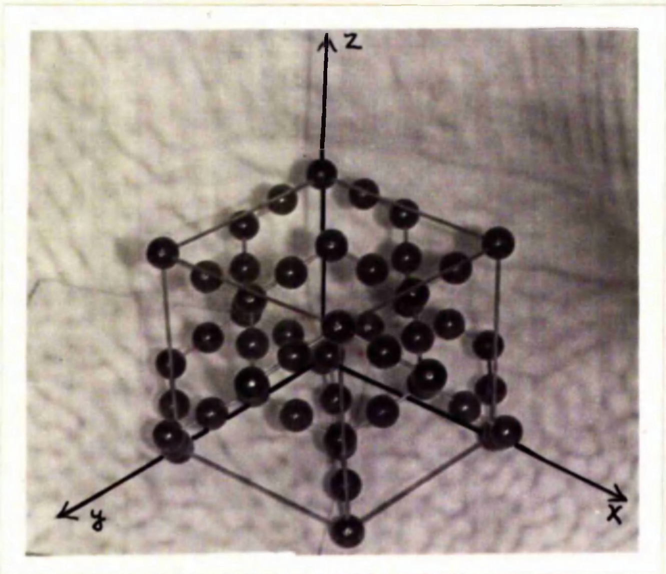

Fig.18 A unit cell of β Cristobolite

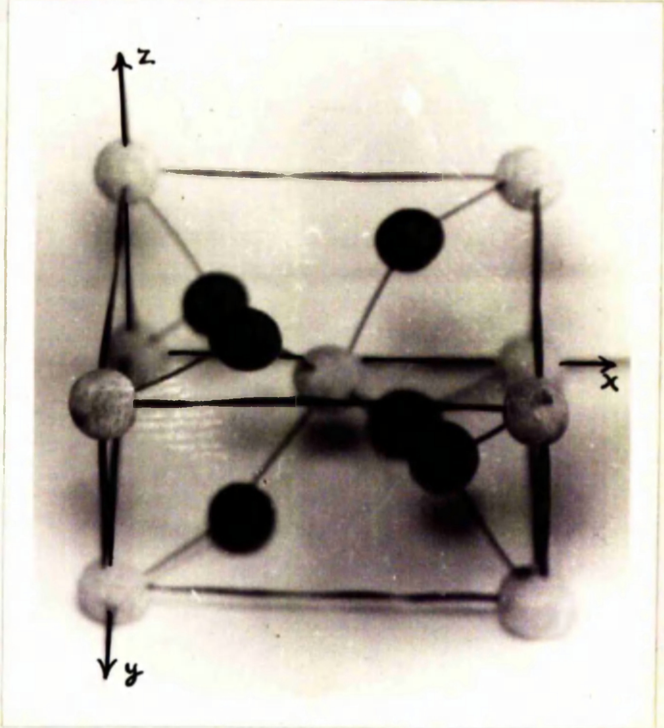

Fig.19 A unit cell of Rutile.

atom being tetrahedral to four atoms of the other type. A model unit cell was constructed from plasticene and wire as in Figure 16, with the four axes drawn in: the thin wires represent the tetrahedral bonds. The two types of atoms are interchangeable as long as each is surrounded by four of the other type.

Four planes were chosen, and bond densities were obtained by counting and by geometry as below:-

Basal + (0001) $\rho = 3 \times 10^{16} \div \frac{3\sqrt{3}}{2} a^2 = \frac{2 \times 10^{16}}{\sqrt{3}\, a^2}$ bonds/cm^2

Perpendicular to axis $(2\bar{1}\bar{1}0)$ $\rho = \frac{4 \times 10^{16}}{\sqrt{3}\, a.c.}$ " "

Parallel to axis + $(30\bar{3}0)$ $\rho = \frac{3 \times 10^{16}}{\frac{3}{2} a.c.} = \frac{2 \times 10^{16}}{a.c.}$ " "

Inclined $(10\bar{1}\,\tfrac{3}{2})$ $\rho = \frac{4 \times 10^{16}}{\frac{3}{2} a \sqrt{4/9\, c^2 + 3a^2}} = \frac{8 \times 10^{16}}{3a \sqrt{4/9\, c^2 + 3a^2}}$ bonds/cm^2.

+Note: In Fig.16 if the basal cleavage plane were "below" (0001) instead of "above" it, the bond density and surface free energy would be three times as great. This large factor would make it extremely unlikely that cleavage would occur thus. Similarly ρ and γ for $(30\bar{3}0)$ could be twice as great.

Each atom is four-coordinated giving $\sigma = \frac{H_s \times J}{8N}$

For BeO: $a = 2.693$Å, $c = 4.37$Å, $H_s = 155$ Kcal/mole and $T_c = 6680$°K, giving:-

	(0001)	(2110)	(3030)	(101)	
γ°	2140	2640	2290	2420	erg/cm^2
$\frac{d\gamma}{dT}$	-0.321	-0.395	-0.343	-0.363	erg/cm^2/°C.

An average value is suggested as: $\gamma_s^T = 2400 - 0.359T$

The coefficient of expansion was estimated from data by Rigby[124] and by Hummel[126] to be about 11×10^{-6} °C, giving, at 2550°C, $a = 2.77$Å and $c = 4.39$Å. In this case γ is lowest for (0001), for which $A = \sqrt{3}a^2$ and $B = \frac{1}{4}$. With $\Delta H_f = 17$ Kcal/mole, $-\Delta\gamma = 222$ erg/cm^2. Thus $\gamma_L^{2550} = 1013$ erg/cm^2 and $\gamma_L^T = 1955\left(1 - \frac{T}{6680}\right)^{1.2}$

Considering the $(30\bar{3}0)$ plane, $-\Delta\gamma = \frac{17 \times 10^3 \times J}{4.a.c.N} = 243$ erg/cm^2 giving $\gamma_L^{2550} = 1080$ erg/cm^2. This value is only slightly greater than that obtained from the (0001) plane, indicating the possibility of a $(30\bar{3}0)$ type of structure in the surface of the liquid, perhaps co-existing with a more pronounced (0001) structure.

5.3 Sphalerite Structure:-

This structure, as in Figure 17, shows a F.C.C. modification with tetrahedrally coordinated atoms. The bond densities are:-

$$(100)\ \rho = \frac{4 \times 10^{16}}{a^2},\ (110)\ \rho = \frac{3 \times 10^{16}}{\sqrt{2}\,a^2},\ (111)\ \rho = \frac{2\sqrt{3} \times 10^{16}}{a^2}$$

As in Wurzite, $\sigma = \frac{H_s \times J}{3N}$

The example of this system is β SiC. No data on T_b are available as it decomposes about 2250°C, though its melting point is 2700°C or above, so T_c was assessed at 5500°K. Many hexagonal forms have been allotted to SiC but the figures below only refer to this cubic modification - β SiC.

SiC: $a = 4.357$ Å, $H_s = 205$ Kcal/mole, $T_c = 5500$°K

	(100)	(110)	(111)	Average	
γ°	3840	2030	3100	3000	erg/cm^2
$-\frac{d\gamma}{dT}$	0.698	0.370	0.563	0.546	erg/cm^2/°C.

The average value was obtained by using $R = 1.5$ with reference to the (110) plane by a rough analogy to the simple cubic system. The possible error for these figures may be in the region of 50%. With the (110) plane as reference the ratios (also for Cristobalite, below) are $R_{(111)} = 1.6$, $R_{(100)} = 1.9$; being so large it would be difficult to produce other faces than {110} in granular material. Fracture would always tend to produce or conserve {110} faces: this may account in part for the excellent abrasive properties of SiC, if it were β SiC, due to renewal of sharp edges. The cohesive strength ($= 2\gamma$) is very high, explaining the hardness of SiC.

5.4 Cristobalite:

This is the form of SiO_2 stable from 1470°C to the melting point, and this range covers most of its refractory applications. A model was available for this substance, as seen in Figure 18. It is a cubic structure with oxygen atoms tetrahedrally bonded to silicon. The bonds in this case may be regarded as "Normal" chemical bonds, in distinction to coordination bonds, thus there are four bonds per molecule, giving $\sigma = \frac{1}{2} \cdot \frac{H_s \times J}{4N}$

The three simplest planes were found to have the same bond densities as in Sphalerite, showing an unexpected similarity between these structures.

$a = 7.09$ Å, $H_s = 168$ Kcal/mole, $T_c = 4800$°K, giving:-

	(100)	(110)	(111)	Average.	
γ°	1160	616	1005	925	erg/cm^2
$-\frac{d\gamma}{dT}$	0.242	0.128	0.209	0.193	erg/cm^2/°C.

As with β SiC, granular material will probably exhibit chiefly {110} faces with an average surface energy in the region of 650 erg/cm^2 at 0°K. The shape effect receives some additional support from the following observations:-

1) the very angular character of crushed SiO_2 brick
2) the high R.u.L. of SiO_2 bricks
3) the difficulty of sintering, would indicate that surface free energies were already close to a minimum.

The other forms of SiO_2 are similar in structure to β Cristobalite, but not so symmetrical, so they possibly have rather similar surface free energies. Tridymite has a lower density (2.26 gm/cm^3) than Cristobalite (2.32 gm/cm^3), and Quartz is denser (2.65); energetic and geometric considerations being very similar the surface free energies will be in proportion. Thus Tridymite will have a lower surface free energy (620 erg/cm^2?) and Quartz a higher (700-750)erg/cm^2?) than Cristobalite. The high temperature stable form is probably closest in structure to the liquid.

The coefficient of expansion is very irregular in this case and there is poor agreement amongst published figures. 'a' at 1713°C was extrapolated from 'a' values up to 1300°C given by Donnax and Nowacki[119], at about 7.145 Å. In this case there are 5½ molecules per $\sqrt{2}\,a^2$, and $B = \frac{1}{4}$. Due to the large unit cell and low ΔH_f (3.6 Kcal/mole) $-\Delta\gamma = 30.3$ erg/cm^2 showing very little change in surface free energy in the solid/liquid transformation. This is possibly one

reason for the ease with which SiO_2 and its mixtures tend to form glasses. By the usual method $\gamma_L^{T_m} = 331.5$ and $\gamma_L^{T} = 628\left(1 - \frac{T}{4800}\right)^{1.2}$

5.5 Rutile Structure:-

This structure is tetragonal and care must be exercised in describing the planes: in general only h and k may be interchangeable in $(hk\ell)$; the planes chosen below exemplify this point. Figure 19 shows the model of this structure, with the unusual three-coordination of the oxygen (black), and the six-coordination of the titanium (white). This gives a total of six bonds per molecule, and thus:-

$$\sigma = \frac{1}{2}\frac{H_s \times J}{6N}$$

With the rather low symmetry of this structure, two neighbouring unit cells had to be considered to obtain some of the bond densities, as below:-

$$(100) \text{ and } (010)\ \rho = \frac{4 \times 10^{16}}{a.c} \qquad (001)\ \rho = \frac{4 \times 10^{16}}{a}$$

$$(110)\ \rho = \frac{10^{16}}{\sqrt{2}\, a.c} \qquad (1\bar{1}0)\ \rho = \frac{\sqrt{2} \times 10^{16}}{a.c}$$

$$(011) \text{ and } (101)\ \rho = \frac{3 \times 10^{16}}{a\sqrt{(a^2 + c^2)}} \qquad (111) \text{ and } (11\bar{1})\ \rho = \frac{5 \times 10^{16}}{a\sqrt{(a^2 - 2c^2)}}$$

$$(\bar{1}11)\ \rho = \frac{6 \times 10^{16}}{a\sqrt{(a^2 - 2c^2)}}$$

$a = 4.4923$ Å, $c = 2.8930$ Å, $H_s = 135$ Kcal/Mole, $T_c = 4800$ °K, giving:-

	(100)	(001)	(110)	$(1\bar{1}0)$	(101)	(111)	$(\bar{1}11)$	Average	
γ°	2405	1550	426	851	976	2530	3040	(800)	erg/cm^2
$-\frac{d\gamma}{dT}$	0.500	0.323	0.089	0.177	0.203	0.528	0.633	(-0.167)	" "/°C

In this case the {110} family have much lower energies than the {100}, which latter are lower than those for the {111} family.

With such a very wide variation in energies (the ratio (111) to (110) is 7.1), from the low symmetry of the structure, it is difficult to suggest an average value, so that the value (800 − 0.167 T) must be tentative only.

5.6 Corrundum Structure:-

There are quite a number of important oxides in this group (e.g. sesquioxides of Al, Cr, Fe, V, Th, etc.) all conforming to this structure, which is shown in Figure 20 shown in plan and elevation. The metal atoms occur in vertical rows at the corners and at the centre of the unit cell, and in five layers in the elevation: the oxygen atoms occur in six rows and four layers between the metal atoms. The metal is six-coordinated and the oxygen four-coordinated, giving a total of twelve bonds per molecule, thus:- $\sigma = \frac{1}{2}\frac{H_s \times J}{12N}$

As in the other hexagonal systems, six planes were investigated, as below:-

$$(0001)\ \rho = \frac{4 \times 10^{16}}{\sqrt{3}a} \qquad (20\bar{2}0)\ \rho = \frac{16 \times 10^{16}}{3ac} \qquad (10\bar{1}0)\ \rho = \frac{9 \times 10^{16}}{ac}$$

$$(2\bar{1}\bar{1}0)\ \rho = \frac{12 \times 10^{16}}{\sqrt{3}ac} \qquad (1\bar{\tfrac{1}{2}}\bar{\tfrac{1}{2}}0)\ \rho = \frac{10 \times 10^{16}}{\sqrt{3}ac} \qquad (10\bar{1}\bar{4})\ \rho = \frac{12 \times 10^{16}}{3a\sqrt{(3a^2 + 4c^2)}}$$

Al_2O_3: $a = 4.75$ Å, $c = 13.00$ Å, $H_s = 470$ Kcal/mole, $T_c = 5180°K$, giving:

	(0001)	$(20\bar{2}0)$	$(10\bar{1}0)$	$(2\bar{1}\bar{1}0)$	$(1\bar{\tfrac{1}{2}}\bar{\tfrac{1}{2}}0)$	$(10\bar{1}\bar{4})$	Average	
$\gamma°$	1390	1175	1985	1560	1270	1120	1200	erg/cm^2
$-\frac{d\gamma}{dT}$	0.268	0.227	0.383	0.295	0.246	0.216	0.232	erg/cm^2/°C.

Figures for the expansion of a compact of Al_2O_3 were obtained from Whitmore and Ault[125] were extrapolated to give a coefficient of

$10.4 \times 10^{-6}\ {}^{\circ}C^{-1}$ up to 2030°C. In this case however the coefficients for the 'a' and 'c' values probably differ significantly. By comparison with values for Fe_2O_3 in the Critical Tables[126], α_a was assessed at $10.3 \times 10^{-6}\ {}^{\circ}C^{-1}$ and α_c at $10.5 \times 10^{-6}\ {}^{\circ}C^{-1}$, giving at 2030°C, $a = 4.875$ Å and $c = 13.277$ Å. The lowest energy plane is the $(10\bar{1}\bar{4})$, which has $\frac{4}{3}$ molecules per $\frac{3a}{2}\sqrt{3a^2 + \frac{1}{4}c^2}$ Å^2, and $B = \frac{3}{16}$. With $\Delta H_f = 26$ Kcal/mole, $-\Delta\gamma = 57.5$ erg/cm^2, giving $\gamma_L^{T_m} = 565$ erg/cm^2 and $\gamma_L^{T} = 1144\left(1 - \frac{T}{5180}\right)^{1.2}$

Cr_2O_3: $a = 4.94$ Å, $c = 13.57$ Å, $H_s = 399$ Kcal/mole, $T_c = 4620$°K, giving:-

	(0001)	$(20\bar{2}0)$	$(1\frac{\bar{1}}{2}\frac{\bar{1}}{2}0)$	$(10\bar{1}\bar{4})$	Average	
γ°	1090	919	995	857	925	erg/cm^2
$-\frac{d\gamma}{dT}$	0.236	0.199	0.215	0.186	0.200	" " /°C.

Fe_2O_3: $a = 5.025$ Å, $c = 13.735$ Å, $H_s = 389$ Kcal/mole, $T_c = 5000$°K (c.f. FeO):-

	(0001)	$(20\bar{2}0)$	$(1\frac{\bar{1}}{2}\frac{\bar{1}}{2}0)$	$(10\bar{1}\bar{4})$	Average	
γ°	1030	869	940	807	870	erg/cm^2
$-\frac{d\gamma}{dT}$	0.206	0.174	0.188	0.161	0.174	" " /°C.

5.7 Spinel Structure:-

This large class of oxides conforms to a cubic system, having the general formula $M''O.M_2'''O_3$ where the metal may be one element (e.g. Fe_3O_4) or more (e.g. MgO, Al_2O_3 - from which the class obtains its name). Extensive solid solution between members may occur within limits according to the ionic radii. The cell parameter is in the region 8.00 - 8.75 Å.

A model was available for this well known, if complex, structure, to which a photograph, as in Figure 21, cannot do justice.

It consists of close-packed oxygen atoms, with the metals occupying their respective octahedral and tetrahedral positions, thus:-

$$M'' \text{ is 4-coordinated } \therefore \sigma_2 = \frac{1}{2}\,\frac{{}^{2}H_s \times J}{4N}$$

$$M''' \text{ is 6-coordinated } \therefore \sigma_3 = \frac{1}{2}\,\frac{{}^{3}H_s \times J}{12N}$$

MgO $\sigma_2 = 1.123 \times 10^{-12}$ erg/bond. Al_2O_3 $\sigma_3 = 1.364 \times 10^{-12}$ erg/bond.

FeO $\sigma_2 = 1.097 \times 10^{-12}$ " Cr_2O_3 $\sigma_3 = 1.158$ " "

Fe_2O_3 $\sigma_3 = 1.129$ " "

The heat of formation of spinels is of the order of 2-3% greater than that of their constituent oxides, therefore the above bond strengths have been increased by 2½%, due to a corresponding increase in H_s, as accurate figures are not available in most cases. This increased stability is reflected in the melting points of the iron oxides (see Table XVIII below).

The bond densities were counted for the three simple planes as below:-

$$(100)\ \rho = \frac{4b_2 + 8b_3}{a^2}; \quad (110)\ \rho = \frac{4b_2 + 14b_3}{\sqrt{2}\ a^2}; \quad (111)\ \rho = \frac{12b_2 + 6\tfrac{1}{2}b_3}{\sqrt{3}/_2\ a^2};$$

where b_2 is the M'' -O bond and b_3 is the M''' -O bond. A higher bond density of $\frac{22b_3}{\sqrt{3}/_2\ a^2}$ is possible for (111), as before, and is not considered for similar reasons.

The critical temperatures were obtained from a consideration of those for the constituent oxides, $MgO.Al_2O_3$ = 5200°K and the other three about 5000°K, giving:-

	(100) γ^{T}	(110) γ^{o}	(111) γ^{o}	Average γ_{A}^{T}
$MgO.Al_2O_3$	2540 - 0.451T	2540	3920	3000 - 0.577 T
Fe_3O_4	1890 - 0.379T	2010	3340	2450 - 0.490 T
$MgO.Cr_2O_3$	1980 - 0.397T	2110	3500	2570 - 0.514 T
$FeO.Cr_2O_3$	1940 - 0.388T	2070	3400	2520 - 0.504 T

It is not possible to make a simple comparison with the other cubic systems due to the two different bonds involved; this also makes comparisons between the spinels difficult. Accordingly the average surface free energy was taken in all cases as approximately 1.3 $\gamma_{(100)}$.

5.8 Gehlenite ($2CaO.Al_2O_3.SiO_2$):-

This rather complex lattice belongs to the Melilite class, with a tetragonal unit cell containing two molecules of Gehlenite. Due to lack of structural members the model built was not very stable or photogenic, so a plan of the cell, looking along the 'z' axis is shown in Figure 22. The four atoms marked with a cross are two each of Al and Si, which are to some extent interchangeable, but with two of each per unit cell the bond densities were unaltered by interchanging them. The numbers against each atom are the heights relative to a 'c' dimension of 100: the Ca atoms are at the "foot" and the "top", thus being '1' and '100' respectively. Some continuity is sought by showing bonds, and parts thereof, not in the unit cell.

There are three types of bonding: Ca - O, denoted 'c' where Ca is eight-coordinated; Al - O, denoted 'a', where Al is four-coordinated; and Si - O, denoted 's' where Si is four-coordinated. As

before only metal-oxygen bonds are considered. The bond strengths are:-

$$\sigma_c = \frac{142 \times 10 \quad \times J}{16N} = 6.169 \times 10 \quad \text{erg/bond.}$$

$$\sigma_a = \frac{470 \times 10 \quad \times J}{16N} = 2.046 \times 10 \quad ''$$

$$\sigma_s = \frac{168 \times 10 \quad \times J}{8N} = 1.460 \times 10 \quad ''$$

The heats of sublimation for the constituent oxides are used due to lack of data on the heat of formation of Gehlenite from the oxides: small increases should possibly be made to the bond strengths of the order of 1-2%.

$a = 7.69$ Å, $c = 5.10$ Å, T_c is taken as 4500°K, giving:-

(001)	14 'c' bonds per a^2	$= 1460 - 0.325T$ erg/cm^2
(002)	6 'a' and 2's' bonds per a^2	$= 2570 - 0.571T$ "
(100)	5 'c', 2'a' and $\frac{a + s}{2}$ bonds per a.c	$= 2280 - 0.506T$ "
(110)	6'c' and 3'a' bonds per $\sqrt{2}$ a.c	$= 1770 - 0.394T$ "
	Average	$= 1600 - 0.356T$ "

The large difference in values for the (001) and (002) planes ensures cleavage to occur preferentially by the former plane, consequently the value for the latter was not considered in assessing the approximate average value. There are no data on the latent heat of fusion or on the coefficient of expansion; they were assessed at 70 Kcal/mole and 10^{-5}°C^{-1} respectively. The area per molecule in the (001) plane is a^2, and B is $\frac{1}{4}$, giving $-\Delta\gamma = 230$ erg/cm^2 at 1590°C, giving an approximate liquid surface free energy of 624 erg/cm^2: thus

$$\gamma_L^T = 1180\left(1 - \frac{T}{4500}\right)^{1.2}.$$

This example was chosen as representative of simple ferrous slags.

The above results are collated in Table XVIII.

Table XVIII.

Calculated Surface Free Energies of Refractory Substances (erg/cm^2).

	Solid				T_m (°K)	T_c (°K)	Liquid	
	Plane	γ^T	γ_A^T	γ_A^{1773}			$\gamma_L^{T_m}$	k
MgO	(100)	1680-0.308T	2600-0.476T	1750	3073	5470	515	1387
CaO		1420-0.246T	2200-0.381T	1525	2863	5770	-	-
FeO		1580-0.306T	2440-0.472T	(1600)	1644	5170	987	1562
BeO	(0001)	2140-0.321T	2400-0.359T	1760	2823	6680	1013	1955
β SiC	(110)	2030-0.370T	3000-0.546T	2030	2970	5500	-	-
SiO_2	(110)	616-0.128T	925-0.193T	580	1986	4800	332	628
TiO_2	(110)	426-0.089T	800-0.167T	505	2403	4800	-	-
Al_2O_3	(10$\bar{1}$1)	1120-0.216T	1200-0.232T	790	2303	5180	566	1144
Cr_2O_3		857-0.186T	925-0.200T	570	2713	4620	-	-
Fe_2O_3		807-0.161T	870-0.174T	(560)	1733	5000	-	-
M.A.	(100)	2340-0.451T	3000-0.577T	1975	2308	5200	-	-
Fe_3O_4		1890-0.379T	2450-0.490T	1580	1860	5000	-	-
M.C.		1980-0.397T	2570-0.510T	1660	?	5000	-	-
F.C.		1940-0.388T	2520-0.504T	1625	?	5000	-	-
C_2AS	(001)	1460-0.325T	1600-0.356T	990	1863	4500	624	1180

Notes: Col.1. "SiO_2" refers to β Cristobalite, "MA" refers to $MgO.Al_2O_3$; "M.C", "F.C." and "C_2AS" are self evident.

Col.5. These figures are for comparison of values at a representative high temperature (1500°C). The bracketed values are for unstable phases.

Col.9. "k" is from the general equation 3:- $\gamma_L^T = k(1 - \frac{T}{T_c})^{1.2}$.

By use of the bond strength factors (σ) and bond densities (ρ), with appropriate H_s and T_c, the surface free energy, for several planes of a substance with any of the above lattices, may easily be obtained. For example for the $(20\bar{2}0)$ plane of the Th_2O_3 reference should be made to part 5.6 above (Corrundum) to obtain:-

$$\gamma^T = \frac{2H_s \times J}{9\; N.a.c}\left(1 - \frac{T}{T_c}\right).$$

The similarity in average surface free energies for FeO and Fe_3O_4 is rather noteworthy; also the large difference between these values and that for Fe_2O_3. This suggests that substances containing oxides of iron may tend to have an effective surface high in Fe_2O_3 in relation to FeO: this is suggestive of a reason for the non-stoichiometry of Wüstite ($Fe_{0.95}O$).

The relative values for the various systems decrease approximately in the order Spinels > Monoxides > Sesquioxides and Dioxides. High surface energies are a possible explanation for the well known catalytic properties of Spinels.

6. Comparison with published values:

MgO. Due to its simple structure MgO has been investigated theoretically more than any other oxide; also due to the relative ease of preparing good crystals, it has had a large share of experimental investigations. Benson and McIntosh[107] discussed the wave-mechanical results, which they considered unreliable. Fricke's[114] result for $\gamma^{o}_{(100)}$ was 1459 erg/cm^2, while Jura and Garland[104] obtained 1040 erg/cm^2 by heat of solution, and Jura[104] 1400 erg/cm^2 by heat capacity determinations. The present result is higher than any of these; the low experimental results may be attributed

possibly to adsorption of O_2, N_2 or H_2O, which could occur on very short exposure to a normal laboratory atmosphere.

CaO. Fricke[103] and Lennard-Jones[105] give $\gamma^{\circ}_{(100)}$ as 979 and 1032 erg/cm^2 respectively. A recent heat of solution value[127] at 23°C is 1310±200 erg/cm^2 and is in good agreement with the author's value of 1346 erg/cm^2 at this temperature.

FeO. The best previous figure is from the work on liquid FeO by Kosakevitch[128], who obtained $\gamma_L^{1420^\circ C} = 585$ erg/cm^2; the present figure is 970 erg/cm^2. Kosakevitch admitted his slag to be contaminated by perhaps as much as 5% of Fe_2O_3, which has a much lower surface free energy and would tend to be preferentially adsorped at the surface. No data are available for ΔH_f for Fe_2O_3 which we may assume to be in the region of 20 Kcal/mole, giving $-\Delta\gamma$ in the region of 30 erg/cm^2 for either $(10\bar{1}4)$ or $(20\bar{2}0)$ planes. Assuming that the Fe_2O_3 on the surface were in the liquid state at 1420°C (T_m for Fe_2O_3 is 1460°C), the $(10\bar{1}4)$ or $(20\bar{2}0)$ planes would possess surface free energies of about 540 or 550 erg/cm^2. Inspection of the structures of FeO and Fe_2O_3 suggests that a $(20\bar{2}0)$ surface would give rather a better "fit" on a (100) surface of FeO; the fit would not be close, giving the surface Fe_2O_3 some strain which would raise the surface free energy; also the Wüstite surface would probably not be completely covered with Fe_2O_3 so that the lowering would not be maximal. These factors together could easily account for a value of 585 erg/cm^2, and the agreement between theory (here) and experiment (Kosakevitch) is considered to be good.

SiO_2. By extrapolation from the work of Kosakevitch[128] and of King[7] on liquid silicates the respective values are 273 erg/cm^2 at 1420°C and 180-240 erg/cm^2 at 1570°C. These figures ignore possible changes in slope of the γ/concentration curves near the SiO_2 end, due to excess surface concentration, which would have the effect of raising these figures by an uncertain amount. Parikh[102] obtained a value of 290 erg/cm^2 at 1100°C on quartz fibres, which is possibly low due to adsorption. Triboluminescence, physiological activity (cf. silicosis) and the production of ozone from freshly crushed quartz, would lead one to expect high values, though this may be due to strain energy. From crushing experiments[129] values in the region 70,000 to 80,000 erg/cm^2 have been obtained for quartz, and a value of 107,000 erg/cm^2 has been reported[130] from ball-mill calorimetry; though these values are out of all proportion to a surface free energy they indicate the possibly large effect of strain energy. The author's result is about twice the best (Parikh) experimental value, again possibly due to adsorption.

Al_2O_3. From heat of solution Fricke[103] obtained a value of 560 erg/cm^2 at 25°C, and from dihedral angles Kingery[69] obtained 905 erg/cm^2 at 1850°C: the author's value is closer to the latter but rather lower. These figures incidentally show that the heat of solution method does not always give results too high, although a high proportion of high energy faces may exist and this argument is frequently evoked to show that $\gamma_{(100)}$ for MgO should be lower than the calorimetric values. Von Wartenberg et al[131], and Kingery[132] obtained values for the liquid of 577 ± 30 erg/cm^2 at 2050°C and 700 ergs/cm^2 at 2080°C respectively;

the former value is in good agreement with that of the author, but Kingery's value is again higher. The high values may be due to a preponderance of high energy planes in the surface which do not readily change to lower energy planes due to high activation energies, or to the relative complexity of the structure reducing the probability of occurrence of low energy planes.

Fe_2O_3. Fricke[103] found $\gamma^{25°C} = 350$ erg/cm^2, again lower than the author's figure.

Gehlenite. From the work of King[7] on $CaO/Al_2O_3/SiO_2$ slags, it is estimated that $\gamma_L^{1570°C} = 500$ erg/cm^2, which is only about 75% of the author's value.

7. Conclusions:

This method of calculating the surface free energy of a particular plane is theoretically applicable to any crystalline substance at any temperature. Predictions are also possible for the surface energies of liquids, though with greater possible error due to uncertainty of the critical temperature, and the rather oversimplified effects of temperature and melting, though better methods have not yet been suggested. Ideas concerning surface configurations may be obtained, but their dimensions and distribution are, at the moment, only conjectural, so that accurate bond densities cannot be obtained. Also, due to the mobility of the particles in the liquid state estimations of bond strength are difficult to make. The simple formula (equation 29) has been shown to yield values of the correct order.

The results are generally higher than those previously

published. Experimental values are believed to be low, chiefly due to the virtual impossibility of avoiding adsorption, or perhaps due to inaccurate determinations of surface areas for the calorimetric values. The results obtained here are in approximately the same order as most published results, though possible errors in some cases (e.g. SiC) may be large.

Jura and Garland[104] have done the only experimental work found on the temperature coefficient of solids much below the melting point; extrapolation of their results leads to a critical temperature (5500°- 5800°K) very similar to the author's (5470°K) though the agreement is possibly fortuitous. The only other applicable work has been done on glasses and low melting slags, where the temperature coefficient is usually in the region of -0.1 erg/cm^2/°C, which figure is frequently and wrongly applied to substances like Al_2O_3: the figures found here are generally much higher than this figure and naturally show as wide a variation as do the figures for the surface free energy. On the other hand positive values for this coefficient (e.g. King[7]) cannot easily be predicted by this method which can only consider one surface species at a time (c.f. part 6, FeO) and cannot yet predict their interaction.

Chapter IV - Experimental Work

A. Apparatus and Technique:

The furnace used is as sketched in Fig.23, in its final form developed from an earlier investigation by the author[133]. The winding, A, is 60 feet of platinum/13% rhodium wire of 20 s.w.g., wound over 18 inches on a thin layer of "101" alumina cement on a tube of "C60" Alundum (materials supplied by the Thermal Syndicate), and covered with another layer of "101" cement before firing. The leads, not shown, were of treble wires to insulated terminals in the case. This furnace tube was buried in a primary shell, B, of -10 mesh fused alumina, in a cylindrical cavity cut in the high temperature insulating bricks, C, the whole being enclosed in a frame of welded angle iron, with sides (as in the figure) of ¼ inch thick Sindanyo board, the other plates being of aluminium. A working tube, D, of alumina was eventually found to be satisfactory. It was closed by brass fittings, E_1 and E_2, with "O" ring seals of rubber; fitting E_1 is shown in more detail in Fig.24; it had a window of optical quality glass cemented to it by Canada Balsam. The working tube was found to bend after some time at high temperatures, chiefly due to the weight of fittings E_1 and E_2: to counteract this, a loose clamp F_1 and a support F_2, were fitted to the side walls. The side-arm G was connected by pressure tubing to a "speedivac" pump, and a mercury manometer, capable of reading to 0.5 m.m in the range zero to 86 cm. of mercury. Gas was

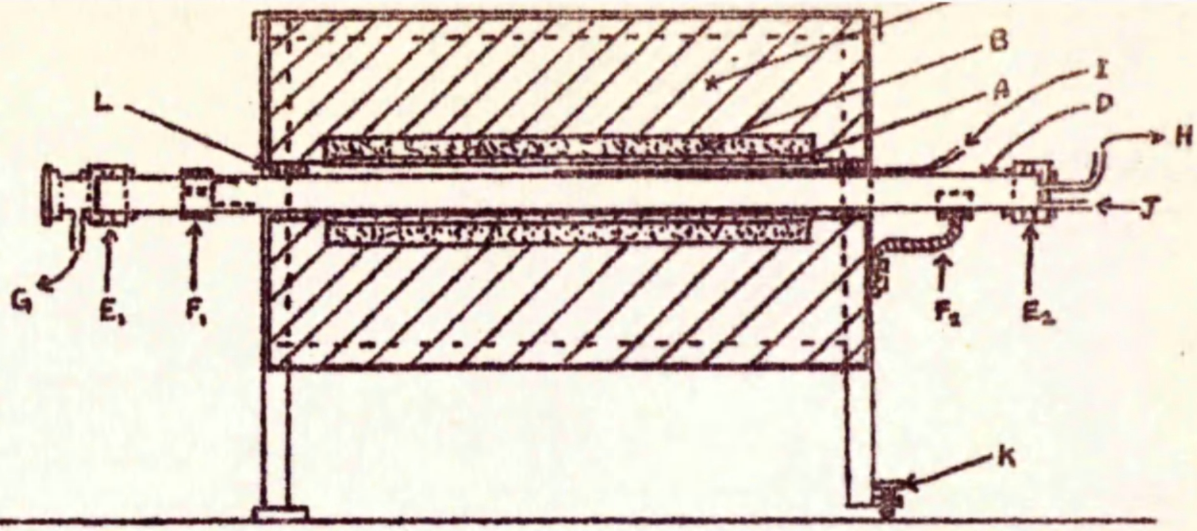

Fig. 23 Construction of Furnace and Working Tube. Scale ~ 1:10

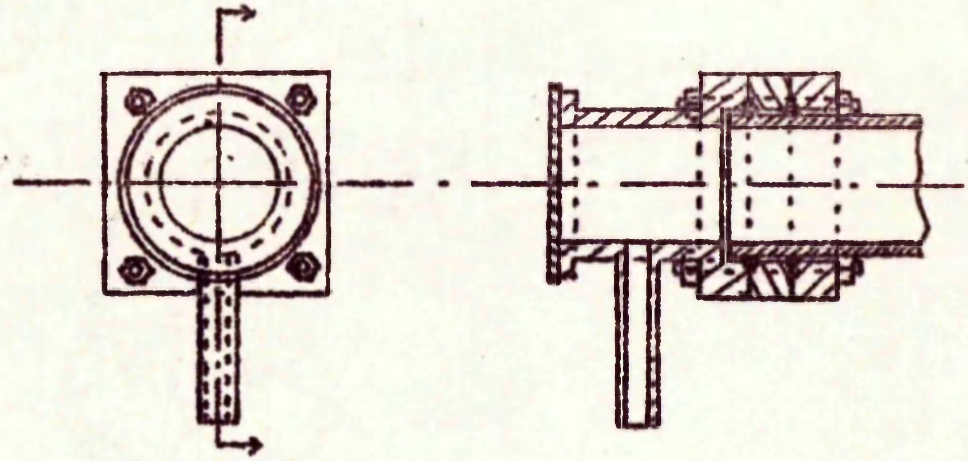

Fig. 24 Detail of Fitting E₁. Scale ~ 1:2

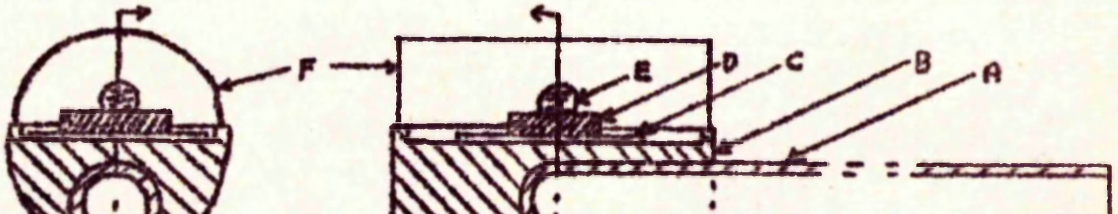

Fig. 25 Construction of Boat, and Specimen Assembly. Actual Size

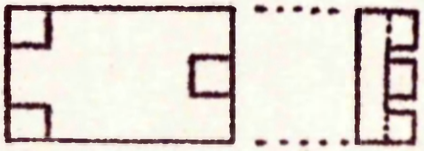

Fig. 26 Levelling Device. Actual Size

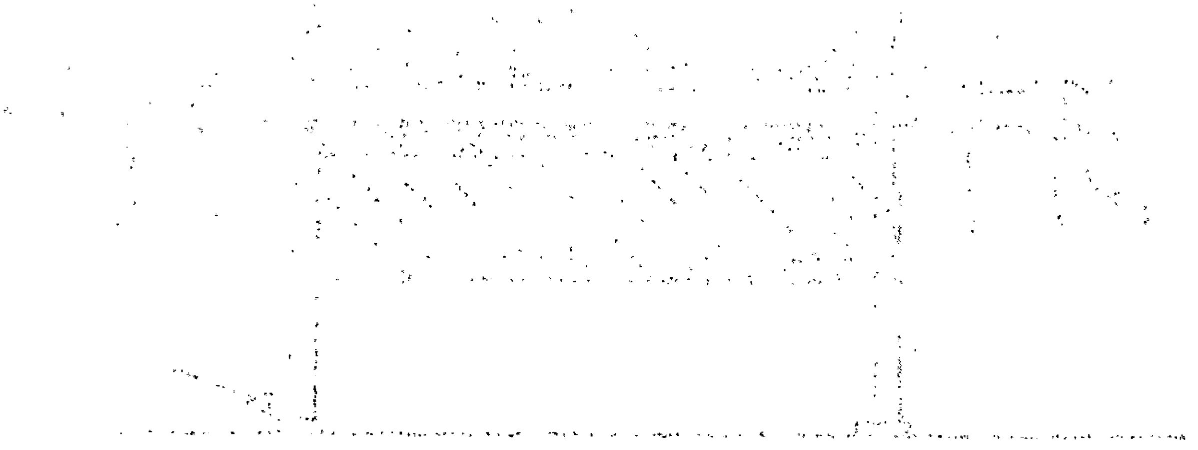

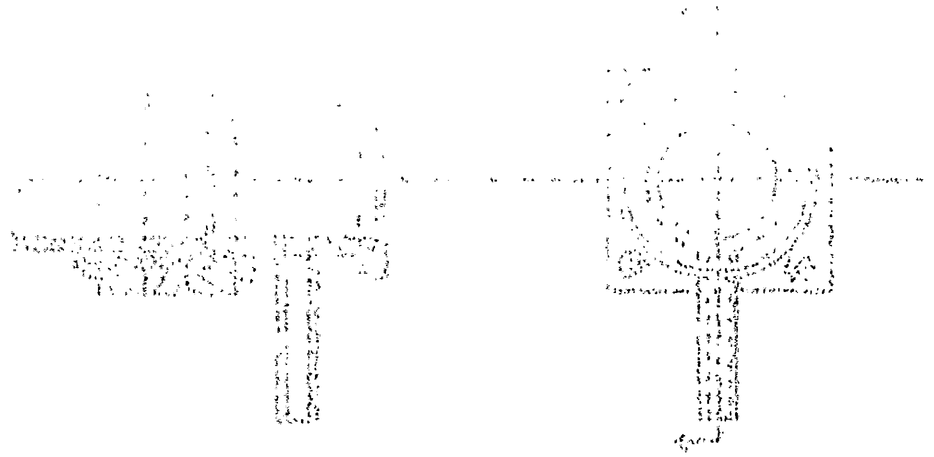

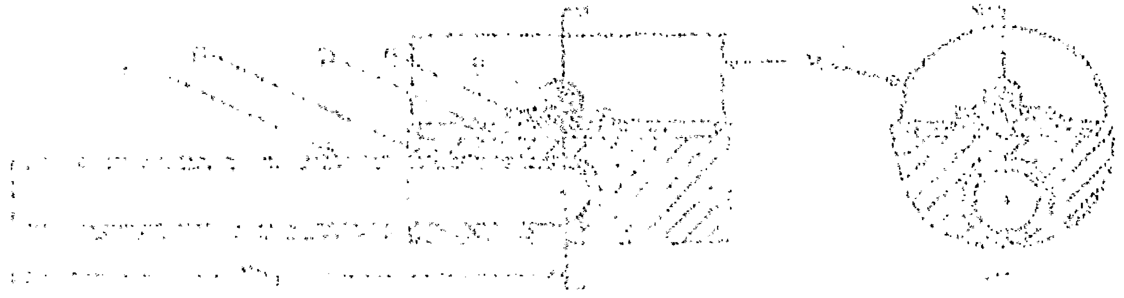

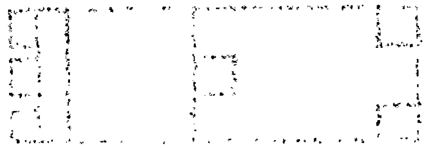

passed, if required, through H. The brass fittings E_1 and E_2 were cooled, to preserve the rubber "O" rings, by a single turn of 1 inch broad degreased wick whose ends dipped into a beaker of water: this method, originated by the author, kept the fittings under 60°C, when the furnace was at 1600°C.

The platinum/rhodium thermocouple, I, was cemented to the outside of the working tube and used for control purposes; another thermocouple was introduced through J and sealed in, to measure the temperature of the specimens, but its use was discontinued as adequate accuracy (± 3°C or better) was obtained by use of the control couple alone, which latter was standardised against palladium about every six months.

Temperature control was achieved by a Kelvin-Hughes controller, which indicated the temperature in °C from the thermocouple I, Fig.23, to which it was linked by compensating cable, and operated a mercury switch on the output side of a two-gang, 16 amp., Variac : the controller could be set to any value from room temperature up to the limit of the furnace, about 1650°C, and the position of the central thermocouple allowed the temperature of the specimen to be maintained to within 3°C.

The specimen assembly is shown in Fig.25. A mullite thermocouple sheath, A, had a boat, B, of 1/3 fused alumina grog plus "O 60" Alundum, carefully moulded round the end. The sheath, A, contained the measuring thermocouple, and facilitated insertion of the assembly into the furnace with minimum vibration so as not to dislodge the

specimens. A separator, C, was used to prevent interaction of the plaque, D, and the boat, it was either of parallel sided graphite or molybdenum sheet, which latter proved to be admirable in most cases with oxide plaques. The specimen, E was placed centrally and covered by an open ended shield of molybdenum, F, as the working tube was found to powder occasionally. The powdering was most severe when the specimens were temporarily fixed, to aid insertion, by a small drop of glycerine, so this practice was discontinued. Boats similar to Fig.25 but machined from electrode graphite were sometimes used for slag/graphite runs, with no effect on the results obtained: they had no shield, and the thermocouple sheath was replaced by a lug.

The assembly was carefully levelled longitudinally, about once a month, by placing the levelling device, Fig.26, on the boat in position in the furnace: this device was machined accurately parallel from mild steel, and kept in a desiccator when not in use. The telescope of an accurately levelled cathetometer was sighted on the device, and the screw K Fig.23, was adjusted until the tops of the flats on the device were in a straight, horizontal line. Lateral levelling was done by rotating the tube, D, Fig.23, until the top of the plaque was parallel to the horizontal cross-wire in the cathetometer telescope; this was checked several times every run.

The chief object of this work was to measure the contact angle θ as in Fig.1, under different conditions of temperature and atmosphere. This was achieved by fixing an aluminium pointer to the eyepiece of the cathetometer telescope, on which the cross-wires were fixed; and a large protractor, calibrated to $\frac{1}{2}^{\circ}$, was fixed to the body of the

telescope, enabling the contact angle to be obtained to better than 1°. Due to minor differences in specimens, and hysteresis, θ frequently varied by about 2°, or occasionally as much as 5°, for identical experiments, so variation of less than 3° was not considered as very significant. To allow observation of the specimens without undue eye-strain, filters were added to the optical system. Trial showed that the best place for them, with minimum distortion to the image, was in front of the eyepiece of the telescope, where they were fixed firmly but temporarily in a wire holder clipped to the eye-piece, and normal to the telescope axis. In addition to being of a suitable intensity, the filters had to be of optical quality to prevent distortion: two blue Wratten filters were eventually selected, one for below and the other above 1400°C. Apart from personal comfort such filters were essential for a reasonable degree of accuracy.

Great care was taken to prevent contamination of the specimens by any impurity which might have had a large effect on the interfacial relations. They were kept in a desiccator and handled by tongs of chromium plated brass. The plaques were usually polished on their top surface, which was then brushed with a camel hair brush to remove most of the detritus; as they were stored in envelopes in the desiccator, they were again brushed prior to use. If E, Fig.25, was of iron, its surface was carefully filed prior to use; such specimens were stored dry, as xylene and toluene were not found to be efficient in preventing rusting.

The specimens were placed in position, and the working tube

evacuated while the temperature was raised to at least 1000°C, to remove as much of the adsorbed fluids (air, water, etc.) as possible, then purified gas was admitted to a pressure of one atmosphere or perhaps a little more to nullify any small leaks. As soon as the specimens were visible by their emitted light, about 650°C, the tube level was checked. Practically continuous observation was made from several hundred degrees Centigrade below the melting point of the specimen to the end of the run, which sometimes amounted to more than eight hours. Allowing for final preparation of the specimens, and cooling of the furnace, three runs per week were the maximum which could be accomplished. Occasionally two liquid specimens (E, Fig.25) were placed side by side, but this did not result in much saving of time as they moved about slowly and coalesced in about 50% of such duplex runs: this method was of some use for comparisons under identical conditions.

Two readings were taken of the contact angle at each side of the liquid drop every five minutes, or at periods up to 15 minutes, depending on the trend of the values. The difference between the right and left angles for one drop was generally less than 5°, usually in the region of 1°, unless one side touched the edge of the plaque when large differences, up to about 15°, occurred due to disturbance of the normal equilibrium: the apparent contact angle at an edge can have any value between the true contact angles for each face meeting at the edge, thus a true angle of 90° may show an apparent angle between 90° and 180° for two faces at right angles. In such a case the angle at the edge was ignored. Quite long times were required for these angles to settle down

to equilibrium values, generally from one to eight hours, depending on the difference between the actual temperature and the melting point; near the melting point equilibrium was attained very sluggishly. A more detailed discussion for each system is given in the relevant section below, but in general a temperature of at least 50°C above the melting point was necessary for equilibrium to be attained in about an hour.

B. Materials Used and Specimen Preparation:

1. Gas: The chief gas used was special quality argon supplied by the British Oxygen Company. It had been passed over heated magnesium after fractionation, and the chief impurities were other inert gases and nitrogen, amounting to about 0.5%; so it was considered that further purification was unnecessary. It was passed from a pressure reducing valve in the cylinder, through a bubbler containing concentrated sulphuric acid which acted as a rough flow meter; it was then passed up a drying tower containing soda asbestos and anhydrone in that order, then over two zinc boats, each about four inches long, containing phosphorus pentoxide. Two-way glass taps were inserted at strategic points so that the apparatus could be flushed, cylinders could be changed or different gases could be supplied, with minimum delay and risk of contamination. Rubber pressure tubing was used and kept to a minimum; all joints with glass or metal were sealed with collodion and bound with wire. The glass taps were lubricated with high vacuum silicone grease to reduce possible contamination. As mentioned above the mercury manometer was connected at the exit side of the working tube so that there was practically no risk of contamination with mercury vapour.

Carbon monoxide and hydrogen were used, after passing through identical and parallel trains to that mentioned above for the argon, when all undesirable contamination (CO_2 and H_2O respectively) were removed. Slight traces of carbon deposition were found when graphite plaques were used in a CO atmosphere; these were in zones in the working

tube where the temperature was favourable for the reaction:-

$$2\,CO \rightarrow C + CO_2$$

Such deposits were removed by steel wool after each such run.

Nitrogen was passed through a train consisting successively of copper gauze, steel wool and magnesium turnings, all heated to about 700°C; it was then stored in a large flask over freshly distilled water, connected to a supply of more distilled water which was used to displace the nitrogen when required. This gas was dried by a tower containing only anhydrone.

Argon containing a small known amount of water vapour, was obtained by passing it from the cylinder over $CuSO_4 . H_2O$ obtained by heating the usual pentahydrate (Analar quality) for two days at 110°C. The system $CuSO_4/CuSO_4.H_2O$ gives an invariant p_{H_2O} of 0.8 mm Hg at 25°C (Glasstone[134]). Twenty-five grams of the pentahydrate were sufficient, after treatment, to give damp argon enough for more than 150 times the volume of the apparatus at 1 atmosphere. Using this gas, the apparatus was first filled with dry argon which was displaced by a steady flow of the damp argon for 15 minutes. This was done to avoid exposing the copper sulphate hydrate to a pressure less than 1 atm. when the final partial pressure of the water vapour would have been above 0.8 m.m.Hg at 1 atm.

2. Irons: Two grades of iron were used as received and alloyed with carbon. They were electrolytic iron ("Sintrex Super Pure Iron", supplied by George Cohen, Sons & Co.Ltd.)and Armco iron, of the following analyses:-

	C	Si	S	P	Mn	O_2	Al	Mo	
Electrolytic[†]	0.003	0.001	0.004	0.004	-	-	0.01	0.01	% by weight
Armco	0.02	0.002	0.02	0.008	0.02	0.04	-	-	% by weight

[†] These figures are below the limit of accuracy of the spectrographic analysis and are therefore only approximate. Slight traces of gas were found on melting, too meagre to analyse, but presumably H_2.

A hypoeutectic alloy of Armco and carbon was first prepared by heating about 100 gm. iron lumps and filings mixed with graphite powder in a crucible made from a 2 inch diameter Atcheson graphite electrode contained in an outer crucible of Alundum to protect from oxidation. The crucibles and contents were heated to 1200°C for about half an hour, in a carbon granule furnace, then the iron was chill cast in an iron mould, broken up to small pieces with a hammer when cold, and stored in an air-tight bottle. Analysis showed it to contain 3.95%C.

Crucibles about 1½ inches diameter by 2½ inches high were slip cast from ball-milled, acid washed Alundum, in the usual manner, and fired at 1500°C in a carbon granule furnace. All iron alloys, other than the above, were made in these crucibles, placed in an outer crucible, made from a graphite electrode, as an additional safeguard in case the Alundum crucible cracked; they were melted in a vertical molybdenum wound furnace in an atmosphere of pure nitrogen (purified as in the preceding section).

The 3.95%C Armco alloy was remelted and specimens taken. The best method of making specimens was eventually found to be by a

suction sampling technique. A piece of approximately 3/16 inch internal diameter fused silica tubing about 9 inches long had a piece of heavy gauge copper wire about 2 inches long fixed inside it at the top, where it was joined by rubber tubing to a similar tube about 2 feet long, with a rubber suction bulb at the other end. In taking a sample, the metal was held about 50°C above its liquidus, and not more than 100°C above it or it did not solidify fast enough to give a good specimen. The rubber bulb was compressed by hand as fully as possible and the silica tubing was lowered into the furnace, held in the hot zone for about 30 seconds then the pressure on the bulb was very slightly relaxed to draw in a little nitrogen, and then the end of the tube was inserted below the surface of the liquid metal; the pressure on the bulb was fully released and about 2-3 seconds later the tube plus sample was quickly removed from the furnace and the whole lower 9 inches quenched in a nearby vessel of cold water. The copper wire was to prevent the sample rising up the tube too far. Such samples were usually solid rods 3-9 inches long, and analysis proved them to be quite homogeneous in composition over their length. They were broken up with a hammer and percussion mortar to pieces approximately 1/8 inch diameter or slightly larger, and some material was further crushed for analysis. The top bung on the furnace was removed during sampling (usually less than 1 minute) and some air gained access to the furnace; so that when a second sample was taken, about five minutes later, it contained less carbon than the first. Three such samples of 20-30 gm.each were taken, with carbon in the range 3.6-3.3%, and stored separately.

96 gm. of small pieces of electrolytic iron and 4.5 gm. graphite powder were melted and sampled directly as above; a repeat was made with 4 gm. graphite, giving a total of six alloys with carbon in the range 4.5 to 3.3%.

3. Carbon Plaques: Two different pieces of Atcheson electrode with ash at 0.14% and 0.85%, but little significant difference was discovered in their behaviour so they are both termed "electrode graphite" below: the purer was used to make the iron alloys. The electrodes were carefully sawn and polished to give plaques about $\frac{5}{8} \times \frac{1}{2}$ inch and 3/32"-$\frac{1}{8}$" thick, with large faces as parallel as possible: this was done by rough polishing a large radial slice, 2" diameter, testing with a micrometer, and then cutting to plaques which were given a very light final polish on 600 mesh SiC paper. The plaques were dried at 110°C for about a day, and then stored in a desiccator. The approximate analysis of the ash is given below:-

SiO_2	CaO	FeO	V_2O_5	NiO	Al_2O_3	Na_2O	S^+	Resid.	
32	27.5	16	14	2.5	2	2	2	2	% by weight.

+ From S in the graphite.

Flake graphite of uncertain origin had 8.55% ash of the following analysis:-

SiO_2	Al_2O_3	Fe_2O_3	MgO	CaO	Alkalis(K_2O,Na_2O) etc.
52.1	26.3	13.4	2.2	0.5	5.5

It was purified by boiling gently in 1:1 HCl for about two days, followed by a boil for ½ hour with strong H_2F_2 solution: it was then boiled for ½ an hour each with four lots of distilled water, each of which was decanted; then it was dried at 110°C for one day. It was

then found to have 0.46% ash, of a pure white colour, but which was not analysed. The flakes were about 1/16 inch diameter and smaller.

B.D.H. sugar charcoal was ground to -120 mesh and found to have negligible ash.

Difficulty was experienced making good plaques from the flake graphite and from charcoal. Graphite was considered to be the more difficult so more work was done on it. Dry pressing at 5 tons per square inch produced fairly good plaques, with better surfaces than when small additions of water or benzene were made; but these plaques tended to revert to the original loose condition on heating above about 1000°C. (Incidentally, pure dry flake graphite was found to extrude through small orifices quite easily at this pressure). Dextrin and sucrose were tried in various ways, and the best and simplest method was dry mixture of flake graphite with 10-12% dry, finely ground sucrose, mixing was done by careful shaking in a glass tube of the weighed dried components, each mixture being sufficient for only one plaque (1.308 gm.graphite) at a time. Difficulty was also experienced with moulds to contain the plaques during heat treating: the final form, as in Fig.27, was quite successful. It consisted of a mild steel cylinder, internally screwed as shown, and plated with copper to act as a barrier to carbon diffusion. The plugs were machined from electrode graphite, as mild steel seized to the cylinder. The plugs were grooved and drilled as at B (Fig.27) to allow easy escape of gas. A temporary anvil (C), plunger (D) and guide (E) were used to press the plaques, but were replaced by the graphite plugs before the final heat treatment. Separators about 1/32 inch thick, accurately fitting inside

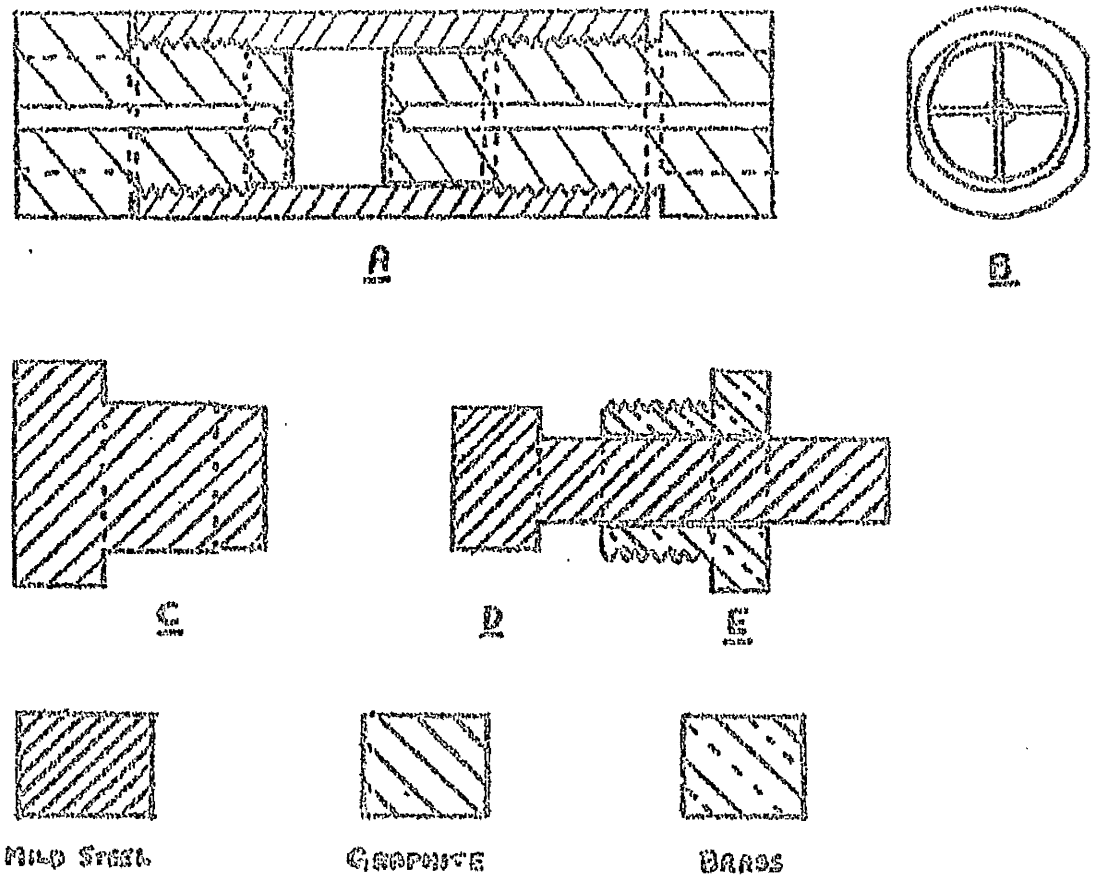

Fig. 27. Mould and Fittings for Graphite Plaques. Actual Size

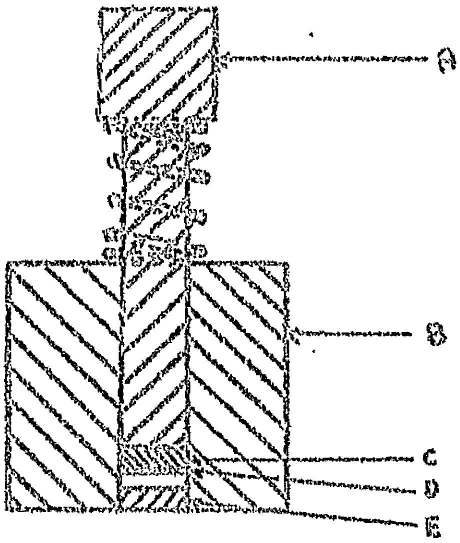

Fig. 28. Press for Refractory Plaques. Half Size

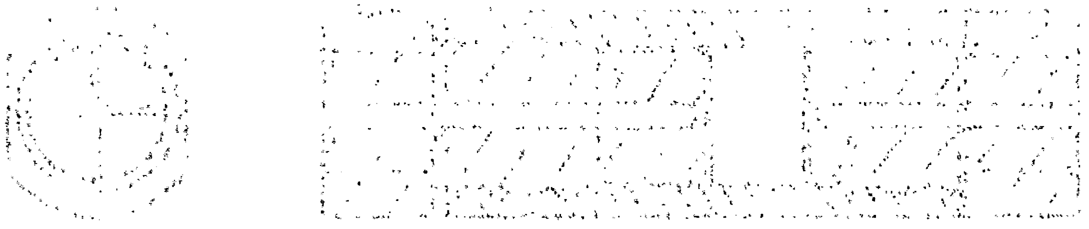

the mould, were used, for which 18/8 stainless steel or pure copper were found to be successful; they were polished carefully before each use. A separator was placed on the anvil (C) and the appropriate end of the cylinder (left, as in Fig.27) lowered into a vertical position on it. The graphite/sugar mixture was carefully added in small amounts, with frequent, gentle tapping to align the flakes horizontally. When sufficient was added, and levelled, for one plaque, another separator was carefully placed in position; the plunger and guide were now fitted and about 15-20 lbs. weight applied by hand. The plunger and guide were removed and the process repeated till four crude plaques were in position, each with a separator on either side of it. The assembly, complete with anvil, plunger and guide were placed on the platform of a mounting press, and a heater placed over the assembly. The heater was $3\frac{1}{2}$ inches of mullite tube fitting quite closely on the cylinder, wound with nichrome wire seated in Alundum and insulated with asbestos rope. Light pressure was put on the plunger (about 10-20 lbs), and $2\frac{1}{2}$ amps were passed through the heater, to heat it to 160°C, as measured by a thermocouple (chromel/alumel) on the anvil. The pressure was then increased to 800 lbs. weight ($\approx$ 1 ton/sq.in) on the plunger, and this pressure and temperature (which is just above the melting point of sucrose) were maintained for 15 minutes. The assembly was then allowed to cool to 60° - 70°C under that pressure before it was removed. The plugs replaced the other fittings, care being taken not to disturb the plaques or separators, and were screwed in as tightly as the fingers only could screw them. The mould (now as in Fig.27A, plus plaques and separators)

was now heated to 750°C for half an hour (which temperature was adjudged to give a balance between risk of carburisation of the cylinder and removal of gases from the sugar) then cooled in position, the whole being done in vacuo, with continuous pumping and with a soda-asbestos tower between the pump and furnace tube to absorb most of the water produced. These plaques were found to be excellent to temperatures above 1600°C; their surface was such that no polishing needed to be done: the flakes were observed microscopically to be orientated to within 2°; and their voidage was only 6.6 to 8.5%, which was good, considering the amount of sugar charcoal likely to be present. Some plaques were made as above but about ½ an inch thick, which were then cut and carefully polished to give plaques with the flakes perpendicular to the surface. These plaques had a slightly higher porosity (9.1 - 9.2%).

Charcoal plaques were made in a similar manner to above, but about 20% of sucrose was required with 0.45 gm. charcoal, and the porosity was very high (in the region of 45-55%).

The theoretical density of graphite is 2.265 gm/cm³ at 25°C, but the densities of the powdered materials only approximated to this value, so the experimental values, (found by the density bottle method, filled in vacuo, each material duplicated or triplicated) were used to ascertain the porosities. The densities for the graphites done in water or xylene were in good agreement, but those for the charcoal varied widely as below:-

Atcheson	Purified Flake	Charcoal	
2.128	2.280	1.61 (xylene)	1.31 (water) gm/cm³

If the vertically orientated flake graphite compacts were not dusted very carefully after polishing, the detritus tended to give a surface with the appearance of very fine velvet on heating to high temperatures (~ 1200°C or above). This also applied to the plaques from Atcheson electrodes. The dusting was done by blowing and by a camel-hair brush.

The electrodes had crystallites roughly orientated[94] so that their [0001] poles were perpendicular to the axis of extrusion, and plaques made as above would have surface free energies very similar to the perpendicularly orientated flake plaques, though in the latter all the [0001] poles would be parallel. In the horizontally orientated flake plaques, virtually only (0001) faces would be in the plaque surface. Thus three quite distinct graphite surfaces were prepared; the charcoal coming into rather a different class, with highly random orientation, extremely small crystallites, and high porosity.

<u>5. Slags and Compound Plaques:</u> The Al_2O_3 and MgO used were pure fused oxides (supplied by the Thermal Syndicate Ltd.) ball-milled for about 24 hours. The Cr_2O_3 was polishing powder, reputedly pure, but found to contain at least 3% volatile compounds, which tended to stain neighbouring furnace equipment. The SiO_2 was derived from quartz, finely crushed, thoroughly boiled with 1:1 HCl, and well washed in distilled water before drying at 110°C for a day, and grinding to -120 mesh. The usual volatilisation with H_2F_2 left no measurable residue in a platinum crucible. All prepared oxides were stored in air-tight bottles. When CaO was required, the requisite amount of dry Analar $CaCO_3$ was used, and mixtures containing the carbonate were roasted to

about 1050°C before melting.

Five slags were made up with analyses as in Table XIX.

Table XIX - Slag Analyses, % Weight.

Slag	%CaO	%MnO	%Al_2O_3	%SiO_2	M.Pt.(°C)
I	38	-	20	42	1265
II	23.25	-	14.5	62.25	1166
III	53	-	47	-	c.1400
IV	35	-	-	65	c.1440
V	-	20.3	18.3	61.4	1345

50 or 100 gm of slag was made up at a time, by weighing out four separate lots of materials, each of which was shaken in a bottle and ground in a mechanical agate mortar for 20 minutes to ensure thorough mixing. Two lots were put into a graphite crucible (from a 2 inch electrode, as for the irons) and melted by high frequency induction heating: when melted the other lots were added and quickly melted, holding for 5-10 minutes above the melting point, and quickly casting in a chill iron mould. Only slag IV showed slight signs of having reacted with the graphite (highest melting point) by exhibiting some light grey areas, which were discarded. These slags were broken up by light blows in a percussion mortar: pieces approximately 2-3 m.m diameter were selected and stored in air-tight bottles.

A mixture termed "CA", of 33% CaO, 67% Al_2O_3, and an approximate Gehlenite (41% CaO, 37% Al_2O_3, 22% SiO_2; stoichiometric - 40.9: 37.2 : 21.9) were made up, each in four lots to 50 gm. as above, but due to their high melting points (> 1590°C) the risk of reaction with graphite was

considered to be too great, so they were separately melted in a platinum/10% rhodium basin in a carbon granule furnace. They too were ground to -120 mesh and stored in air-tight bottles, and used to make plaques. Spinel ($MgO.Al_2O_3$) and picrochromite ($MgO.Cr_2O_3$) were made by a method similar to that used by Rigby, Lovell and Green[135]. Materials were weighed out to give 25 gm. of stoichiometric composition, with the addition of 5% (1.25 gm) of boric acid to act as a mineraliser, and mixed as above. The spinel mixture was dry pressed to a rod at about 10 tons per sq.in., slowly heated in a platinum crucible, in an atmosphere of air to 1550°C (over about 2 days), held for 3 hours, and furnace cooled. This rod proved very difficult to break up prior to grinding to -120 mesh. The picrochromite mixture was dry pressed to plaques about ½ inch thick which were piled, wrapped in platinum foil, and the whole placed in a magnesia crucible and heated in a carbon granule furnace to 1580°-1620°C for an hour; these plaques were much more easily crushed prior to grinding. This method, by analogy to the method of Rigby et al[135], together with the experimental true densities (MA = 3.549, MC = 4.405) which were at least as good as those found by Rigby et al (viz.3.55 and 4.39 respectively), was considered to give practically pure spinels, so no X-ray analysis was done. Mullite was obtained from J.G.Stein and Co. Ltd., which was ground, washed with dilute HCl to remove traces of iron, dried and ground to -120 mesh. Plaques were also made from MgO, Al_2O_3, Cr_2O_3, SiO_2 and technical SiC ("Carborundum").

The following method, after some less successful trials, was found to give good plaques, except in the case of SiO_2 which is treated

separately below. A press was made as in Fig.28. The plunger A, body B and plug E were carefully machined in E.N.24 air cooled from 750°C to give a bainitic structure, and proved to be very successful. An accurately fitting fibre disc C expanded under pressure and prevented abrasive material from wearing the plunger and the major part of the body. It was faced with a polished 18/8 stainless steel disc D, also accurately fitting, to give a good surface to the plaques. The inner face of the plug E was also polished. Repolishing was necessary after pressing 5-10 plaques, depending on the material being used. A scoop was made with a volume sufficient to give a plaque about ⅛ inch thick, allowing for 70% porosity for the loose material. Six or ten scoopfuls of powder were placed in a small evaporating basin and about 3% (0.4 or 0.75 gm. respectively) of a binder, "Carbowax 4,000", dissolved in a few c.c's of warm benzene, were mixed in. When the benzene had evaporated, the cake was reduced to powder. To make a plaque, the scoop was filled, or ¾ filled, according to a trial; this amount of powder was slowly pressed in a mounting press to 10 tons per sq.in.: the whole was inverted, a spacer placed in position, and the body pushed down to reveal the plaque; the spring (see Fig.28) prevented the body from falling on to the plunger head.

The SiO_2 was first heated, in a crucible cut from silica brick, to 1600°C for about half an hour to try to convert it to cristobolite. Very little sintering occurred, and density measurement showed it to consist of approximately equal parts of cristobolite and tridymite, which latter had probably formed in cooling. The above method of compaction was not successful on this material, as the plaques

burst on releasing the pressure. About 5% of "Carbowax 1500", together with careful pressing up to about 9 tons per sq.in., gave quite good plaques.

These plaques were sintered in the carbon granule furnace, on a plate of material which did not react significantly with them. Details of the sintering, together with the porosities and changes in the diameter ($d\ell$) of the resultant plaques are given in Table XX. The densities were found from literature or obtained by experiment on the powder of a crushed plaque. Sintering was tried using several forms of graphite inductors in a high frequency coil, but was unsuccessful chiefly due to poor temperature control; some plaques were poorly sintered, some melted and some partly reduced.

Table XX - The Sintering and Properties of Compound Plaques.

Material	MgO	Al_2O_3	Cr_2O_3	SiO_2	"CA"	Mullite	Gehlenite	M.A.	M.C.	SiC
Temp.(°C)	1600	1550	1600	1600	1500	1550	1450	1550	1550	1600
Time (mins)	30	60	30	20	15	20	10	60	60	60
Plate	MgO	Al_2O_3	Cr_2O_3	SiC	Al_2O_3	Al_2O_3	Al_2O_3	SiC	SiC	SiC
Density (gm/cm^3)	3.65	3.99	5.21	2.35	2.93	2.31	2.94	3.55	4.41	3.23
Porosity (%)	22.3	24.9	36.3	22-35	20.9	20.1	20.1	22.3	30.5	26.9
$d\ell$(%)	-3.97	-1.9	-2.27	+5.7 to -6.4	-0.9	-3.4	+0.3	-4.2	-0.8	-1.8

The Cr_2O_3 at first showed an expansion ($d\ell$ = + 0.8%) on firing to 1500°C with a very high porosity (c.68%), so the plaques were re-fired, as above. The Cr_2O_3 and picrochromite plaques had high porosities, though the rest were in the region 20-25%: it was intended to have all the

plaques as similar as possible (made from -120 mesh material sintered to 20-25% porosity), but the Cr_2O_3 and picrochromite specimens, though outside this limit, were similar to each other. After sintering the SiO_2 plaques, they were quickly removed, on the plate, and the whole placed in a furnace at 500°C, and cooled with the furnace, to avoid risk of spalling and to try to retain most of the cristobalite: the density is seen to be close to that of α cristobalite (viz. c. 2.32 gm/cm^3). Their porosities varied considerably, so only the plaques with porosities in the region 22-25% were used: the very variable change in length possibly was due to inhomogeneity in the amounts of the allotropes present in the original material, though low porosities were associated with high expansions.

These plaques were polished on four grades of silicon carbide papers, from 220 mesh to 600 mesh, apart from the Al_2O_3 plaques. It was very difficult in most cases to avoid contamination with particles of SiC, very slow polishing with frequent cleaning of the paper, and dusting of the plaque with a camel hair brush was necessary. The Al_2O_3 plaques were too hard for successful use of SiC; they were polished using dry ball-milled Al_2O_3 on a sheet of glass followed by light, slow rubbing on the flat surface of an Al_2O_3 boule. All plaques were stored in a desiccator and dusted before use.

C. Experimental Results:

1. Slags on Graphite: The relationships in gas/slag/graphite systems is of interest in the iron blast furnace; chiefly in respect of slag passing over coke; the greater the contact angle the quicker the slag will tend to run off the coke, so that interfacial relations may affect the rate of slag collection and the efficiency of the coke in removing as much iron as possible from the slag. The composition of the slag changes as it passes down the furnace, so it is interesting to examine the wettability of various forms of carbon by slags of various compositions.

Towers[26] examined the wetting of electrode graphite by a blast furnace type slag (40% CaO, 20% Al_2O_3, 40% SiO_2) in nitrogen of deliberately varied purity. She found that the contact angle decreased from about 160° to about 20° over a period of five or six hours. The production of SiO and SiC was examined thermodynamically, and their possible effects on the interfacial relations were discussed, together with the effect of p_{CO}.

Some twenty runs were done by the author on different varieties of graphite, in atmospheres of A (dry and wet), CO, N_2 and in vacuo, over the range 1250°C to 1550°C with six different slags. The general practice was to allow at least 20 minutes (longer at lower temperatures) at each temperature at about 50°C intervals from the melting point upwards. Then the temperature was reduced to about 1000°C to prevent further reaction; the gas was evacuated and replaced, when a new series of readings was commenced. When observations were made in vacuo, they were the last in that run, due to possible change in the composition of the slag: also

the maximum temperature, before the final observations, was limited to 1450°C or below, for the same reason.

Due to their method of manufacture the slags were glassy and softened over a range of temperature. They took a long time to reach equilibrium just above the melting point, and to achieve equilibrium in a period of a few hours, a temperature of at least 100°C above the melting point was necessary. On melting they showed angles from about 90° to 150° but generally approached equilibrium from about 5°-10° above the equilibrium angle. On heating the silicious slags to the region of 1500°C, reaction frequently occurred and will be discussed in more detail below. Between those temperatures (T_m + 100°C and 1500°C), temperature was found to have no significant effect within the limits of error (~ 2°) if the equilibrium angle was attained. Accordingly the results given in Table XXI are those obtained in the region 1400°- 1450°C for presumed equilibrium values.

The surface free energies of the slags in nitrogen (γ_{LG}) were obtained from King[7]: extrapolation being necessary except for Slag V so the figures are only approximate with an error of 5% or less. The atmospheres are self-evident except perhaps for line 25 where A_{H_2O} means argon with p_{H_2O} of 0.8 mm Hg as described in B1 above. Plaques A and B are two different specimens of electrode graphite with ash contents of 0.85% and 0.14% respectively: the sign "=" means flake graphite plaques with the flakes parallel to the surface, and "⊥" signifies one with vertically orientated flakes: as before, θ is the contact angle, and W_{AD} the work of adhesion. Only those results

Table XXI.

Contact Angles and Work of Adhesion of Slags on Graphite, at 1400°-1450°C.

Slag					γ_{LG} erg/cm^2	Atm.	Plaque	θ°	W_{AD} erg/cm^2	line
No.	CaO	MgO	Al_2O_3	SiO_2						
I	38	-	20	42	437	A	A	127	174	1
							B	125.5	178	2
							=	125	186	3
							⊥	134	133	4
						CO	A	124.5	190	5
							B	126	180	6
							=	124.5	190	7
							⊥	132	145	8
						Vac.	A	146	75	9
							B	147.5	69	10
							=	132	145	11
							⊥	136	123	12
II	23.25	-	14.5	62.25	360	A	A	131.5	121	13
							=	126	138	14
							⊥	128	148	15
						N_2	A	125	154	16
							=	125	154	17
						CO	A	139.5	83	18
							=	126	148	19
						Vac.	A	(150)	(43)	20
							=	(140)	(84)	21
III	53	-	47	-	580	A	A	135	170	22
IV	35	-	-	65	345	A	A	(140)	(81)	23
V	-	20.3	18.3	61.4	390	A	⊥	128	154	24
						A_{H_2O}	=	127	156	25
I (+ 3.3% FeO)					437	A	=	(130)	(156)	26

which were derived from runs regarded as successful are included: for example, one plaque gave persistently high contact angles (~ 150°) with two different slags, this may have been due to a difference in purity in that plaque from the others, so these results are not included. The bracketed values are uncertain chiefly because a reaction was in progress so that equilibrium values were not obtained; the bracketed values are the mean of the advancing and receding angles.

From lines 1-10 it is at once seen that there is no significant difference in the wetting properties of the two electrode graphites: from lines 1-15 the values of θ and W_{AD} for those specimens are seen to be between those for the horizontal and for the vertical flake specimens, or θ is above and W_{AD} below those values, showing that the electrode graphite was on the whole more similar to the vertical flake compacts than to the horizontal. This was expected from structural considerations already mentioned (part B3, this chapter). Results for the electrode specimens were poorly reproducible, due to poor orientation and perhaps variations in purity. In lines 3,4,7,8,11, 12,14 and 15, θ is seen to be lower and W_{AD} higher for the horizontal flake than for corresponding values for the vertical flake, though the differences are not consistent. This is a case where a surface with a lower surface free energy (c.2300 erg/cm^2) is wet slightly better than a similar surface with a higher surface free energy (c.3850 erg/cm^2), and is rather exceptional in this respect.

It is also clear from lines 1-21, that the contact angle is greater in vacuo than with a gas present. Evacuation would tend

to cause desorption of gas, and increase the surface free energies: increase in γ_{SG} would cause an obtuse θ to decrease; a similar increase in γ_{LG} would cause θ to decrease; and an increase in γ_{SL} would cause θ to increase. Since an increase in θ was observed, the change in γ_{SL} must be of major importance. This is rather surprising as the solid/liquid interface is the least accessible to adsorption and desorption. With the exception of line 18, the contact angles are lower in CO than the corresponding angles in A; this would be expected as CO is likely to be chemisorped and have a larger effect on the surface free energies than A. N_2 would also be expected to behave more like CO than A, but the differences in wetting are not significant in this case (lines 13-19). Line 25 shows the effect of about 1.05% of water in the argon, comparing the values in this line with those in lines 14, 15 and 24, it is seen that this amount of water has a negligible effect on the wetting of graphite by slag. The time required to regain equilibrium after changing the atmosphere was similar to, or less than, the time required to reach it in the first place when the gas was already present at the interface; so that solution and diffusion of the gas to or from the interface is not the rate controlling factor; the chief factors in this respect are possibly the high viscosity of the slags and the time required to attain favourable orientation of the slag molecules/ions at the solid/liquid interface.

Comparing slags I, II and IV, θ increases slightly as the percentage of SiO_2 increases; a similar effect was found by Towers[26] on platinum. Increase in SiO_2 lowers γ_{LG} (second column, Table XXI); so this is a case of an obtuse contact angle being increased by a

decrease in γ_{LG}, as would be expected from the Dupré equation. From lines 1, 13, 22, and 23, variation of Al_2O_3 is seen to have an indeterminate effect on wetting, although it is well known to raise γ_{LG}, so that Al_2O_3 must have a similar but smaller effect on γ_{SL}. From lines 14 and 25, 15 and 24, θ is seen to be virtually the same whether the slag contains MgO or CaO; the slight increase (30 erg/cm^2) on replacing CaO by MgO produces a slight increase in W_{AD}, and a slight increase in γ_{SL} must also result.

The silicious slags tended to be reduced by the graphite in the region of 1500°C, due to their SiO_2 content, as CaO and Al_2O_3 are quite stable in the present of carbon at this temperature. With slags I and II in argon, faint luminous clouds, possibly of SiO were observed near the three phase boundary below 1490°C, but no bubbles of gas were observed to form in the slag below 1500°C : such bubbles would form when the total pressure of the gases present was in the region of one atmosphere, but the gas clouds were presumably formed by diffusion from the slag and the reaction pressure in this case was indeterminate. In vacuo slag I showed bubbles bursting from the slag at 1500°C, and slag II showed a similar effect as low as 1250°C for electrode graphite and 1300°C for horizontal flake graphite (see lines 20 and 21, Table XXI) which indicates a faster rate of reaction was obtained with the specimen of higher surface free energy. Slag III, with no SiO_2 showed no visible reaction up to 1550°C. Slag IV had an unfortunately high melting point but reacted rather violently at 1500°C in A. Slag V seemed to show slightly less reactivity than the comparable CaO slag (II), which is rather surprising as a_{SiO_2} would be higher due to the

lower basicity of MgO. Water in the atmosphere had no noticeable effect on reaction. Towers[26] found a reaction temperature of 1520°C at which gas bubbles were evolved, and assumed that this represented evolution of CO at a pressure of one atmosphere due to the reaction $SiO_2 + 3C \rightarrow SiC + 2CO$. This assumption was in good agreement with the then accepted thermodynamic data. More recent work by Baird and Taylor[136] on this reaction showed that reaction pressures are much lower than those calculated by Towers, and for a slag of the composition used by Towers the reaction temperature for p_{co} of one atmosphere is above 1600°C. It would appear therefore that the above reaction could only take place at a temperature as low as 1520°C if the p_{co} were less than one atmosphere and the total pressure of the gas evolved were raised by an inert gas such as N_2 evolved from the plaque.

When reaction produced bubbles of gas in the slag, the slag swelled and collapsed giving variable contact angles, varying by as much as 30° in some cases. On cooling till the reaction ceased the contact angle always fell to lower values than obtained before the reaction; this may be due both to the smaller amount of SiO_2 left and to the effect of the reaction products (CO, SiO & SiC) chiefly on γ_{SL} . In line 23 Table XXI, where reaction was allowed to proceed quite far before reducing the temperature below 1490 °C when reaction ceased, θ dropped to 77° which was the lowest contact angle observed in this series. Towers[26] found the contact angle, for a slag similar to slag I, to fall below 90° in about two hours and to approach values in the region of 20°. The author melted slag II on a SiC plaque in A at 1250°C, and θ was observed

to fall to between 6° and 10° in two hours, so it seems likely that wetting is produced by SiC in slag/graphite systems: the SiC would be produced at the solid liquid interface, and when present in sufficient quantity it would tend to give the graphite an effective surface of SiC over which the slag would spread to a low contact angle. This spreading tendency was observed after reaction in low p_{co} atmospheres when production of SiC is thermodynamically possible. However spreading was not observed at any time in this series when the specimens had not been heated above 1490°C, even when new graphite boats were used to avoid possible contamination. Two reasons can be suggested why Dr. Towers found low contact angles, whereas the author did not. Firstly, Dr. Towers granulated her slag by pouring it into water, for which a high temperature would be required, possibly causing reaction with the graphite crucible, whereas the author took care to melt his slags at as low a temperature as possible (see B.5 above). The solubility of SiC in slags is not known, but the slag/SiC run indicated that it is low, so this reason is not very likely. Secondly, large differences can exist in the ash composition of different samples of electrode graphite, and it is possible that some constituent in the graphite was responsible for the wetting found by Dr. Towers: in the present series with purified graphite such a constituent was not actively present. This active constituent could act as some form of catalyst to the SiO_2/C reaction speeding up the formation of SiC, or it could be in the form of a carbide which is wet by the slag. This explanation is regarded as the more likely. From the analyses quoted, vanadium

compounds are seen to be present in some electrode graphites but absent in the flake graphite, and these may act as catalysts, or VC films may cause wetting. It is well known that the reaction between SiO_2 and carbon is very slow, and kinetic studies of this system would be very interesting. After reaction had occurred the slag was always found to be of a grey colour, possibly due to a dispersion of carbon, but due to the very small amount of this impurity analysis was not attempted.

In line 27 the FeO slag melted at a slightly lower temperature than the pure slag I, but the contact angles varied rather more than usual due to iron coming out round the periphery of the slag and interfering with the equilibrium. The reduction of FeO caused no other effect on the wetting, nor did the small amount of Feo left after the run (a faint blue colour in the slag was just visible).

The wetting of coke by slag in an iron blast furnace may be greatly influenced by traces of impurities (vanadium compounds?), but in their absence coke is not likely to be wet till fairly low in the furnace where the production of SiC is more feasible.

<u>Conclusions:-</u>

1. Slags containing only CaO, MgO, Al_2O_3 and SiO_2 do not wet graphite, the contact angles being 125° to 150°, and $W_{AD} \sim 50$ to 200 $ergs/cm^2$.
2. Temperature does not seem to affect the equilibrium value of θ, provided negligible reaction occurs, but higher temperatures give a quicker attainment of equilibrium for any slag.
3. θ is lower and W_{AD} higher for low surface free energy graphites than for those with high surface free energy.

4. θ is reduced and W_{AD} increased when a gas is present, CO and N_2 having slightly more effect than A.
5. Increase in SiO_2 results in slightly higher θ and lower W_{AD}. The wetting properties of a slag do not seem to vary, whether it contains of CaO or MgO; and Al_2O_3 has an indeterminate effect on θ.
6. When reaction has occurred, the wetting tendency of silicious slags is increased, probably due to some reduction product of SiO_2, such as SiO.
7. A small quantity of water (~ 1%) in the atmosphere has no effect on the wetting, and small quantities (< 3.3%) of FeO do not affect it either.

2. Iron on Graphite: Little previous work seems to have been done on iron/graphite systems, though the results are of importance in connection with wetting of coke and carbon bricks in a blast furnace, and of graphite moulds in foundry work. The interfacial relations could perhaps be extrapolated to a solid iron/graphite system when they would be very interesting from a point of view of graphitisation and nucleation phenomena in cast irons.

Before considering the experimental results it is as well to review some of the work on the surface free energy of liquid iron/carbon alloys: many workers have essayed this field and produced a very wide range of results. Bickerman[137] quotes results on five impure irons in the range 820-1200 ergs/cm^2, four of which have positive temperature coefficients - which are quite common in reports on work on cast irons. For pure iron Becker, Harders and Kornfeld[138] found an improbable value of about 900 ergs/cm^2 at 1540°C: Sauerwald, Schmidt and Pelka[139] obtained

1350 erg/cm^2 at 1550°C with a coefficient of about −0.04 erg/cm^2/°C. Bondi[28] quotes a value of 1700 at 1550°C. Kingery et al have given several values, their most recent[140] being 1720 erg/cm^2 at 1570°C: Kozakevitch et al have also done much work in this field and their most recent value[141] is 1835 ± 15 erg/cm^2 at 1550°C. These last five results are all for electrolytic iron and in approximately chronological order, so the tendency is towards higher results as experimentation presumably improves. A likely value at 1550°C is then 1800 ± 50 ergs/cm^2. One unreliable result[139] has been found for the temperature coefficient for pure iron: by analogy with gold, which has a similar boiling point and presumably a similar critical point to iron, from values in Bondi[28], this coefficient has been estimated at about −0.71 erg/cm^2/°C. Armco iron has a value about 150 erg/cm^2 lower than electrolytic iron, as found by Kingery and Humenik[142], so we may assess its value to be 1650 ± 100 erg/cm^2 at 1550°C with a coefficient of about −0.65 erg/cm^2/°C. Theoretical results for pure iron (e.g. 37 and 143) give γ_{SG} = 4,000–5,000 ergs/cm^2, with γ_{LG} about 1600 erg/cm^2 lower at 1550°C (using $\frac{d\gamma}{dT} = -0.7$, and $\Delta\gamma$ on melting about −400 erg/cm^2 from Bondi[28] p.433): these results are almost twice the values obtained from experimental work, and do not seem to be reliable, so they are disregarded here.

The effect of carbon is not very clear; most work indicates that it lowers γ_{LG} for example Kozakevitch, Chatel and Sage[144] give the equation:–

$$\gamma_{LG} = 1600 - 100\ (\%C).$$

However the more recent work of Halden and Kingery[140] seems preferable,

and it shows that carbon has no effect on γ_{LG} up to 3.39%.

Again about twenty runs were done, and they met with rather less success initially than with the slags. Electrode graphite was first used, with Armco/C alloys, and gave contact angles in the range $63^\circ - 130^\circ$, the lower results were obtained with the graphite with lower ash content. After the runs were completed, examination of the plaques showed minute particles of glassy material scattered over the surface, derived from the mineral content of the graphite as they were more abundant with the high ash graphite. Thus minerals in the graphite interfered with the wetting and gave high contact angles. Some part of this glassy material was also derived from a powder which fell from the tube, above about 1100°C, so a molybdenum shield was fitted over the specimens: this powdering was associated with the use of very small amounts of glycerine which were used temporarily to hold the specimens in position during insertion, possibly due to cracking of the glycerine to some products which slightly attacked the tube, and the powdering became negligible when the use of glycerine was discontinued.

Due to the effect of minerals in the graphite it was thought that small amounts of oxides in the Armco iron could also interfere with the wetting, so electrolytic iron/carbon alloys were used and gave contact angles down to 60° with parallel flake compacts, and down to 53.5° with vertical flake compacts. When the polishing detritus was not removed, it adhered to the surface of the drop and also hindered wetting (c.f. water on a dusty surface). Further to investigate the effect of the iron on wetting, specimens of Armco and of electrolytic iron were observed on parallel flake compacts in argon, with results as below:-

Temp.	1350°C	1450°C
Armco	61°	59°
Electrolytic	52.5°	51.5°

The steady difference in θ of about 8° was observed throughout these runs. Similar runs with perpendicular flake compacts showed angles about 50° for the electrolytic iron, with those for Armco 4° - 6° higher. So that oxides and perhaps other minor impurities in the Armco hindered wetting. The tendency for the contact angle to decrease with increasing temperature was also general in these runs, but was due to the iron dissolving the plaque beneath it and forming a shallow cavity which deepened at higher temperatures due to increased solution: the walls of these cavities were at 1°- 2° to the surface of the plaque, so that the true contact angles were at least 1°- 2° greater than those observed, so it was considered desirable to try to avoid cavitation, by experimenting with hypereutectic carbon alloys at their liquidus temperatures. Hypo-eutectic irons melted in the region of 1250°C and took close to 2 hours to reach equilibrium at 1350°C; the time to reach equilibrium was decreased at higher temperatures, so long periods of observation for runs at the liquidus temperature were expected. Runs in vacuo and in argon showed lower and higher contact angles rather indiscriminately, but the differences were not greater than about 2° so were not significant.

A series of runs, each lasting for two to four days, was carried out with three hypereutectic electrolytic iron alloys, with results as in Table XXII.

Table XXII.

Contact Angles of Hypereutectic Iron Alloys on Graphites.

%C	Temp. °C	Run	Graphite	Atmosphere	θ°	Time(hrs.)
4.51	1247	1	=	A	62	11
				Vac.	59	2
		2	⊥	A	58	10
4.40	1205	3	=	Vac.	69	13
				A	65	2
		4	⊥	Vac.	55 59	5½ ½
				A	54	5
4.30	1160	5	=	A	58.5	19
				H_2	38	2½
				Vac.	42	1½
				A	42.5	4
		6	⊥	Vac.	55.5 59	2½ 3½
				A	58	1
				H_2	37	5

The irons for runs 1 and 6 melted with initial angles of 130° and 140° respectively, and all the others melted at 110°; the iron tends to sphere on melting much more readily than the slags, chiefly due to the lower viscosity and higher surface free energy. The types of graphite are represented as previously. In the second and subsequent days of these runs, the specimens were reheated to 1000°C in vacuo and then the atmosphere altered as desired; it was not thought advisable to leave the experiment in progress overnight. The contact angle was seldom affected by more than 2° by this cooling and repeating, run 5 with a change of 10° was the worst. The whole of run 5 is shown graphically in Fig.29. The first day of this run the results were rather erratic but a more normal decrease in θ took place on the second day with a slight pause in the fall at 90° which was very common in these runs. The first day of run 4 (Fig.30) also shows this pause quite clearly, and a more regular drop in θ for the first 5½ hours. Apart from run3, parallel flake graphite shows an angle of 59° in vacuo with no change with temperature in the range 1160°-1247°C, and the time to reach equilibrium decreases with increasing temperature: unfortunately the rather erratic manner of this drop in θ precludes calculation of an activation energy. For the perpendicular flake graphite, runs 4 and 6 show a primary angle of 55° and a secondary angle of 59°, run 2 does not show the primary value. This increase, as shown in Fig.30 at about 6 hours, was quite marked and reproducible, and it was believed that the surface structure of the graphite was somehow altered; by solution and deposition of carbon by the iron as the self diffusion of graphite is quite negligible at this temperature. It was not at all likely that a

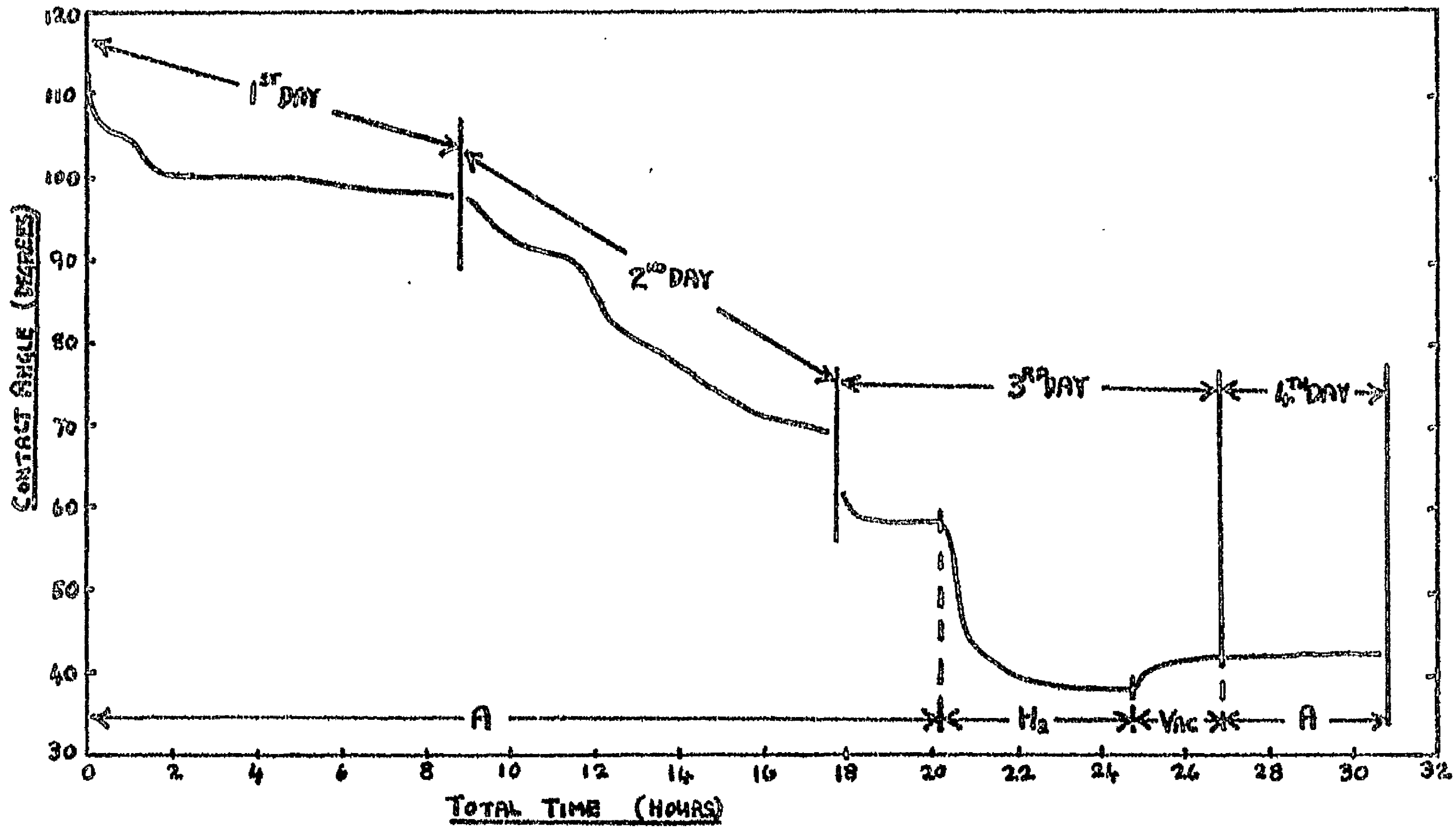

FIG. 29. VARIATION OF CONTACT ANGLE WITH TIME, IRON + 4·30%C ON HORIZONTAL FLAKE GRAPHITE, AT 1160°C.

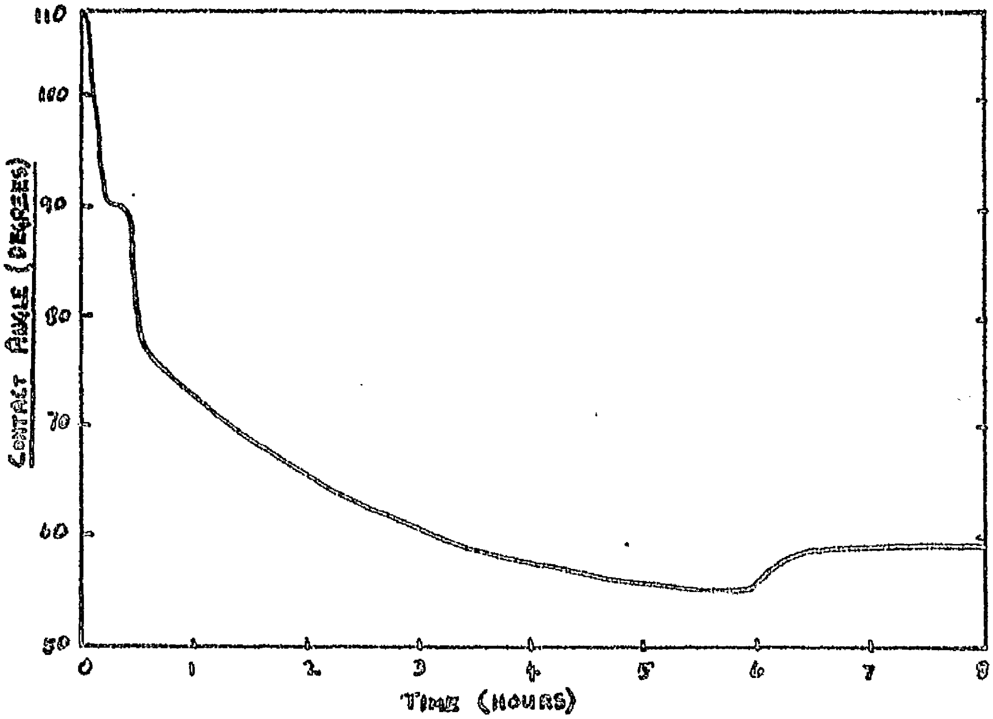

FIG. 30. VARIATION OF CONTACT ANGLE WITH TIME, IRON + 4·40%C ON VERTICAL FLAKE GRAPHITE AT 1205°C, IN VACUO.

surface similar to (0001) was produced, so another structure was sought and found, the $(3\bar{3}00)_M$ as discussed in Chap.IIIA. The normal $(3\bar{3}00)$ possibly changed to the modified form with a higher contact angle, in about 6 hours. Run 2 did not exhibit this change in A as equilibrium was not attained in under 11 hours by which time the structure would have been altered and only the secondary angle (59°) was observed.

The change from vacuum to argon had an indeterminate effect on the contact angle. The lowering in θ on change to hydrogen is however quite definite (runs 5 and 6) with θ at 38° and 37° with parallel and perpendicular graphites respectively, the difference (1°) is not regarded as significant. This change was not quite reversible, as is seen from Fig.29, possibly due to desorption of hydrogen not being complete. Reductions in acute contact angles on admission of a gas must be due to the reduction of either or both γ_{LG} and γ_{SL}, as a reduction in γ_{SG} only would increase θ. The effect of A is not determinate, but H_2 is quite soluble in iron and could lower γ_{LG} and eventually γ_{SL} - it must lower at least one of these parameters. The effect of H_2 on γ_{LG} is not known, but N_2 is quite surface active and can lower γ_{LG} by about 200 erg/cm^2 at 0.093% in iron[140], so H_2 may have a similar or greater effect.

If a value of $\gamma_{LG} = 1800$ erg/cm^2 is accepted, since all the contact angles are in the region of 60° in A, $\gamma_{LG}\cos\theta = 900$ erg/cm^2; thus $(\gamma_{SG} - \gamma_{SL}) = 900$ erg/cm^2. Since γ_{SL} cannot be less than zero, γ_{SG} cannot be less than 900 erg/cm^2 in the region of 1200°C, or less than about 1100 erg/cm^2 at 0°K. The lowest reported value for 4-5% C

[illegible]

[illegible]

[illegible]

[illegible]

[illegible]

alloys is 600 erg/cm^2 and is very doubtful in view of the above review. Thus the surface free energy of the basal plane cannot be 150 erg/cm^2 and the van der Waal's calculation in Chap. IIIA cannot be upheld, leaving only the approximate Ruff's method values, which are of the correct order. Using these values, various parameters for this system in vacuo are given in Table XXIII, in erg/cm^2 or degrees.

Table XXIII - Values of Various Parameters for Carbon Saturated Iron on Graphite in Vacuo.

	1247°C			1205°C			1160°C		
	=	⊥	⊥'	=	⊥	⊥'	=	⊥	⊥'
γ_{LG} (erg/cm^2)	2015	2015	2015	2045	2045	2045	2077	2077	2077
θ°	59	(55)	59	59	55	59	59	55	59
W_{AD} (erg/cm^2)	3050	(3170)	3050	3100	3220	3100	3150	3270	3150
γ_{SG} (")	2440	3995	3930	2460	4025	3960	2480	4055	3990
γ_{SL} (")	1402	(2840)	2892	1406	2852	2906	1410	2864	2920

In the third column the contact angle and derived parameters are based on an assumption, as mentioned above. The temperature coefficient of at about 1200°C is negative and in the region -0.093 to -0.325 erg/cm^2/°C, which would lead to a hypothetical critical solution temperature between iron and graphite in the region of 10,000° to 15,000°C : since this is well above the critical temperature of either component, it may be assumed that they will never be completely miscible.

A plaque was made from pure sugar charcoal in a similar manner to the graphite plaques, but with 20% sucrose added and the whole finely ground before pressing: it had a porosity of 55% (using the true density

of graphite). A specimen of 4.5% C iron was observed on this plaque at about 1300°C, when the contact angle fell gradually, and the specimen was completely absorbed into the plaque in about an hour. Examination when cold showed the plaque to contain a slight cavity with a small amount of kish in it. 1300°C is above the liquidus temperature (1247°C) for this alloy, so kish could only have remained if the iron preferentially dissolved carbon from the charcoal, so it would seem that charcoal was more soluble in iron than is graphite up to at least 1300°C, which would be expected as charcoal is metastable with respect to graphite. This dissolution of charcoal and possible precipitation of kish may have been responsible for the complete absorbtion of the iron into the plaque.

The only previous work found with reference to this system is by Humenik and Kingery[146]. They melted Armco iron on electrode graphite at 1550°C : their results in He and H_2 (viz. $\theta = 51^\circ$ and 37° respectively) are similar to those above, though it would be expected that their angles would be lower by an uncertain amount due to solution cavities much more severe than any found by the author, and higher than such values for electrolytic iron(8°?), the two effects being approximately equal and opposite. However they also observed a contact angle of zero in vacuum. It is difficult to account for this result, but it remains as an isolated observation against the author's many in which the contact angle never fell below 37°.

With impure iron, containing oxygen, sulphur and nitrogen, as does pig iron, the surface free energy will possibly be about 1200 ergs/cm^2, and it will probably wet graphite with a contact angle less

[illegible]

[illegible]

[illegible]

[illegible]

[illegible]

[illegible]

than 60°, giving an iron/graphite interfacial free energy less than $(\gamma_G - 1200\cos 60^\circ)$ viz. $(\gamma_G - 600)$ erg/cm^2, where γ_G is the surface free energy of the graphite. With representative figures of $\theta = 130^\circ$ and $\gamma_{LG} = 400$ erg/cm^2 in a slag/graphite system, the interfacial free energy is about $(\gamma_G + 260)$ erg/cm^2. Thus the difference in interfacial free energies (slag/graphite − iron/graphite) is 860 erg/cm^2 or more. In a system containing liquid slag, liquid iron and graphite, $\gamma_{LL} \cos\theta = 860$ erg/cm^2, so if the interfacial free energy between liquid slag and liquid iron (γ_{LL}) is not greater than 860 erg/cm^2, θ will be zero and iron will displace slag from graphite surfaces. Work is later shown (Part 4) which suggests $\gamma_{LL} = 1500$ erg/cm^2 so it is not very likely that iron will thus displace slag; but γ_{LL} is also shown to be possibly 1000 erg/cm^2 or slightly lower, and this would constitute a borderline case. No observations of such a displacement are known to the author so γ_{LL} is probably > 1000 erg/cm^2.

Conclusions:

1. Pure iron in equilibrium with graphite at 1160°-1247°C in vacuo, wets it with angles from 55° to 59°, with work of adhesion in the range 3270 to 3050 erg/cm^2.
2. From these figures it is shown that $\gamma^{\circ}_{(0001)}$ for graphite cannot be < 1100 erg/cm^2.
3. Temperature does not affect θ at equilibrium in this temperature range, though higher temperatures speed the attainment of equilibrium. Very long times (c.19 hrs) are required to reach equilibrium at 1160°C suggesting a high activiation energy of wetting.
4. The normal perpendicular flake compacts exhibit better wetting with iron than do the parallel flake compacts

with the lower surface free energy. A modified structure for the perpendicular flake surface has been postulated to form, from a change in θ after about 6 hours in the region 1100°- 1200°C.

5. Wetting is enhanced by an atmosphere of H_2, which may be surface active with respect to γ_{LV} or to γ_{SV} or to both.
6. Wetting is hindered by small amounts (0.85%) of mineral matter in the graphite, and by very small amounts of impurity in the iron, probably by acting as physical barriers to the advance of the three phase boundary; graphite detritus also acts in this manner.

3. Iron on Oxides: These runs were, in general, the least satisfactory of this series, because of their poor reproducibility, due to the large effect of traces of contaminants and possibly also due to the high porosities of the plaques. Iron is particularly susceptible to contamination due to its reactivity, and high surface free energy which is easily lowered by traces of impurities such as oxygen and nitrogen[140], silicon[69] and sulphur[147]. In the previous runs the graphite plaque helped to control any traces of oxygen, but with oxide plaques retained, adsorped air possibly supplied some of these gases to the iron. With most of the plaques chemical reaction occurred and precise measurements were not possible due to irregular pitting of the plaque and products of the reaction obscuring the interface. About two dozen runs were done, generally using at least three irons (pure, hypo-eutectic and hypereutectic samples) for each type of plaque. Only A and vacuo were used for the atmosphere, when vacuo exhibited generally lower contact angles by 5°- 20°: all the results quoted below are for atmospheres of A, unless stated otherwise.

The initial melting, in the absence of pronounced reaction, gave angles of 160°- 170° for alloys of carbon close to the eutectic point (4.40%C), which angles were quickly assumed; with lower carbon (c.3.5%) the initial angles were in the region of 150° presumably due to the range between solidus and liquidus; and pure iron showed initial angles of 145°- 147°. These angles fell slowly to equilibrium values, the speed again depending on the difference in temperature above the liquidus. When reaction occurred the specimen melted irregularly with angles from about 60° to 160°, depending on how much reaction had already occurred. The standard free energies of formation of some relevant oxides are given below (from Kubaschewski and Evans[116]).

Table XXIV - Free Energies of Formation at 1500°C from elements in their Standard States (+ $\frac{1}{2}O_2$).

Oxide	CO	FeO	MgO	$\frac{1}{3}Al_2O_3$	$\frac{1}{2}SiO_2$	SiO	$\frac{1}{3}Cr_2O_3$	CaO
$-\Delta G$(Kcal/mole)	63.85	36.42	89.85	101.95	67.85	55.95	52.55	107.45

Given unit activities carbon will reduce SiO_2 and Cr_2O_3 but iron will not reduce any of these oxides: the activities of carbon and the products from the reduction of these oxides will be far from unity so it is not possible to predict reactions without further data. Each plaque material is considered individually below.

Al_2O_3 No reaction was observed, as would be expected from Table XXIV; except in one case when some air was inadvertently admitted with the argon when using pure iron, when "slag" (FeO) was observed to run off the iron on to the plaque, and when molten, contact angles of 50°- 60° were observed. In one or two other such accidents was also lowered due to the surface activity of FeO. With electrolytic iron in A,

θ was 141.5° and in vacuo θ was 118° both at 1550°C. Carbon decreased θ and γ_{SL}, with a change in θ with %C close to − 1.8°/%C, and in γ_{SL} of about − 35 erg/cm^2/%C. The relevant figures are given in Table XXV with those for other oxides.

Table XXV - Interfacial Data for Irons on Oxide Plaques in Argon.

Plaque	%C	Temp. (°C).	θ°	γ_{LG} (erg/cm^2)	W_{AD} (erg/cm^2)	γ_{SG} (erg/cm^2)	γ_{SL} (erg/cm^2).
Al_2O_3	0	1550	141.5	1800	390	778	2190
	3.67	1350	145	1942	350	823	2410
		1450	135	1870	550	800	2120
	4.40	1350	143	1942	390	823	2370
		1450	133.5	1870	580	800	2090
MgO	0	1550	130	1800	640	1730	2890
	3.54	1300	131.5	1977	670	1850	3160
	4.40	1300	132	1977	650	1850	3170
Gehlenite	-	1450	133	1870	600	600	1880
Mullite	4.4	1250	130	2013	720	350	1040
C.A.	-	1450	130	1870	670	650	1850
Spinel	-	1450	131.5	1870	650	2000	3240

MgO: Since Mg boils at 1105°C, reduction above this temperature may lead to a low p_{Mg} so that reduction is more likely than would be expected from Table XIV. There is no significant difference in the data in Table XXV for 3.54 and 4.40%C, and θ is close to that for pure

iron, so that the effect of carbon is indeterminate or negligible. When the temperature of the iron/carbon alloys was raised to 1400°C, their contact angles rose by 10° to 142°. This was observed in yet another run with 4.4%C iron. On raising the temperature to about 1500°C a tiny cloud of gas was observed near the interface which could be CO and Mg vapour, so presumably, since the contact angle now remained constant, some reaction occurred between 1300° and 1400°C and θ was raised. This could be brought about by a small amount of FeO in the iron lowering γ_{LG} (Halden and Kingery[140]) and causing θ to increase: any FeO at the solid/liquid interface would lower γ_{SL} and decrease θ, so presumably most of the FeO produced went to the iron; only very faint discolourations of the plaques after these runs, showed little FeO to be present in them. Again, an electrolytic specimen observed in A with an inadvertent trace of O_2 in it, showed contact angles down to 110°, and quite heavy contamination of the plaque with FeO. So it is possible that a trace of FeO chiefly affects γ_{LG} raising θ, and more FeO affects γ_{SL} lowering θ.

SiO_2 : With every alloy from 0 to 4.4%C reaction was observed with considerable lowering of θ. This lowering occurred in a very erratic manner, as is seen from Fig.31 where both left and right angles for one specimen of electrolytic iron are plotted; equilibrium seems established at about 55° after about 2½ hours at 1540°C. Results for Armco iron were similar but 3°-5° higher. Gas clouds were observed near the specimens (not bubbles of gas), which could only be SiO from the reduction of SiO_2 by iron, and these clouds were observed to increase markedly on cooling from 1540°C until recalescence was observed at

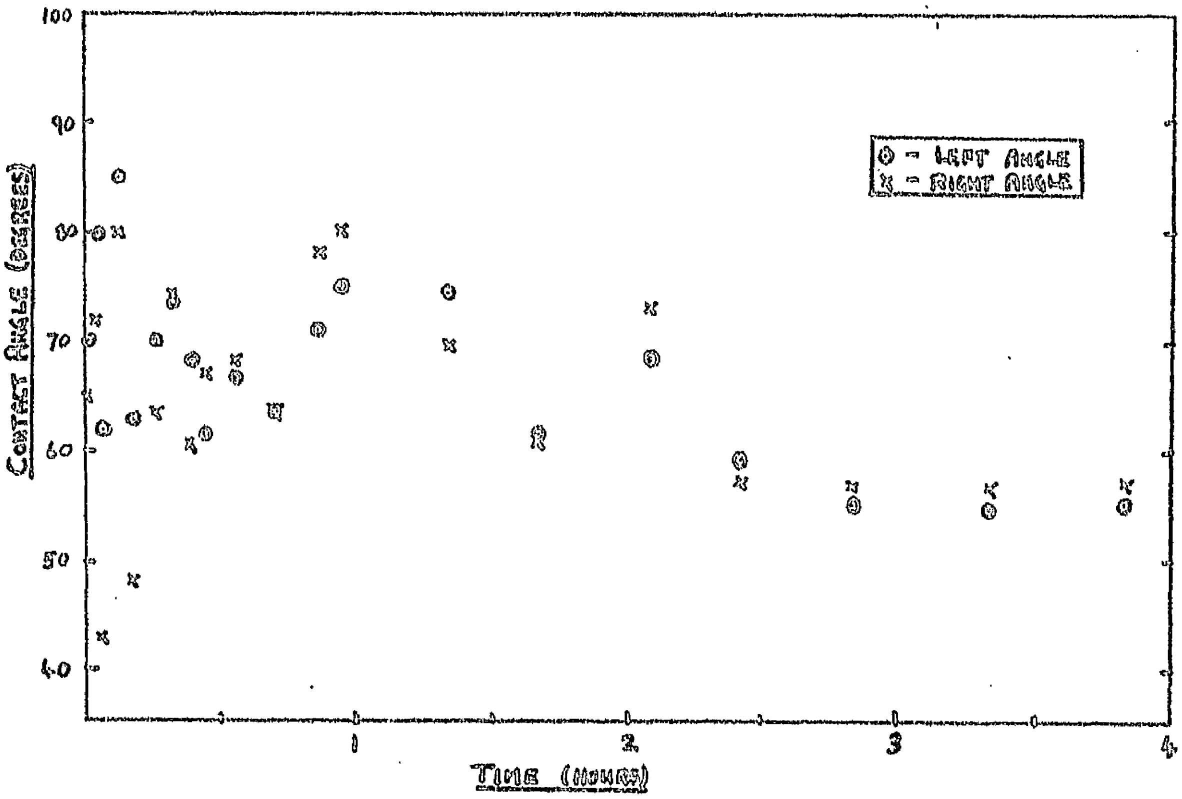

Fig. 31. Change of contact angle with time for pure iron on a silica plaque in argon at 1540°C.

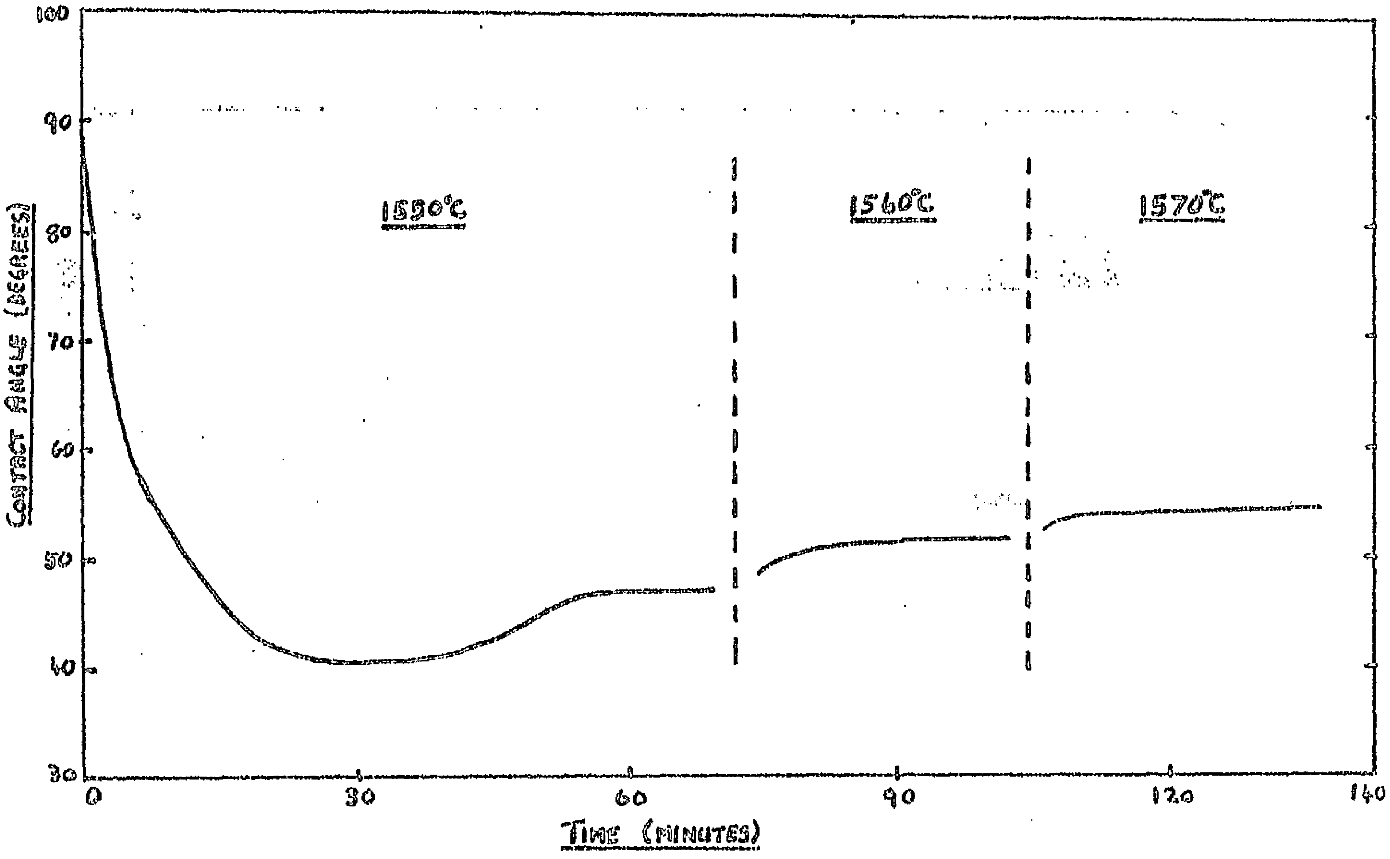

Fig. 32. Contact angles for pure iron on chromium trioxide in argon.

about 1400°C. SiO could possibly assist FeO in lowering γ_{SL} and γ_{LG}. Unfortunately FeO also permeated the plaque and γ_{SG} was also indeterminate, so the contact angle was the only numerical observation which could be obtained concerning interfacial phenomena. From Kubaschewski and Evans[116], the reaction:- $Fe + SiO_2 = FeO + SiO$ ......(1) has an equilibrium constant about 6×10^{-6} at 1540°C, so that the products would have very low activities. The reaction:- $Fe + \frac{1}{2}SiO_2 = FeO + \frac{1}{2}Si$.....(2) has an equilibrium constant about 1.2×10^{-4} at 1540°C, which is rather more favourable to the production of FeO, provided SiO does not escape from the system.

Fe/C alloys quickly solidified at each temperature from their melting points up to about 1530°C, as their carbon contents were lowered by reaction with SiO_2. At 1550°C reduction by carbon to SiO has an equilibrium constant about 116×10^{-2}, and reduction to Si has a constant about 1.07×10^{-1}. If all the carbon in a 4.4% alloy reacted to give only Si, an alloy with 5.1% Si would result; whereas the figure found after such a run was only 0.66%Si, showing that the chief product of the reduction was SiO, as could be the case if SiO diffused away from the interface. Lower contact angles were observed for these alloys than for pure iron, the lowest being 25° for the formerly 4.4%C. The formerly pure iron showed only about 0.12% Si after the run, and a higher contact angle (55°). These alloys have a ratio of Si contents about 1:6, and from equation (2) above, their systems would be expected to have FeO in the ratio of approximately 2:1. Since the carbon alloy system contained less FeO its contact angle would be expected to be greater than for the pure iron: this effect is apparently more than

balanced by the much higher Si in the carbon alloy. Kingery[69] has shown the large effect of Si in reducing γ_{SL} of Fe/Al_2O_3. The resultant surface excess of Si apparently persists to the solid state, as when the 0.66%Si specimen was dissolved in acid, the centre dissolved more quickly than the outside of the specimen, which was more corrosion resistant presumably due to a higher percentage of Si.

<u>Gehlenite:</u> Up to 1450°C both 3.6% and 4.4% C alloys showed contact angles between 132° and 134° at equilibrium. Several attempts to observe pure iron on this plaque failed due to reaction in the region of 1500°C, and as Gehlenite is at a maximum in the liquidus surface of the CaO: Al_2O_3: SiO_2 system, minor alteration would cause it to melt below 1590°C, this effect added to the fluxing effect of the FeO produced, caused the plaque to soften and results above 1450°C were not obtainable. Above 1450°C the carbon in the iron also reacted and the contact angle dropped to about 120°, possibly due to traces of Si in the iron. Up to 1450°C and between 3.6% and 4.4%C, neither temperature nor carbon content was found to have a significant effect on the wetting. Representative values are shown in Table XXV.

<u>Mullite:</u> The 4.4% carbon alloy assumed a contact angle of 130° on Mullite at 1250°C. Above this temperature all carbon alloys reacted with the plaque, and contact angles of 110° were observed when the iron finally melted, about 1530°C. Analysis of the Mullite gave 30.3% SiO_2 which is some 2% higher than the stoichiometric amount of 28.17%: this was possibly due to the acid washing treatment, or more probably, to an impure original material. This free SiO_2 may have been responsible for

the observed reaction at such low temperatures, compared to the iron/Gehlenite system.

The values of γ_{SG} for this material and the CaO/Al_2O_3 material below were obtained by extrapolation from King[7].

C.A.: Again temperature and amount of carbon showed no significant effect on θ which was within 3° of 130°, in the regions 1250°-1550°C, and 3.6% to 4.4%C. Just above 1590°C, which is the solidus temperature for this plaque, it softened, and apparent contact angles down to 80° were observed.

Cr_2O_3: All the iron/carbon alloys from zero to 4.4%C, reacted with this plaque in A at or below their melting points. The high carbon alloys, at their melting points, showed incipient fusion only at the top due to removal of some carbon near the plaque/metal interface: whereas the pure irons showed incipient fusion near the interface below 1535° due to pick up of some Cr. With rising temperature the high carbon alloys could be maintained partly liquid up to about 1540°C. quite violent bubbling of gas (CO) occurred up to this temperature, with receding contact angles down to 20°, and when reaction ceased the angles assumed values in the region 50°-60° at about 1550°C. The variation of θ with time and temperature for electrolytic iron is shown in Fig.32. In this figure is seen a tendency to low contact angles as reaction is proceeding, then an increase to the equilibrium value of 46.5°. At 1560°C an equilibrium value of 51° is quickly achieved, and similarly at 1570°C with an angle of 54.5°. Thus the contact angle increased about 4° per 10°C temperature increase, this change was quite reproducible and reversible, in the range

1550°- 1570°C, in a period of minutes (5-15), except for one Armco specimen which showed a steady decrease in θ with temperature increase to values in the range 60° - 70°. The most probably products are Cr and the spinel, $FeO.Cr_2O_3$:- $3Fe + 4Cr_2O_3 = 3FeO.Cr_2O_3 + 2Cr$...(3) Increase in temperature would be expected to yield more Cr, and if Cr had any marked effect on γ_{SL} and γ_{LG} it would be expected to reduce these parameters with a consequent reduction in an acute contact angle. However it is possible that Cr is not interfacially active and that it slightly increases γ_{LG} (cf. the Fe/Ni system, Kingery and Humenik[146]) with a slight increase in θ. Analysis of similarly treated specimens of Armco and electrolytic iron showed chromium contents of 3.77% and 4.13% respectively. The reaction, as in equation (3) above, is not the only one possible, the work of Hilty, Friedel and Crafts[148] indicates the possibility of the formation of a mixed spinel $XO.Cr_2O_3$ where X is Fe or Cr, and it seems that the system Fe/Cr/O is worthy of further investigation.

The contact angles quoted above are lower than the true values by an uncertain amount in the region of 5°, due to cavitation of the plaques, so that the true angle for electrolytic iron at 1550°C may be about 50°. However the changes in contact angle for any one specimen (~ + 4°/10°C increase) remain true.

<u>$MgO.Al_2O_3$:</u> This material showed a marked resemblance to MgO in its behaviour towards Fe/C alloys. No change in wetting occurred with temperature (1300°C - 1550°C) or with carbon (0 - 4.4% C), and the contact angles were within 1° of 131.5° at equilibrium. Faint clouds of gas were observed to gather near the interface in most of these runs,

presumably due to reduction of MgO: but in this case θ was lowered to about 125°, and not raised as in the case with pure MgO.

In one run with electrolytic iron, a trace of oxygen was inadvertently admitted with the argon, and observations were continued till a steady angle of 47° was observed at 1550°C: the plaque was badly contaminated with FeO, and the surface of the iron was oxidised. With both the spinels quite a lot of trouble arose due to traces of oxygen, far more persistent than in any other systems, and this was attributed to desorption from the plaques. The adsorptive power of the spinels has already been considered (Chap.IIID). On evacuating for longer periods up to higher temperatures (about 1100°C) this trouble was decreased.

In cooling down after these runs a solid was observed to separate from the iron before recallescence was observed. Examination when cold showed several iron specimens to be partly covered with this white substance. A similar phenomenon had been observed in several cases with Al_2O_3 plaques, and a similar white powder had been observed on the top surface of iron which had been melted in Alundum crucibles to prepare the specimens (Part D2, this chap.), so it was attributed to an interaction between Fe and Al_2O_3. There is some doubt[149] about the thermodynamics of Aluminium and oxygen in iron, and there is a possibility of the occurrence of some suboxide, Al O or Al_2O (e.g. Hock and Johnson[150]). The presence of this powder seems to suggest that the equilibrium concentration of oxygen in iron in the presence of aluminium is higher than is commonly believed. By weighing specimens this powder was about 0.05% of the iron.

$MgO.Cr_2O_3$: This material showed reaction with all the alloys observed, though to a much smaller extent than the pure Cr_2O_3. Pure iron at 1550°C showed contact angles from 100° dropping to about 70° in about 40 minutes before rising to a steady 108°. The Fe/C alloys remained partially molten up to about 1530°, due to removal of carbon; over this range θ was in the region of 130° - 160°. At 1550°C the contact angles dropped to 95° - 105°, then rose to a steady 109° ± 2°, which angle was not changed with temperature, as was observed with the pure Cr_2O_3. Very little Cr (0.08%) was found in the iron after these runs.

Discussion:

The contact angles for the iron/carbon alloys on Al_2O_3 are similar to those (147°-100°) found by Kingery et al[140,146] who also quoted interfacial free energies in the range 1400-1550 ergs/cm^2. The values for γ_{SL} in Table XXV are higher due to the higher γ_{SG} used here. A contact angle of 130° has been reported[146] for iron on MgO in He which agrees well with those found here. No published work seems to have been done on any of the other systems, although the author had done some previous work[133] with Gehlenite and CaO/Al_2O_3 plaques, the results of which agree quite well with those discussed above.

When a significant amount of FeO occurred in these plaques the wetting by Fe was always increased, with contact angles down to 110° with MgO, and about 50° with Al_2O_3 and $MgO.Al_2O_3$; and systems containing SiO_2 or Cr_2O_3 may be considered to show similar effects. Very few examples have been given in literature of metals with a contact angle less than 90° on oxides. The best known of these is the wetting of Al_2O_3 by Al[28,113]; in this case the possibility of the

formation of suboxides is high[150]. Na is reported to wet glass[28], and iron is reported[146] to wet TiO_2. In all of these systems there is a possibility of the formation of some oxides of the metal, the mutual solubility of this oxide in the metal and in the solid may be the factor responsible for the wetting. In the case of the iron/SiO_2 system the wetting agent may be Si in addition to FeO. Sulphur is reported[147] to be interfacially active in iron/oxide systems, when FeS may be the mutually soluble component. So it seems that when wetting occurs in metal/oxide systems it is due to a mutually soluble component, usually the oxide of the metal in question. The only doubtful case reported[113] is the wetting of UO_2 by Na; thermodynamically little Na_2O should form, but this small amount may be sufficient to cause the observed wetting.

Silicious refractories are well known to have poor resistance to liquid steel. This is due not only to the thermodynamics of the Fe/SiO_2 systems, but to the low contact angles of the steel with these materials, giving an increased area of reaction. This is of little consequence in casting steel or iron into sound moulds due to the speedy formation of a solid skin cutting down the reaction, but the low contact angles would have a beneficial effect in promoting complete filling of the mould and giving a casting with good edges and corners.

Cr_2O_3 and $MgO.Cr_2O_3$ exhibit large differences in contact angles and reactivity with iron, as discussed above, so one would expect much better corrosion resistance to be found with Chrome-Mag bricks than with Chrome.

Conclusions:

1) Liquid iron does not wet those oxides investigated with which it

does not react significantly: the contact angles being 130°-133° and work of adhesion ~ 600-650 erg/cm^2, except for Al_2O_3 where θ is higher and W_{AD} lower.

2) In the non-reacting systems examined, the surface free energy of the solid (350 to 2,000 erg/cm^2) had no significant effect on the contact angles.

3) In the non-reacting systems, except for Fe/Al_2O_3, no significant effect on wetting was found on varying either temperature (1250°-1550°C) or carbon in the iron (0 - 4.4%).

4) Fe and Fe/C alloys react with plaques containing SiO_2 or Cr_2O_3, with a resultant low contact angle, being in the region of 50° for the pure oxides, and in the region 110°-120° for oxide compounds (Gehlenite, Mullite and Picrochromite). An unexplained reversible change in contact angle with temperature was found with iron and pure Cr_2O_3.

5) In every case when a significant amount of FeO was found in the plaque, low contact angles were observed; 110° for MgO and about 50° for Al_2O_3 and $MgO.Al_2O_3$.

4. Slags on Iron:

Although results[151] have been reported for the wetting of other metals by liquid oxides, none was found on the wetting of iron. The contact angles for silicates and borates on metals are generally in the region of 40° - 70° in inert atmospheres, so low contact angles would be expected with silicates on the relatively more reactive iron.

A slice about 1/8 inch thick was cut from an Armco iron bar, perpendicular to the axis, and ground flat and parallel sided. It was

polished by hand on abrasive papers down to 600 mesh SiC, and stored in a desiccator. When required, pieces about 1/2 inch square were cut and their top surface cleaned on 600 mesh paper. The same slags were used, as described earlier in this chapter, and the experimental procedure was also the same. The results are shown in Table XXVI.

Table XXVI: Contact Angles and Work of Adhesion for Slags on Iron in Argon.

Slag	Composition				θ° at T°C.				W_{AD} at 1450°C
	CaO	MgO	Al_2O_3	SiO_2	1300	1350	1415	1450	
I	38	-	20	42	78	69	54	43.5	755
II	23	-	15	62	75	72.5	55	52	580
III	53	-	47	-	-	-	30	33	1060
V	-	20	18	62	-	60	50	50	640

These slags showed about 10% FeO by analysis after the runs. Accurate figures, for the surface free energy of these slags with FeO, were not available so that the work of adhesion quoted is not very accurate being derived from values of γ_{LG} for the pure slags.

There is a tendency for θ to decrease with temperature increase; this effect was not reversible in a period of about half an hour, and it is attributed to the production of more FeO at higher temperatures. Another run with slag I up to 1450°C showed a contact angle substantially constant at about 73°, and when this specimen was analysed it was found to contain only 3.8% FeO. This suggests that FeO has quite a marked effect in decreasing θ.

Although the range of slag compositions is not all that might be desired, there seems a tendency, from Table XXVI, for θ to decrease with increasing basicity. FeO would contribute to this basicity, in

[illegible]

[illegible]

[illegible]
[illegible]

[illegible]

[illegible]

addition to having a possible surface activity. The rate of change of θ with temperature seems to increase in the region 1350°- 1415°C, indicating that δ iron is wet better than γ iron, though this effect is not clearly separable from the temperature effect, and a marked decrease in θ in passing 1410°C was not observed.

Discussion:

With a $CaO/Al_2O_3/SiO_2$ slag on iron at 1400°-1450°C,   is in the region of 50°. From Bondi[28], the change in the surface free energy of iron on solidifying is shown to be about 430 erg/cm^2, so that the surface free energy of solid iron will be approximately 2320 erg/cm^2 in the region 1400°- 1450°C, and this will give γ_{SL} about 2060 erg/cm^2.

For iron on such a slag/(Gehlenite) γ_{SL} is about 1880 erg/cm^2 at 1450°C. So that γ_{SL} in both cases is about 1970 ± 90 erg/cm^2. If a similar change in surface free energy of the interface occurs, as is the case with iron, we may have an interfacial free energy with both phases liquid of $\gamma_{LL} \sim 1540 \pm 100$ erg/cm^2. This figure applies to pure iron; where large amounts of surface active alloys are present this figure may be about 500 erg/cm^2 lower.

The figures quoted for   are in good agreement with those given by Kingery and others[69,140,142,146]. The only work known to the author on γ_{LL} was done by Popeil, Esin and Geld[152], who examined sessile drops by X-ray photography. They found values of γ_{LG} for 4.6%C, 0.4%Si of 675 erg/cm^2: this value is considerably below any other for a similar alloy found by the author in literature; so it is possible their results are only about 50% of the true figures. Their values for γ_{LL} for iron in $CaO/Al_2O_3/SiO_2$ slags were in the region 600-800 erg/cm^2

which are considered to be in agreement with the estimated value of 1000 - 1500 erg/cm^2 found here.

It has frequently been observed that the non-wetting of solid oxides by liquid metals is due to the repulsive effect of the polarised oxygen ions on the electron cloud in the metal. In non-reactive iron/oxide systems a contact angle of about 130° was found. In reacting systems FeO occurred and the oxygen in the iron would tend to lower the electron concentration, lessening this repulsion; also the iron ions in the oxide being possibly of lower polarising power than the other cations present would lessen the polarisation; giving lower contact angles, as found. In the case of liquid slags on solid iron, a similar reaction would take place, but it is not clear, atomistically, why the contact angles should be so low for non-reacting systems such as slag on platinum[26]. Only the thermodynamic explanation may be used in this case: the values of surface free energy for slags being much lower (c.400 erg/cm^2) than for metals (1000 - 1800 erg/cm^2), the liquid phase conforms to a shape of minimum total free energy.

——— xxx ———

Literature.

1. S.D.Poisson, "Nouvelle Theorie de l'Action Capillaire",Bachelier, Paris, 1831.

2. W.Thomson, Proc.Roy.Soc.,9,255,1858.

3. K.F.Gauss,"Werke", Gottingen, 5,29,1867.

4. P.S.LaPlace,"Oeuvres", 4, 348, 1880.

5. J.W.Gibbs, "On the Equilibrium of Heterogeneous Substances", Longmans, Green & Co., 1928.

6. J.Frenkel, "Kinetic Theory of Liquids", Clarendon,Oxford,1946(p.308).

7. T.B.King, Trans.Soc. Glass Tech., 35, 241, 1951.

8. J.R.Partington, "Advanced Treatise on Physical Chemistry", 1951.

9. N.K.Adam, "The Physics and Chemistry of Surfaces", Oxford U.Press, London, 1944 (p.157).

10. R.von Eotvos, Ann.Physik, 27, 448, 1886.

11. W.Ramsay & J.Shields, Z.phys.Chem., 12,443, 1893.

12. N.Lovgren, Svensk Kem. Tid., 53, 359, 1941; Amer.Chem.Abstr.,36, 3077, 1942.

13. E.K.Rideal, "Introduction to Surface Chemistry",Cambridge U.Press, 1930 (p.146).

14. J.W.McBain, "The Sorbtion of Gases and Vapours by Solids", Routledge & Sons, London, 1932.

15. R.A.Beebe, "Handbuch der Katalyse, IV", Springer-Verlag,Vienna, 1943 (p.473).

16. W.E.Garner & D.McKie, J.Chem.Soc., 2455, 1927.

17. G.J.Parkes, Phil.Mag., 6, 5, 517,1903.

18. H.Udin, E.R.Funk & J.Wulff, J.Metals, 3,1206, 1951.

19. E.Orowan, Nature, 154, 341, 1944.

20. I.Sawai & K.Kubo, Z.anorg.allgem.Chem., 232,425,1937.

21. G.Tamman & K.A.Rabe, " " " , 162,17, 1927.

22. W.A.Weyl, "Structure and Properties of Solid Surfaces", Nat. Research Council Conf'ce, Wisconsin, U.S.A., Sept. 1952, p.147.

23. J.E.Lennard-Jones, Proc.Roy.Soc., A 109, 476, 1925.

24. A.K.Schellinger, Trans.A.I.M.E., 179, 379, 1952.

25. G.Tammann & F. Arntz, Z.anorg.allgem.Chem., 192,45,1930.

26. H.Towers, Trans.Brit.Ceram.Soc., 53,3,180,1954.

27. W.D.Harkins, "The Physical Chemistry of Surface Films",Reinhold, New York, 1952.

28. A.Bondi, Chem.Rev., 52,417,1953.

29. R.N.Wenzel, Ind.Eng.Chem.,28,988,1936.

30. F.E.Bartell & J.W.Shepard, J.Phys.Chem., 57,211 & 455, 1953.

31. H.B.Bell,A.B.Murad & P.T.Carter, J.Metals,4,718,1952.

32. D.Turnbull, J.Chem.Phys., 20,411, 1952.

33. P.Kosakevitch, Rev.de Met., 9,578, 1949.

34. J.Okaga & T.Ikegawa, J.Appl.Phys., Sept., 1249, 1953.

35. J.A.Hedvall & Runehagen, Naturewissenschaften, 28,27,429,1940; Ceram.Abstr., 20,3,76,1941.

36. A.T.Gwathmey & A.F.Benton,J.Phys.Chem.,44,35,1940: A.T.Gwathmey & H.Leidheiser, J.Amer.Chem.Soc., 70,1200,1948.

37. J.Friedel,B.D.Cullity & C.Crussard, Acta Met. I, 79, 1953.

38. J.Friedel, Private Communication to Author.

39. J.P.Roberts, Metallurgia, 1, August, 1950.

40. N.W.Taylor, J.Amer.Ceram.Soc., 17,155, 1934.

41. G.Tammann, Z.anorg.allgem.Chem., 149, 29, 1925; Kolloid Zeit., 98, 275, 1942.

42. M.Volmer, "Kinetik der Phasenbildung", Dresden, 1939, p.56.

43. J.Hutchins & J.P.Roberts, R.A.E.Farnborough, Tech.Note Met.170,1953.

44. A.G.Allison, E.C.Sesler, N.L.Haldy & W.H.Duckworth, J.Amer.Ceram. Soc., 39, 151, 1956.

45. P.W.Clark, J.H.Cannon & J.White, Trans.Brit.Ceram.Soc., 52,1,1953.

46. W.K.Burton & N.Cabrera, "Crystal Growth", Disc.Faraday Soc. No.5, 1949, p.35.

47. W.Jander, Z.anorg.allgem.Chem., 163,1,1927.

48. R.M.Barrer, "Diffusion in and through Solids", Cambridge U.Press,1941

49. A.H.Cottrell, Met.Reviews, 1, 479, 1956.

50. H.Towers, M.Paris & J.Chipman, J.Metals, 5, 1555, 1953.

51. J.F.Laurent & P. Bernard, Compt.Rend., 241, 1204, 1956.

52. B.Bengtson & R. Jagitsch, Arkiv.Kemi., A 24, 18, 1947; Amer.Chem. Abstr., 42, 7146, 1948.

53. G.Wulff, Z.Krist., 34, 449, 1901.

54. P.Curie, Bull.soc.franc.Mineral., 8, 145, 1885.

55. P.R.Landon, J.L.Lytton, L.A.Shepherd & J.E.Dorn,
Trans.Amer.Soc.Met., Vol.51, Preprint 73.

56. P.Duwez & C.B.Jordan, J.Metals, 188, 943, 1950.

57. L.Navias, J.Amer.Ceram.Soc., 39, 141, 1956.

58. J.K.Mackenzie & R.Shuttleworth, Proc.Phys.Soc., B62, 833, 1949.

59. P.W.Clark & J. White, Trans.Brit.,Ceram.Soc., 49,305, 1950.

60. G.C.Kuczynski, J.Metals, 1,169,1949.

61. E.B.Allison & P.Murray, Acta.Met., 2, 487, 1954.

62. I.N.Stranski, Z.physik.Chem., B11, 342, 1931.

63. P.Murray, E.P.Rodgers & A.E.Williams, A.E.R.E.Harwell, Report M/R 893, 1952.

64. A.R.Verma, "Crystal Growth and Dislocations", Butterworth,London,1953

65. F.H.Horn, Phil.Mag., 43, 1210, 1952.

66. A.H.Cotrell, "Dislocations and Plastic Flow in Crystals",Clarendon, Oxford, 1953.

67. Internat.Crit.Tables, II, p.48.

68. N.F.Mott,Proc.Phys.Soc., 60,391,1948.

69. W.D.Kingery, J.Amer.Ceram.Soc., 37, 42, 1954.

70. C.S.Barrett, "The Structure of Metals", McGraw-Hill,London,1953.

71. H.Udin,"Metal Interfaces", Amer.Soc.Metals, 1952, p.114.

72. C.S.Barrett, G.Ansel & R.F.Mehl, Trans.A.I.M.E.,125,516,1937;
C.S.Barrett & L.H.Levenson, ibid, 145, 281, 1941.

73. R.Arnold, Z.fur angew.Physik, 7,9,453,1955.

74. P.Debye & P.Scherrer, Phys.Zeit., 18, 291, 1917.

75. J.D.Bernal, Proc.Roy.Soc., A 106, 749, 1924.

76. G.I.Finch & H. Wilman, Proc.Roy.Soc., A 155, 345, 1936.

77. A.Taylor & D. Laidler, Nature, 146, 130, 1940.

78. H.Lipson & A.R.Stokes, Proc.Roy.Soc., A 181, 101, 1942-43.

79. H.P.Rooksby & E.G.Steward, Nature, 159, 638, 1947.

80. H.Arnfelt, Ark.Mat.Astron.Fysik, B 23, 1, 1932.

81. G.Herzberg, J.Chem.Phys., 10,306, 1942.

82. F.R.Bichowski & F.D.Rossini, "Thermochemistry of Chemical
Substances", Reinhold, New York, 1936.

83. G.J.Kynch & W.G.Penney, Proc.Roy.Soc., A 179, 214, 1941.

84. J.Glocker, J.Chem.Phys., 21, 313, 1954.

85. L.Pauling, J.Amer.Chem.Soc., 57, 2705, 1935.

86. C.A.Coulson, "Valence", Oxford U.Press, 1952.

87. O.Ruff, Trans.Faraday Soc., 34, 1002, 1938.

88. Y.K.Syrkin & M.E.Dyatkina, "The Structure of Molecules and the
Chemical Bond", London, 1950.

89. L.A.Girifalco & R.A.Lad, J.Chem.Phys., 25,693,1956.

90. W.D.Harkins, J.Chem.Phys., 10, 268, 1942.

91. "Structure Reports", 1947-48, Internat.Union of Crystallography.

92. J.Basset, Brenstoff-Chemie, 23, 127, 1942.

93. D.A.Melford & T.P.Hoar, J.I.M., 3, 17, 197, 1957.

94. R.H.Bruce, Met.Club J., Royal College of Science and Technology, No.10, p.41, 1957-58.

95. O.Maas & A.L.Geddes, Phil.Trans.Roy.Soc., A 236, 303, 1937.

96. M.G.Mayer, "Statistical Mechanics", J.Wiley & Sons Inc., N.Y., 1940, Chap's 13 & 14.

97. K.A.Kobe & R.E.Lynn, Chem.Rev., 52, 117, 1953.

98. C.M.Guldberg, Z.physik.Chem., 5, 374, 1890.

99. D.T.Lewis, J.Chem.Soc., 261, 1938.

100. H.P.Meissner & E.M.Redding, Ind.Eng.Chem., 34, 521, 1942.

101. R.Herzog, Ind.Eng.Chem., 36, 997, 1944.

102. N.M.Parikh, Sc.D.Thesis, M.I.T., 1953 (See Kingery[132]).

103. R.Fricke, Kolloid Z., 96, 213, 1941; R. Fricke & E. Denger, Z.anorg. Chem.,253,2, 1945.

104. G.Jura, J.Chem.Phys., 12, 1335, 1949; G.Jura & C.W.Garland, J.Amer.Chem.Soc.,74,6033,1952.

105. J.E.Lennard-Jones & P.A.Taylor, Proc.Roy.Soc., A 109,476,1925;
ibid. A 117, 230, 1926: J.Biemuller, Z.Physik.,38,759,1926:
R.Shuttleworth, Proc.Roy.Soc., A 62, 167, 1949.

106. R.Brill, C.Hermann & C.Peters, Z.anorg.Chem., 257, 151, 1948.

107. G.C.Benson & R.McIntosh, Canad.J.Chem.,33,1677,1955.

108. B.M.Dent, Phil.Mag., 7,8, 530, 1929.

109. L.Pauling, "The Nature of the Chemical Bond", Cornell U.Press, 1948, p.346.

110. K.Moliere, W.Rathje & I.N.Stranski, Disc.Faraday Soc., No.5, 1949, p.21.

111. F.M.Jaeger, Z.anorg.allgem.Chem., 101,1,1917.

112. S.G.Lipsett,F.M.G.Johnson & O.Maas,J.Amer.Chem.Soc.,49,1940,1927;

(contd.)

112.(cont'd). ibid, 50, 2071, 1928: W.D.Harkins, J.Chem.Phys., 10,268,1942: G.C.Benson & G.W.Benson, Canad.J.Chem., 33, 232,1955.

113. D.T.Livey & P.Murray, 2nd Plansee Seminar, June, 1955, p.375; J.Amer.Ceram.Soc., 39,11,363, 1956.

114. R.Fricke, "Handbuch der Katalyse", IV, Springer-Verlag,Vienna, 1943, p.1.

115. M.Volmer, "Kinetik Der Phasenbildung", Dresden,Steinkopff,1939,p.87.

116. O.Kubaschewski & E.Ll.Evans."Metallurgical Thermochemistry", Pergamon Press, London, 1956.

117. L.Brewer, Chem.Rev.52, 1, 1953: T.L.Cotrell, "The Strength of Chemical Bonds",Butterworth,London,1954

118. G.Herzberg, "Molecular Spectra and Molecular Structure; I,Spectra of Diatomic Molecules", New York, 1950.

119. J.D.H.Donnay & W.Nowacki, "Crystal Data", Geol.Soc.of Amer. Mem. 60, 1954.

120. G.R.Rigby, Trans, Brit. Ceram.Soc., 50, 175, 1951.

121. W.L.Bragg, "Atomic Structure of Minerals", Oxford U.Press, 1937.

122. A.F.Wells, "Structural Inorganic Chemistry", Clarendon Press,1950.

123. O.J.Whitmore & N.N.Ault, J.Amer.Ceram.Soc., 39, 443, 1956.

124. G.R.Rigby, G.B.H.Lovell & A.T.Green, Trans.Brit.Ceram.Soc., 45, 251, 1945-46.

125. F.A.Hummel, J.Amer.Ceram.Soc., 33, 102, 1950.

126. Internat.Crit.Tables, vol.II, p.83.

127. S.Brunauer, D.L.Kantro & C.H.Weise,Canad.J.Chem., 34,729,1956.

128. P.Kosakevitch, Rev.de Met., 46,505, 1949.

129. J.F.Johnson, J.Axelson & E.L.Piret, Chem.Eng.Prog., 45,708,1949.

130. A.K.Schellinger, Trans.A.I.M.E., 179, 379, 1952.

131. H.von Wartenberg, G.Welmar & E.Saran, Nachr.Gottingen,Math.Phys.Kl., Fachgruppe 2 (N.F.), 2,73, 1936.

132. W.D.Kingery, Bull.Amer.Ceram.Soc., 353, 108, 1956.

133. R.H.Bruce,Thesis to the University and the Royal College of Science and Technology, Glasgow, May,1954.

134. S.Glasstone, "Elements of Physical Chemistry",D.van Nostrand & Co., N.Y., 1948, p.368.

135. G.R.Rigby,G.B.N.Lovell & A.T.Green,Trans.Brit.Ceram.Soc.,45,137,1946.

136. J.D.Baird & J.Taylor, Trans.Faraday Soc., 424, 54, 4, 526, 1958.

137. J.J.Bickerman, "Surface Chemistry", Academic Press Inc.,1947,pp.4-19.

138. G.Becker,F.Harders & H.Kornfeld,Z.anorg.Chem.,258,363,1949; Amer. Chem.Abstr.,44,4396, 1950.

139. F.Sauerwald,B.Schmidt & F.Pelka, Z.anorg.Chem., 223, 84, 1935; Amer.Chem.Abstr., 29, 5392, 1935.

140. F.A.Halden & W.D.Kingery, J.Phys.Chem., 59, 557, 1955.

141. P.Kosakevitch & G. Urbain, Compt.Rend., 244, 335, 1957.

142. W.D.Kingery & M.Humenik, J.Phys.Chem., 57, 359, 1953.

143. D.S.Kothari & F.C.Auluck, Nature, 159, 204, 1947.

144. P.Kosakevitch, S.Chatel & M.Sage, Compt.Rend.,236,2064, 1953.

145. B.V.Stork & S.I.Filsppov, Isvestia Acad.Nauk., S.S.S.R., Otd.Tekh. Nauk., 3, 413, 1949.

146. M.Humenik & W.D.Kingery, J.Amer.Ceram.Soc., 37,18, 1954.

147. G.Derge & W.O.Philbrook, Rev.de Met., 52, 995, 1955.

148. D.C.Hilty, W.D.Forgeng & R.L.Folkman,Trans.A.I.M.M.E., 203,253,1955.

149. N.A.Gokcen & J.Chipman, J.Metals, 5, 173, 1953.

150. M.Hock & H.W.Johnson, J.Amer.Ceram.Soc., 76, 2560, 1954.

151. B.S.Ellefson & N.W.Taylor,J.Amer.Ceram.Soc.,21,193,205,1938: V.F.Zackay, D.W.Mitchell, S.P.Mitoff & J.A.Pask,J.Amer.Ceram. Soc., 36,84,1953.

152. S.I.Popeil,O.A.Esin & P.D.Geld,Dok.Acad.Nauk.,S.S.S.R., 74,1097, 1950; ibid,75,227,1950.

Acknowledgements

This work was carried out in the Metallurgy Department of the Royal College of Science and Technology, Glasgow.

The author desires to thank Professor R. Hay, D.Sc.,Ph.D., F.R.I.C., F.I.M., who suggested the subject and provided help and encouragement throughout the course of this work. Much help and useful discussion were also freely given by other members of the department, in particular by J. Taylor, M.Sc., Ph.D., F.I.M., to whom the author is also grateful.